Dioxin Inhibits Epicardium Development and Regeneration of the Zebrafish Heart

By

Peter Jacobs Hofsteen

A dissertation submitted in partial fulfillment
of the requirements for the degree of

Doctor of Philosophy

(Pharmaceutical Sciences)

at the

UNIVERSITY OF WISCONSIN-MADISON

2013

Date of final oral examination: 08/15/13

The dissertation is approved by the following members of the Final Oral Committee:

Warren Heideman, Professor, Dept. of Pharmaceutical Sciences

Richard E. Peterson, Professor, Dept. of Pharmaceutical Sciences

Arash Bashirullah, Assistant Professor, Dept. of Pharmaceutical Sciences

Tim Bugni, Assistant Professor, Dept. of Pharmaceutical Sciences

Susan Smith, Professor, Dept. of Nutritional Sciences

Gary Lyons, Professor, Dept. of Cell and Regenerative Biology

Abstract

Zebrafish (*Danio rerio*) are an established vertebrate model for studying heart development, regeneration and cardiotoxicity. Zebrafish embryo-larvae exposed during the temporal window of epicardium development to the aryl hydrocarbon receptor (AHR) agonist 2,3,7,8-tetrachlorodibenzo-*p*-dioxin (TCDD) exhibit severe heart malformation. Thus, we sought to determine if epicardium development was affected by TCDD exposure. TCDD exposure prevents development of the epicardial progenitors (proepicardium; PE) and subsequent formation of the epicardium. Exposure to TCDD later in development, after the epicardium has formed, does not produce acute cardiac toxicity. However, in adult zebrafish, TCDD exposure prior to ventricular resection prevents cardiac regeneration; the epicardially-derived white epithelium that envelops the blood clot fails to form and cardiomyocyte proliferation is markedly reduced. It is likely that TCDD-induced inhibition of epicardium development and cardiac regeneration occur via a common mechanism. Using the embryonic zebrafish, we have identified *sox9b* as a downstream AHR target gene in the heart. We find that while *sox9b* is expressed in the myocardium, it is not expressed in the affected epicardial cells or progenitors. TCDD exposed zebrafish embryos had significantly reduced levels of cardiac *sox9b* during epicardium development. Furthermore, we found manipulation of *sox9b* expression could phenocopy most of the effects of TCDD at the heart. Loss of *sox9b* prevented the formation of epicardial progenitors comprising the PE on the pericardial wall, and prevented the formation and migration of the epicardium around the heart. Zebrafish lacking *sox9b* showed pericardial edema, heart elongation, reduced blood circulation and lacked endocardial valve cushions and leaflets.

Furthermore, *sox9b* mRNA injection prior to TCDD exposure rescued PE formation, but the epicardium failed to form. Myocardial contractility remained severely affected in *sox9b* mRNA injected TCDD-treated fish. This led us to investigate the role of myocardial contractility during epicardium formation. Lack of heart contractility resulted in a phenotype analogous to our *sox9b* rescue experiments; the PE formed but failed to migrate and form the epicardium. These experiments demonstrate myocardial contractility is required for PE cell migration and epicardium formation. Together, zebrafish epicardium development requires *sox9b* and normal cardiac contractility, which in our model, are severely affected by TCDD.

DEDICATION

This dissertation is dedicated to wonderful wife and son, Laura and Sebastian; my parents; Linda and Wayne Antonie-Lusk and James Hofsteen; my brothers and their families: Alex, Brian, Alisha, Lindsay, Malia, Ethan and Owen; and my late grandparents Celestine (CJ) and Betty Antonie. I am lucky to have such a wonderful family! You have all inspired me and your support during graduate school was incredible. I also dedicate this dissertation to my dog, Guddha and cats, Nadi and Suva and to all the chickens and fish that have provided us warmth and entertainment during the long winter months.

ACKNOWLEDGEMENTS

I would like to thank my advisors, Warren Heideman and Richard E. Peterson for providing me the opportunity to train in their laboratory. Their different personalities ad mentoring styles gave me a well-rounded graduate school experience that I'll cherish for many years. I also would like to thank my committee members: Gary Lyons, Arash Bashirullah, Tim Bugni and Susan Smith for all your support and guidance. You have all inspired me in different ways and I am truly grateful.

This experience would not have been nearly as fun without the support and friendship of past and present Heideman-Peterson laboratory members. I'd like to thank Jess Plavicki first and foremost, as our collaborations were a ton of fun and extremely productive. I'll miss randomly getting tackled by Felipe Burns, the ever-so-clever one-liners from Kevin Lanham, safety questions from Joe Gawdzik, talking about the weather with Tracie Baker, cupcakes and cookies from Monica Yue and of course the shots with Min-sik Kim. I'll miss talking to Robert Moore in his office in amazement that he knows where things are and discussing the latest in computers with Tien-Min Lin. I'd also like to thank past lab members: Vatsal Mehta, Kong Xiong, Ofek Bar-ilan Michael Conway, Heather Hardin, Chad Vezina and Doug Grunwald for your help, patience and laugher. Lastly, I'd like to thank Dorothy Nesbit as she is the glue that holds this place together.

TABLE OF CONTENTS

LIST OF TABLES AND FIGURES

CHAPTER 1: Introduction

Epicardium Formation as a Sensor in Toxicology

Peter Hofsteen, Jessica Plavicki,

Richard E. Peterson and Warren Heideman

Journal of Developmental Biology 2013 **1(2)**, 112-125

ABSTRACT

Zebrafish (Danio rerio) are an excellent vertebrate model for studying heart development, regeneration and cardiotoxicity. Zebrafish embryos exposed during the temporal window of epicardium development to the aryl hydrocarbon receptor (AHR) agonist 2,3,7,8-tetrachlorodibenzo-p-dioxin (TCDD) exhibit severe heart malformations. TCDD exposure prevents both proepicardial organ (PE) and epicardium development. Exposures later in development, after the epicardium has formed, do not produce cardiac toxicity. It is not until the adult zebrafish heart is stimulated to regenerate does TCDD again cause detrimental effects. TCDD exposure prior to ventricular resection prevents cardiac regeneration. It is likely that TCDD-induced inhibition of epicardium development and cardiac regeneration occur via a common mechanism. Here, we describe experiments that focus on the epicardium as a target and sensor of zebrafish heart toxicity.

INTRODUCTION

Heart disease remains the leading cause of death worldwide. In the United States, one third of all deaths can be attributed to cardiovascular disease (Lloyd-Jones et al., 2010). It is believed that the etiology of heart disease results from a combination of factors including individual genetic makeup and either intentional or unintentional exposure to environmental factors such as tobacco smoke or environmental contaminants at different stages of life. Here we describe recent work identifying the epicardium as the target for chemicals that cause heart failure in developing embryos.

Although literature searches retrieve hundreds of articles using the keyword epicardium along with toxicity or chemical, the majority of these identify articles that are either about the epicardium as a surface for electrophysiological contact, or articles with the pericardium but no mention of the epicardium. Of the few remaining articles, most examine the epicardium in adults, rather than studies examining epicardium formation or even expansion or maintenance.

It has long been known that drugs used in treating cancer have effects on humans that include damage to the epicardium and other heart structures (Tsibiribi et al., 2006; Yeh et al., 2004). While not directly related to using the epicardium it should be noted that the pig pericardium is of intense interest as a biomaterial used in valve reconstruction. Chemical treatment and effects on this pericardial tissue is of interest both as it pertains to human responses to latent material in the xenograft as well as the effectiveness in treatment in prolonging the material effectiveness,

primarily reducing calcification (Guldner et al., 2012; Guldner et al., 2009; Neethling et al., 2010). Finally among asbestos workers, mesotheliomas arise on various internal tissues. Although primarily associated with the lung, these sometimes arise on the pericardium (Abejie et al., 2008).

Mammalian models have been used to study various aspects of chemical interactions with the epicardium. Iminashi and Arita used ouabain to alter the action potential duration on the epicardium of Japanese monkeys (Imanishi and Arita, 1987). In another study, the effects of kallikrein was studied on the adult dog epicardium, following the effects of exogenous bradykins and proteases as well as bradykin receptor antagonists on blood pressure and heart rate (Staszewska-Woolley and Woolley, 1989). While isolated epicardial cells have been used to test the effects of 4-Aminopyridine in ischemia response models (Lukas and Antzelevitch, 1993). Canine epicardial cells have also been used to test the effects of different adrenergic receptor agonists and antagonists in dogs in the acute stage of Chagas disease (Han et al., 1997). Other studies with dog epicardium examined the effects of captopril on the production of free radicals after electric shock (Pagan-Carlo et al., 1999).

Others have used the epicardium to study the toxic effects of doxorubicin on conduction properties of the ventricle in the rat (Kharin et al., 2012). In another study examining mouse epicardial cells, arsenite was found to inhibit the epithelial to mesenchymal transition (EMT) of the epicardial cells, but not differentiation into smooth muscle cells (Allison et al., 2013). Using the chick embryo as a model,

Olivey *et al* found that transforming growth factor-beta 1 and 2 increase EMT in PE explants (Olivey et al., 2006). Mouse hearts have also been used as whole explants to follow the effects of antiarrhythmic drugs, often focusing on the excitability of the epicardial layer (Sabir et al., 2008).

There are an increasing number of articles showing the ability of different chemicals to cause pericardial edema in developing fish (Incardona et al., 2011; Lefebvre et al., 2004; Li et al., 2012; Lin et al., 2007; Reimers et al., 2004; Tu et al., 2013; Valesio et al., 2013). As will be seen below, the pericardial edema may be a secondary response to effects of the chemical on epicardium formation. Thus, fish models may prove very sensitive in identifying epicardium-toxic compounds.

Due to the paucity of reports investigating epicardium formation following exposure to environmental chemicals, we describe experiments conducted in our laboratory using zebrafish and mouse models that have identified the epicardium as a target underlying cardiotoxicity. As an example, we use 2,3,7,8-tetrachlorodibenzo-*p*-dioxin (TCDD), a cardiotoxic environmental contaminant and prototypical AHR ligand to show how a common form of cardiotoxicity in zebrafish is connected to impaired epicardium development. We also discuss another cardiotoxic compound and non-AHR agonist, valproic acid (VPA), and its role in zebrafish epicardium development. We speculate that formation of the epicardium may be sensitive to disruption by environmental exposures during vertebrate development.

Zebrafish heart and epicardium development

The zebrafish heart is made up of two chambers, an atrium and a ventricle. In addition, the bulbous arteriosus lies directly after the ventricle, storing pulse pressure in a role analogous to that of the mammalian aorta. At the inflow tract, the sinus venosus collects venous blood for delivery to the atrium. Blood flows from the sinus venosus through the 2 contractile chambers and out the bulbous arteriosus to the ventral aorta, which delivers blood to the pharyngeal arch arteries (Hu et al., 2000).

The vertebrate heart is the first internal organ to form and function (Lee et al., 1994). For detailed reviews about early zebrafish heart development see (Bakkers, 2011; Stainier, 2001). Briefly, in the earliest stages of zebrafish heart development, just prior to gastrulation, bilateral clusters of cardiac progenitors cells are located in the lateral marginal zone. During gastrulation, cardiac progenitors migrate to the anterior lateral plate mesoderm where they are positioned near the midbrain-hindbrain boundary. Myocardial and endocardial precursors converge at the embryonic midline forming a cardiac disc at 19 hours post fertilization (hpf). The cardiac disc undergoes morphogenetic movements to form a contractile linear heart tube (24-28 hpf), which consists of an inner endocardial lining continuous with the vascular endothelium and an overlying myocardial layer. Distinct ventricular and atrial chambers form (30 hpf), the heart tube loops (36 hpf) and the atrioventricular (AV) canal becomes visible. Between the chambers, the endocardium gives rise to endocardial cushions, which are later elaborated into cardiac valves. Proper valve development is essential for directional blood flow and heart function. Continued

development of the zebrafish heart is highly dependent on the formation of the third and outer most layer of cardiac tissue, the epicardium.

The epicardium (*epi*: outer, *cardium*: heart) is a mesodermally derived squamous epithelium that is critical for heart development, function and regeneration. Unlike the cells that form the heart tube, the epicardium is derived from a transient pool of progenitors located outside of the heart field, termed the proepicardium (PE) (Manner et al., 2001; Manner et al., 2005; Serluca, 2008). PE cells migrate towards the looped heart and envelop the naked myocardium. In chick, following initial epicardial coverage of the heart, a subset of epicardial cells undergoes an epithelial-to-mesenchymal transition (EMT) to become epicardial derived progenitor cells (EPDCs; reviewed in (Lie-Venema et al., 2007). EPDCs invade the underlying myocardium and differentiate directly to become vascular smooth muscle cells and cardiac fibroblasts. Furthermore, EPDCs play important roles in heart looping, valve and coronary vasculature development, cardiac morphogenesis, cardiomyocyte alignment and proliferation, and maturation of the cardiac conduction system (reviewed in Gittenberger-de Groot et al., 2012; Lie-Venema et al., 2007; Riley, 2012). Furthermore, it is thought that epicardial cells retain plasticity as cardiac stem cells that can assist adult cardiac regeneration (Riley, 2012; Smart et al., 2012b; Smart and Riley, 2012). However, the formation or role EPDCs in zebrafish remains undetermined.

Zebrafish as a model to study cardiotoxicity

Zebrafish are an excellent vertebrate model for studying human health and disease. Development of zebrafish internal organs can be monitored *in vivo* because embryos are translucent and develop externally. These attributes combined with high fecundity and potential for high throughput screening make the zebrafish an ideal model to study heart development and chemical toxicity (Bakkers, 2011; Hill et al., 2005). Zebrafish were first developed as a genetic model, and are highly amenable to forward and reverse genetic screens. These screens have yielded much new information about heart development. Identifying genes required for heart development is greatly facilitated by the fact that zebrafish embryo-larvae are able to rely on passive oxygen diffusion and do not require heart function during the first week of life (Kopp et al., 2005; Stainier et al., 1996; Wells and Pinder, 1996). This is very important, because it means that one can follow the effects of mutations interfering with heart function as the heart ceases to function. In mammals, these mutations often produce immediate death of the fetus at the onset of effect.

DLCs and heart defects

Halogenated aromatic hydrocarbons (HAH) are ubiquitous environmental contaminants produced in industrial manufacturing processes and combustion. Included in this class are polychlorinated biphenyls, polychlorinated dibenzofurans, and polychlorinated dibenzo-*p*-dioxins. A subset of these different chemicals shares a similar molecular shape, matching the binding site of the ligand-activated aryl hydrocarbon receptor (AHR). The prototype agonist for the AHR is 2,3,7,8-tetrachlorodibenzo-*p*-dioxin (TCDD), commonly referred to as “dioxin”. Thus,

members of this group of AHR agonists can be referred to as dioxin-like compounds (DLCs).

Embryonic exposure to TCDD disrupts cardiac development and function in fish, birds, and mammals (Carney et al., 2006; Cheung et al., 1981; King-Heiden et al., 2012; Kopf and Walker, 2009; Peterson et al., 1993; Thackaberry et al., 2005b). TCDD is known to be highly toxic. In humans, epidemiological studies have linked TCDD exposure to congenital heart defects such as hypoplastic left heart syndrome (Cronk et al., 2004; Kuehl and Loffredo, 2006) and ischemic heart disease (Bertazzi et al., 1998; Flesch-Janys et al., 1995).

The most sensitive organisms to the effects of DLCs are fish, especially fish in early life stages (Lanham et al., 2012; Peterson et al., 1993). Using zebrafish as a model, it was quickly determined that TCDD exposure during early development causes decreased cardiomyocyte proliferation, a block and lack of erythrocyte development, reduced blood flow and cardiac output, and lack endocardial valve cushions. Ultimately, this leads to ventricular standstill and death (Antkiewicz et al., 2005; Belair et al., 2001; Carney et al., 2006; Dong et al., 2004; Henry et al., 1997; Mehta et al., 2008). Understanding why TCDD and related AHR agonists cause cardiotoxicity has been a question for quite some time.

TCDD and the zebrafish epicardium.

In zebrafish, the temporal window of cardiotoxicity is peculiar. The first 48 hours of cardiac development proceeds normally when zebrafish were exposed to TCDD immediately following fertilization. The primitive heart tube forms, the heart

loops and heart function is indistinguishable from controls. Circulation appears normal at 48 hpf in these animals. After 48 hpf, TCDD treated hearts diverge from experimental controls: the heart unloops and elongates, the ventricle becomes constricted, and pronounced pericardial edema develops (Antkiewicz et al., 2005). This unusual sensitivity to the cardiotoxic effects of TCDD corresponds to the developmental period in which the PE is specified and migrates over the myocardium to form the epicardium (Plavicki et al., 2013; Serluca, 2008). Furthermore, a similar phenotype was observed in the zebrafish *heartstrings* mutant (Garrity et al., 2002). These fish lack *tbx5a,* which was later shown to be required for PE specification (Liu and Stainier, 2010).

We now know that TCDD-induced activation of AHR prevents the development of both the PE and epicardium. This results in severe heart malformations that culminate in death (Plavicki et al., 2013). This explains the peculiar lag in toxicity until approximately 48 hpf. Furthermore, after the epicardium has formed it is no longer affected by TCDD; in adults a lethal TCDD exposure fails to produce cardiotoxicity (Hofsteen et al., 2013; Lanham et al., 2012). The failure to form an epicardium explains most of the heart malformations caused by TCDD.

Because many other chemicals produce a syndrome including pericardial edema and heart malformations in zebrafish, the epicardium may be useful as a sensor of chemical cardiotoxicity. Furthermore, disruption of epicardial development may prove to be a common cause of cardiotoxicity in developing vertebrates.

TCDD and the murine epicardium

Consistent with the high sensitivity that developing fish have to DLCs, the mouse heart is less sensitive to embryonic TCDD exposure than the zebrafish heart. Unlike zebrafish, TCDD-exposed mice do not exhibit pronounced heart malformations; however, measureable defects such as bradycardia and cardiac hypertrophy have been observed (Thackaberry et al., 2005b). Additionally, in the fetal murine heart, TCDD-exposure causes global transcriptomic changes in genes that regulate the cell cycle and extracellular matrix (Thackaberry et al., 2005a). In contrast to the effect in fish, the changes in the mouse heart are not embryonically lethal. Whether they reduce fitness or affect adult health is not known.

We have recently found that TCDD exposure does affect the developing mouse epicardium. While TCDD did not prevent epicardium formation in the developing mouse, the epicardium appeared detached from the underlying myocardium (Figure 1). Epicardial detachment has also been observed in mice carrying mutations in RXR-alpha (Jenkins et al., 2005), Tcf21 (Acharya et al., 2012), PDGF (Smith et al., 2011), and Flrt2 (Muller et al., 2011). It is generally thought that epicardial detachment in these mutants is due to defects in extracellular matrix composition and EMT processes. Why the epicardium responses differ between mouse and zebrafish is an intriguing question for further investigation.

The zebrafish epicardium as a sentinel for other cardiotoxic compounds

Pericardial edema coupled with an elongated, unlooped heart is a phenotype that is not unique to fish exposed to DLCs. This syndrome has been observed in zebrafish carrying mutations that disrupt the cardiovascular and other systems, as

well as following exposure to a variety of cardiotoxic chemicals (Mitchell et al., 2010; Muto et al., 2011; Pruvot et al., 2012). Based on our results with TCDD, a possible link between these factors and the syndrome of heart malformation and pericardial edema could be effects on epicardium formation. We have made a preliminary test of this idea using valproic acid (VPA), a compound that is not a DLC, yet produces the type of cardiac malformations described for TCDD. VPA is an anticonvulsant known to affect cardiovascular development in zebrafish (Gurvich et al., 2005). Despite critical differences in the mechanism of action, both agents produced an elongated heart with a thin atrium, a compacted ventricle, and failure of epicardium development (Figure 2).

Of particular interest, VPA-exposed zebrafish appeared completely normal until the PE to epicardium transition, in which the cluster of cells forming the PE begins to cross over to the heart to form the epicardium. In VPA-treated zebrafish, there were no signs of pericardial edema during the period from 0 to 72 hpf. While the PE formed in these fish, there was no progression to forming the epicardium. In the ensuing period from ~72 to 120 hpf, during which the epicardial cells would normally envelop the heart, the hearts in the VPA-treated zebrafish became unlooped and elongated. This was accompanied by marked pericardial edema.

While the mechanism remains a mystery, epicardium formation was sensitive to blockade by two compounds with very distinct mechanisms of action. In both cases, the initial patterning of the heart was unaffected, and cardiotoxicity was only manifested at the point at which epicardial cells normally form. It may be that epicardium formation is more sensitive to disruption than other processes needed to

produce a healthy functional heart. If so, the epicardium could be a sentinel for cardiotoxicity.

The epicardium and heart regeneration

Following myocardial infarction (heart attack), the human heart can lose billions of cardiomyocytes, resulting in the loss of a significant portion of myocardium (Reinecke et al., 2008). The damaged myocardium is not replaced with new myocardial cells, but rather healed by formation of non-contractile scar tissue. This inability to replace lost heart tissue with contractile myocardium is critical medical problem (Bolli and Chaudhry, 2010; Malki et al., 2002).

The epicardium has received great interest in the field of regenerative medicine due to the plasticity of epicardial progenitors (reviewed in Gittenberger-de Groot et al., 2012; Riley, 2012; Smart et al., 2012a; Smart et al., 2012b; Smart and Riley, 2012). Furthermore, many reports have identified the epicardium as a critical signaling center following myocardial injury.

Unlike mammals, zebrafish retain the ability to regenerate damaged myocardial tissue into adulthood (Poss et al., 2002). This occurs mainly by differentiation and proliferation of spared resident cardiomyocytes (Jopling et al., 2010; Kikuchi et al., 2010). Following surgical resection of the adult zebrafish ventricle at its apex, profuse bleeding occurs followed by formation of a fibrin-rich blood clot. Subsequently an epicardial-derived white epithelial sheath of tissue migrates and surrounds the newly formed blood clot (Lepilina et al., 2006). The combination of sealing the wound with epithelial-like sheath of tissue, cardiomyocyte

dedifferentiation and proliferation orchestrate regeneration of a new contractile myocardium over a period of 1-2 months.

During heart regeneration in zebrafish, the epicardium is thought to revert to an “embryonic-like” state and act as a signaling center by expressing embryonic genes such as the retinoic acid (RA) synthesizing enzyme, *raldh2* (Choi and Poss, 2012; Lepilina et al., 2006). Expression of *raldh2* in epicardial and endocardial cells during regeneration is thought to secrete trophic RA to assist in cardiomyocyte proliferation. Inhibition of RA signaling during heart regeneration reversed the regenerative capacity by halting cardiomyocyte proliferation (Kikuchi et al., 2011b). While controversy remains regarding the role of the epicardium during heart regeneration, it appears the adult epicardium may play a supportive role by acting as a signaling center to direct differentiation, proliferation and recruitment of cardiac progenitors to the wound site. Thus, embryonic-like epicardial cells may be needed for wound healing in the adult heart.

Once the epicardium has formed, the heart appears to no longer be a target for DLCs in zebrafish, and even when exposed to a lethal concentration of TCDD the adult heart is unaffected (Hofsteen et al., 2013; Lanham et al., 2012). However, as indicated above, embryonic-like epicardial progenitor cells are required for heart wound healing in the adult zebrafish. It is perhaps then not surprising that during wounding, the adult zebrafish regains sensitivity to TCDD. In experiments in which the apex of the adult ventricle were amputated control hearts quickly regenerated the missing tissue, while TCDD-pretreated hearts did not progress past the initial stage of blood clot formation (Hofsteen et al., 2013). TCDD prevented the formation

of the epicardially-derived sheath of tissue that normally envelops the wound, and reduced cardiomyocyte proliferation at the wound site. If TCDD was administered 1 day following surgical amputation, the regenerative capacity was not affected; the epithelial-like sheath of tissue formed and the blood clot was replaced with new contractile myocardium. This suggests that activated epicardial progenitors in the adult partially amputated zebrafish heart are targeted by TCDD.

Conclusions

The epicardium and epicardial progenitors are potentially vital for development, function and regeneration of the vertebrate heart. In zebrafish, the epicardium appears to be sensitive to disruption by xenobiotic chemicals during development, but not once formed. In humans, long-term exposure to TCDD is associated with ischemic heart disease (Bertazzi et al., 1998; Flesch-Janys et al., 1995). It is interesting that other studies of ischemic heart disease have found a reduction in epicardial cell numbers in affected patients (Bertazzi et al., 1998; Di Meglio et al., 2010; Flesch-Janys et al., 1995). We speculate that epicardium development may play an important role in environmentally induced heart disease, worth further study. The zebrafish heart is now being used to screen drug candidates for Q-T prolongation and other forms of cardiotoxicity (Milan et al., 2006; Park et al., 2013; Parng et al., 2002). Due to high throughput screening capability, zebrafish have many advantages in screening for teratogenic effects over other vertebrate models. It may be that the tools available with the zebrafish: transgenic lines that mark the epicardium, translucent external development, and high

fecundity, will make following epicardium development an important screen as well. Thus, we may see future use of epicardium formation as a marker of cardiotoxicity.

ACKNOWLEDGEMENTS

We would like to thank Dorothy Nesbit for technical services and fish husbandry, Andrew Schneider for assisting in procedures with mice, and the entire zebrafish group for helpful discussions.

Supported by the National Institutes of Health (NIH) grant R01 ES012716 from the National Institute of Environmental Health Sciences (NIEHS) and the University of Wisconsin Sea Grant Institute, National Sea Grant College Program, National Oceanic and Atmospheric Administration, U.S. Department of Commerce grant number NA 16RG2257, Sea Grant Project R/BT- 22 and 25.

RESEARCH PROBLEMS TO BE ADDRESSED

It has been known that embryonic-larvae exposure to TCDD results in severe heart malformation in zebrafish. When fish are exposed later in development, juvenile to adult stages, the heart becomes resistant to TCDD (Lanham et al., 2012). This trend overlaps considerably with the temporal window of epicardium development. While we know the heart is a target of embryonic-larvae TCDD exposure, how this toxicity manifests remains a mystery. Thus, the goal of this thesis is to determine how TCDD affects zebrafish heart development by asking the following questions: does TCDD exposure affect epicardium development; If so, what is the molecular mechanism of action; And does TCDD exposure affect other epicardium-dependent events such as adult heart regeneration?

The epicardium plays a crucial role in two distinct growth-like phases of the zebrafish heart: initial heart development and adult heart regeneration. Since TCDD affects embryonic heart development and regeneration of other tissue types in zebrafish, we were curious if TCDD exposure would again be detrimental during heart regeneration. Thus, the aim of Chapter ll is to determine whether TCDD exposure impairs adult zebrafish heart regeneration.

Since TCDD-induced heart malformation manifests during epicardium formation, the aim of Chapter III is to determine if TCDD exposure affects epicardium formation. If so, this could provide mechanistic insight for the peculiar lag in TCDD-induced heart malformation. TCDD activates the AHR/ARNT transcription factor. Thus, cardiotoxicity is secondary to transcriptional changes during heart development and regeneration. The aim of Chapter IV is to identify a

molecular mechanism that results in TCDD-induced heart malformation. A major endpoint of TCDD-induced cardiotoxicity is reduced heart contractility. Furthermore, heart morphology in fish lacking heart contractility resembles that of TCDD-exposed animals. Thus, the aim of Chapter V is to determine the role of heart contractility and epicardium formation. Together, this research will further our understanding of TCDD-induced cardiotoxicity while strengthening our understanding of normal zebrafish epicardium development and heart regeneration.

REFERENCES

Abejie, B.A., Chung, E.H., Nesto, R.W., and Kales, S.N. (2008). Grand rounds: asbestos-related pericarditis in a boiler operator. Environmental health perspectives *116*, 86-89.

Acharya, A., Baek, S.T., Huang, G., Eskiocak, B., Goetsch, S., Sung, C.Y., Banfi, S., Sauer, M.F., Olsen, G.S., Duffield, J.S.*, et al.* (2012). The bHLH transcription factor Tcf21 is required for lineage-specific EMT of cardiac fibroblast progenitors. Development *139*, 2139-2149.

Allison, P., Huang, T., Broka, D., Parker, P., Barnett, J.V., and Camenisch, T.D. (2013). Disruption of canonical TGFbeta-signaling in murine coronary progenitor cells by low level arsenic. Toxicology and applied pharmacology.

Antkiewicz, D.S., Burns, C.G., Carney, S.A., Peterson, R.E., and Heideman, W. (2005). Heart malformation is an early response to TCDD in embryonic zebrafish. Toxicol Sci *84*, 368-377.

Bakkers, J. (2011). Zebrafish as a model to study cardiac development and human cardiac disease. Cardiovasc Res *91*, 279-288.

Belair, C.D., Peterson, R.E., and Heideman, W. (2001). Disruption of erythropoiesis by dioxin in the zebrafish. Dev Dyn *222*, 581-594.

Bertazzi, P.A., Bernucci, I., Brambilla, G., Consonni, D., and Pesatori, A.C. (1998). The Seveso studies on early and long-term effects of dioxin exposure: a review. Environ Health Perspect *106 Suppl 2*, 625-633.

Bolli, P., and Chaudhry, H.W. (2010). Molecular physiology of cardiac regeneration. Ann N Y Acad Sci *1211*, 113-126.

Carney, S.A., Chen, J., Burns, C.G., Xiong, K.M., Peterson, R.E., and Heideman, W. (2006). Aryl hydrocarbon receptor activation produces heart-specific transcriptional and toxic responses in developing zebrafish. Molecular pharmacology *70*, 549-561.

Cheung, M.O., Gilbert, E.F., and Peterson, R.E. (1981). Cardiovascular teratogenicity of 2, 3, 7, 8-tetrachlorodibenzo-p-dioxin in the chick embryo. Toxicology and applied pharmacology *61*, 197-204.

Choi, W.Y., and Poss, K.D. (2012). Cardiac regeneration. Curr Top Dev Biol *100*, 319-344.

Cronk, C.E., Pelech, A.N., Malloy, M.E., and McCarver, D.G. (2004). Excess birth prevalence of Hypoplastic Left Heart syndrome in eastern Wisconsin for birth cohorts 1997-1999. Birth defects research *70*, 114-120.

Di Meglio, F., Castaldo, C., Nurzynska, D., Romano, V., Miraglia, R., and Montagnani, S. (2010). Epicardial cells are missing from the surface of hearts with ischemic cardiomyopathy: a useful clue about the self-renewal potential of the adult human heart? Int J Cardiol *145*, e44-46.

Dong, W., Teraoka, H., Tsujimoto, Y., Stegeman, J.J., and Hiraga, T. (2004). Role of aryl hydrocarbon receptor in mesencephalic circulation failure and apoptosis in zebrafish embryos exposed to 2,3,7,8-tetrachlorodibenzo-p-dioxin. Toxicol Sci *77*, 109-116.

Flesch-Janys, D., Berger, J., Gurn, P., Manz, A., Nagel, S., Waltsgott, H., and Dwyer, J.H. (1995). Exposure to polychlorinated dioxins and furans (PCDD/F) and mortality in a cohort of workers from a herbicide-producing plant in Hamburg, Federal Republic of Germany. Am J Epidemiol *142*, 1165-1175.

Garrity, D.M., Childs, S., and Fishman, M.C. (2002). The heartstrings mutation in zebrafish causes heart/fin Tbx5 deficiency syndrome. Development *129*, 4635-4645.

Gittenberger-de Groot, A.C., Winter, E.M., Bartelings, M.M., Jose Goumans, M., Deruiter, M.C., and Poelmann, R.E. (2012). The arterial and cardiac epicardium in development, disease and repair. Differentiation *84*, 41-53.

Guldner, N.W., Bastian, F., Weigel, G., Zimmermann, H., Maleika, M., Scharfschwerdt, M., Rohde, D., and Sievers, H.H. (2012). Nanocoating with titanium reduces iC3b- and granulocyte-activating immune response against glutaraldehyde-fixed bovine pericardium: a new technique to improve biologic heart valve prosthesis durability? J Thorac Cardiovasc Surg *143*, 1152-1159.

Guldner, N.W., Jasmund, I., Zimmermann, H., Heinlein, M., Girndt, B., Meier, V., Fluss, F., Rohde, D., Gebert, A., and Sievers, H.H. (2009). Detoxification and endothelialization of glutaraldehyde-fixed bovine pericardium with titanium coating: a new technology for cardiovascular tissue engineering. Circulation *119*, 1653-1660.

Gurvich, N., Berman, M.G., Wittner, B.S., Gentleman, R.C., Klein, P.S., and Green, J.B. (2005). Association of valproate-induced teratogenesis with histone deacetylase inhibition in vivo. Faseb J *19*, 1166-1168.

Han, W., Barr, S.C., Pacioretty, L.M., and Gilmour, R.F., Jr. (1997). Restoration of the transient outward potassium current by noradrenaline in chagasic canine epicardium. J Physiol *500 (Pt 1)*, 75-83.

Henry, T.R., Spitsbergen, J.M., Hornung, M.W., Abnet, C.C., and Peterson, R.E. (1997). Early life stage toxicity of 2,3,7,8-tetrachlorodibenzo-p-dioxin in zebrafish (Danio rerio). Toxicology and applied pharmacology *142*, 56-68.

Hill, A.J., Teraoka, H., Heideman, W., and Peterson, R.E. (2005). Zebrafish as a model vertebrate for investigating chemical toxicity. Toxicol Sci *86*, 6-19.

Hofsteen, P., Mehta, V., Kim, M.S., Peterson, R.E., and Heideman, W. (2013). TCDD inhibits heart regeneration in adult zebrafish. Toxicol Sci *132*, 211-221.

Hu, N., Sedmera, D., Yost, H.J., and Clark, E.B. (2000). Structure and function of the developing zebrafish heart. The Anatomical record *260*, 148-157.
Imanishi, S., and Arita, M. (1987). Electrophysiologic properties differ in the ventricular endocardium and epicardium of the Japanese monkey. J Electrocardiol *20*, 185-192.

Incardona, J.P., Linbo, T.L., and Scholz, N.L. (2011). Cardiac toxicity of 5-ring polycyclic aromatic hydrocarbons is differentially dependent on the aryl hydrocarbon receptor 2 isoform during zebrafish development. Toxicology and applied pharmacology *257*, 242-249.

Jenkins, S.J., Hutson, D.R., and Kubalak, S.W. (2005). Analysis of the proepicardium-epicardium transition during the malformation of the RXRalpha-/- epicardium. Dev Dyn *233*, 1091-1101.

Jopling, C., Sleep, E., Raya, M., Marti, M., Raya, A., and Belmonte, J.C. (2010). Zebrafish heart regeneration occurs by cardiomyocyte dedifferentiation and proliferation. Nature *464*, 606-609.

Kharin, S.N., Krandycheva, V.V., Strelkova, M.V., Tsvetkova, A.S., and Shmakov, D.N. (2012). Doxorubicin-induced changes of ventricular repolarization heterogeneity: results of a chronic rat study. Cardiovasc Toxicol *12*, 312-317.

Kikuchi, K., Gupta, V., Wang, J., Holdway, J.E., Wills, A.A., Fang, Y., and Poss, K.D. (2011a). tcf21+ epicardial cells adopt non-myocardial fates during zebrafish heart development and regeneration. Development (Cambridge, England) *138*, 2895-2902.

Kikuchi, K., Holdway, J.E., Major, R.J., Blum, N., Dahn, R.D., Begemann, G., and Poss, K.D. (2011b). Retinoic acid production by endocardium and epicardium is an injury response essential for zebrafish heart regeneration. Developmental cell *20*, 397-404.

Kikuchi, K., Holdway, J.E., Werdich, A.A., Anderson, R.M., Fang, Y., Egnaczyk, G.F., Evans, T., Macrae, C.A., Stainier, D.Y., and Poss, K.D. (2010). Primary contribution to zebrafish heart regeneration by gata4(+) cardiomyocytes. Nature *464*, 601-605.

King-Heiden, T.C., Mehta, V., Xiong, K.M., Lanham, K.A., Antkiewicz, D.S., Ganser, A., Heideman, W., and Peterson, R.E. (2012). Reproductive and developmental toxicity of dioxin in fish. Mol Cell Endocrinol *354*, 121-138.

Kopf, P.G., and Walker, M.K. (2009). Overview of developmental heart defects by dioxins, PCBs, and pesticides. J Environ Sci Health C Environ Carcinog Ecotoxicol Rev *27*, 276-285.

Kopp, R., Schwerte, T., and Pelster, B. (2005). Cardiac performance in the zebrafish breakdance mutant. J Exp Biol *208*, 2123-2134.

Kuehl, K.S., and Loffredo, C.A. (2006). A cluster of hypoplastic left heart malformation in Baltimore, Maryland. Pediatric cardiology *27*, 25-31.

Lanham, K.A., Peterson, R.E., and Heideman, W. (2012). Sensitivity to dioxin decreases as zebrafish mature. Toxicol Sci *127*, 360-370.

Lee, R.K., Stainier, D.Y., Weinstein, B.M., and Fishman, M.C. (1994). Cardiovascular development in the zebrafish. II. Endocardial progenitors are sequestered within the heart field. Development *120*, 3361-3366.
Lefebvre, K.A., Trainer, V.L., and Scholz, N.L. (2004). Morphological abnormalities and sensorimotor deficits in larval fish exposed to dissolved saxitoxin. Aquatic toxicology (Amsterdam, Netherlands) *66*, 159-170.

Lepilina, A., Coon, A.N., Kikuchi, K., Holdway, J.E., Roberts, R.W., Burns, C.G., and Poss, K.D. (2006). A dynamic epicardial injury response supports progenitor cell activity during zebrafish heart regeneration. Cell *127*, 607-619.

Li, X., Ma, Y., Li, D., Gao, X., Li, P., Bai, N., Luo, M., Tan, X., Lu, C., and Ma, X. (2012). Arsenic impairs embryo development via down-regulating Dvr1 expression in zebrafish. Toxicol Lett *212*, 161-168.

Lie-Venema, H., van den Akker, N.M., Bax, N.A., Winter, E.M., Maas, S., Kekarainen, T., Hoeben, R.C., deRuiter, M.C., Poelmann, R.E., and Gittenberger-de Groot, A.C. (2007). Origin, fate, and function of epicardium-derived cells (EPDCs) in normal and abnormal cardiac development. ScientificWorldJournal *7*, 1777-1798.

Lin, C.C., Hui, M.N., and Cheng, S.H. (2007). Toxicity and cardiac effects of carbaryl in early developing zebrafish (Danio rerio) embryos. Toxicology and applied pharmacology *222*, 159-168.

Liu, J., and Stainier, D.Y. (2010). Tbx5 and Bmp signaling are essential for proepicardium specification in zebrafish. Circulation research *106*, 1818-1828.

Lloyd-Jones, D., Adams, R.J., Brown, T.M., Carnethon, M., Dai, S., De Simone, G., Ferguson, T.B., Ford, E., Furie, K., Gillespie, C.*, et al.* (2010). Executive summary: heart disease and stroke statistics--2010 update: a report from the American Heart Association. Circulation *121*, 948-954.

Lukas, A., and Antzelevitch, C. (1993). Differences in the electrophysiological response of canine ventricular epicardium and endocardium to ischemia. Role of the transient outward current. Circulation *88*, 2903-2915.

Malki, Q., Sharma, N.D., Afzal, A., Ananthsubramaniam, K., Abbas, A., Jacobson, G., and Jafri, S. (2002). Clinical presentation, hospital length of stay, and readmission rate in patients with heart failure with preserved and decreased left ventricular systolic function. Clin Cardiol *25*, 149-152.

Manner, J., Perez-Pomares, J.M., Macias, D., and Munoz-Chapuli, R. (2001). The origin, formation and developmental significance of the epicardium: a review. Cells Tissues Organs *169*, 89-103.

Manner, J., Schlueter, J., and Brand, T. (2005). Experimental analyses of the function of the proepicardium using a new microsurgical procedure to induce loss-of-proepicardial-function in chick embryos. Dev Dyn *233*, 1454-1463.

Mehta, V., Peterson, R.E., and Heideman, W. (2008). 2,3,7,8-Tetrachlorodibenzo-p-dioxin Exposure Prevents Cardiac Valve Formation in Developing Zebrafish. Toxicol Sci *104*, 303-311.

Milan, D.J., Jones, I.L., Ellinor, P.T., and MacRae, C.A. (2006). In vivo recording of adult zebrafish electrocardiogram and assessment of drug-induced QT prolongation. Am J Physiol Heart Circ Physiol *291*, H269-273.

Mitchell, I.C., Brown, T.S., Terada, L.S., Amatruda, J.F., and Nwariaku, F.E. (2010). Effect of vascular cadherin knockdown on zebrafish vasculature during development. PLoS One *5*, e8807.

Muller, P.S., Schulz, R., Maretto, S., Costello, I., Srinivas, S., Bikoff, E., and Robertson, E. (2011). The fibronectin leucine-rich repeat transmembrane protein Flrt2 is required in the epicardium to promote heart morphogenesis. Development *138*, 1297-1308.

Muto, A., Calof, A.L., Lander, A.D., and Schilling, T.F. (2011). Multifactorial origins of heart and gut defects in nipbl-deficient zebrafish, a model of Cornelia de Lange Syndrome. PLoS Biol *9*, e1001181.

Neethling, W.M., Glancy, R., and Hodge, A.J. (2010). Mitigation of calcification and cytotoxicity of a glutaraldehyde-preserved bovine pericardial matrix: improved

biocompatibility after extended implantation in the subcutaneous rat model. J Heart Valve Dis *19*, 778-785.

Olivey, H.E., Mundell, N.A., Austin, A.F., and Barnett, J.V. (2006). Transforming growth factor-beta stimulates epithelial-mesenchymal transformation in the proepicardium. Dev Dyn *235*, 50-59.

Pagan-Carlo, L.A., Garcia, L.A., Hutchison, J.L., Buettner, G.R., and Kerber, R.E. (1999). Captopril lowers coronary venous free radical concentration after direct current cardiac shocks. Chest *116*, 484-487.

Park, M.J., Lee, K.R., Shin, D.S., Chun, H.S., Kim, C.H., Ahn, S.H., and Bae, M.A. (2013). Predicted drug-induced bradycardia related cardio toxicity using a zebrafish in vivo model is highly correlated with results from in vitro tests. Toxicol Lett *216*, 9-15.

Parng, C., Seng, W.L., Semino, C., and McGrath, P. (2002). Zebrafish: a preclinical model for drug screening. Assay Drug Dev Technol *1*, 41-48.

Peterson, R.E., Theobald, H.M., and Kimmel, G.L. (1993). Developmental and reproductive toxicity of dioxins and related compounds: cross-species comparisons. Crit Rev Toxicol *23*, 283-335.

Plavicki, J., Hofsteen, P., Peterson, R.E., and Heideman, W. (2013). Dioxin inhibits zebrafish epicardium and proepicardium development. Toxicol Sci *131*, 558-567.

Poss, K.D., Wilson, L.G., and Keating, M.T. (2002). Heart regeneration in zebrafish. Science *298*, 2188-2190.

Pruvot, B., Quiroz, Y., Voncken, A., Jeanray, N., Piot, A., Martial, J.A., and Muller, M. (2012). A panel of biological tests reveals developmental effects of pharmaceutical pollutants on late stage zebrafish embryos. Reprod Toxicol *34*, 568-583.

Reimers, M.J., Flockton, A.R., and Tanguay, R.L. (2004). Ethanol- and acetaldehyde-mediated developmental toxicity in zebrafish. Neurotoxicol Teratol *26*, 769-781.

Reinecke, H., Minami, E., Zhu, W.Z., and Laflamme, M.A. (2008). Cardiogenic differentiation and transdifferentiation of progenitor cells. Circ Res *103*, 1058-1071.

Riley, P.R. (2012). An epicardial floor plan for building and rebuilding the mammalian heart. Curr Top Dev Biol *100*, 233-251.

Sabir, I.N., Li, L.M., Jones, V.J., Goddard, C.A., Grace, A.A., and Huang, C.L. (2008). Criteria for arrhythmogenicity in genetically-modified Langendorff-perfused murine

hearts modelling the congenital long QT syndrome type 3 and the Brugada syndrome. Pflugers Arch *455*, 637-651.

Serluca, F.C. (2008). Development of the proepicardial organ in the zebrafish. Developmental biology *315*, 18-27.

Smart, N., Bollini, S., Dube, K.N., Vieira, J.M., Zhou, B., Riegler, J., Price, A.N., Lythgoe, M.F., Davidson, S., Yellon, D.*, et al.* (2012a). Myocardial regeneration: expanding the repertoire of thymosin beta4 in the ischemic heart. Ann N Y Acad Sci *1269*, 92-101.

Smart, N., Dube, K.N., and Riley, P.R. (2012b). Epicardial progenitor cells in cardiac regeneration and neovascularisation. Vascul Pharmacol.

Smart, N., and Riley, P.R. (2012). The epicardium as a candidate for heart regeneration. Future Cardiol *8*, 53-69.

Smith, C.L., Baek, S.T., Sung, C.Y., and Tallquist, M.D. (2011). Epicardial-derived cell epithelial-to-mesenchymal transition and fate specification require PDGF receptor signaling. Circulation research *108*, e15-26.

Stainier, D.Y. (2001). Zebrafish genetics and vertebrate heart formation. Nat Rev Genet *2*, 39-48.

Stainier, D.Y., Fouquet, B., Chen, J.N., Warren, K.S., Weinstein, B.M., Meiler, S.E., Mohideen, M.A., Neuhauss, S.C., Solnica-Krezel, L., Schier, A.F.*, et al.* (1996). Mutations affecting the formation and function of the cardiovascular system in the zebrafish embryo. Development (Cambridge, England) *123*, 285-292.

Staszewska-Woolley, J., and Woolley, G. (1989). Participation of the kallikrein-kinin-receptor system in reflexes arising from neural afferents in the dog epicardium. J Physiol *419*, 33-44.

Thackaberry, E.A., Jiang, Z., Johnson, C.D., Ramos, K.S., and Walker, M.K. (2005a). Toxicogenomic profile of 2,3,7,8-tetrachlorodibenzo-p-dioxin in the murine fetal heart: modulation of cell cycle and extracellular matrix genes. Toxicol Sci *88*, 231-241.

Thackaberry, E.A., Nunez, B.A., Ivnitski-Steele, I.D., Friggins, M., and Walker, M.K. (2005b). Effect of 2,3,7,8-tetrachlorodibenzo-p-dioxin on murine heart development: alteration in fetal and postnatal cardiac growth, and postnatal cardiac chronotropy. Toxicol Sci *88*, 242-249.

Tsibiribi, P., Bui-Xuan, C., Bui-Xuan, B., Lombard-Bohas, C., Duperret, S., Belkhiria, M., Tabib, A., Maujean, G., Descotes, J., and Timour, Q. (2006). Cardiac lesions induced by 5-fluorouracil in the rabbit. Hum Exp Toxicol *25*, 305-309.

Tu, W., Niu, L., Liu, W., and Xu, C. (2013). Embryonic exposure to butachlor in zebrafish (Danio rerio): endocrine disruption, developmental toxicity and immunotoxicity. Ecotoxicol Environ Saf *89*, 189-195.

Valesio, E.G., Zhang, H., and Zhang, C. (2013). Exposure to the JNK inhibitor SP600125 (anthrapyrazolone) during early zebrafish development results in morphological defects. J Appl Toxicol *33*, 32-40.

Wells, P., and Pinder, A. (1996). The respiratory development of Atlantic salmon. II. Partitioning of oxygen uptake among gills, yolk sac and body surfaces. J Exp Biol *199*, 2737-2744.

Yeh, E.T., Tong, A.T., Lenihan, D.J., Yusuf, S.W., Swafford, J., Champion, C., Durand, J.B., Gibbs, H., Zafarmand, A.A., and Ewer, M.S. (2004). Cardiovascular complications of cancer therapy: diagnosis, pathogenesis, and management. Circulation *109*, 3122-3131.

Zodrow, J.M., and Tanguay, R.L. (2003). 2,3,7,8-tetrachlorodibenzo-p-dioxin inhibits zebrafish caudal fin regeneration. Toxicol Sci *76*, 151-161.

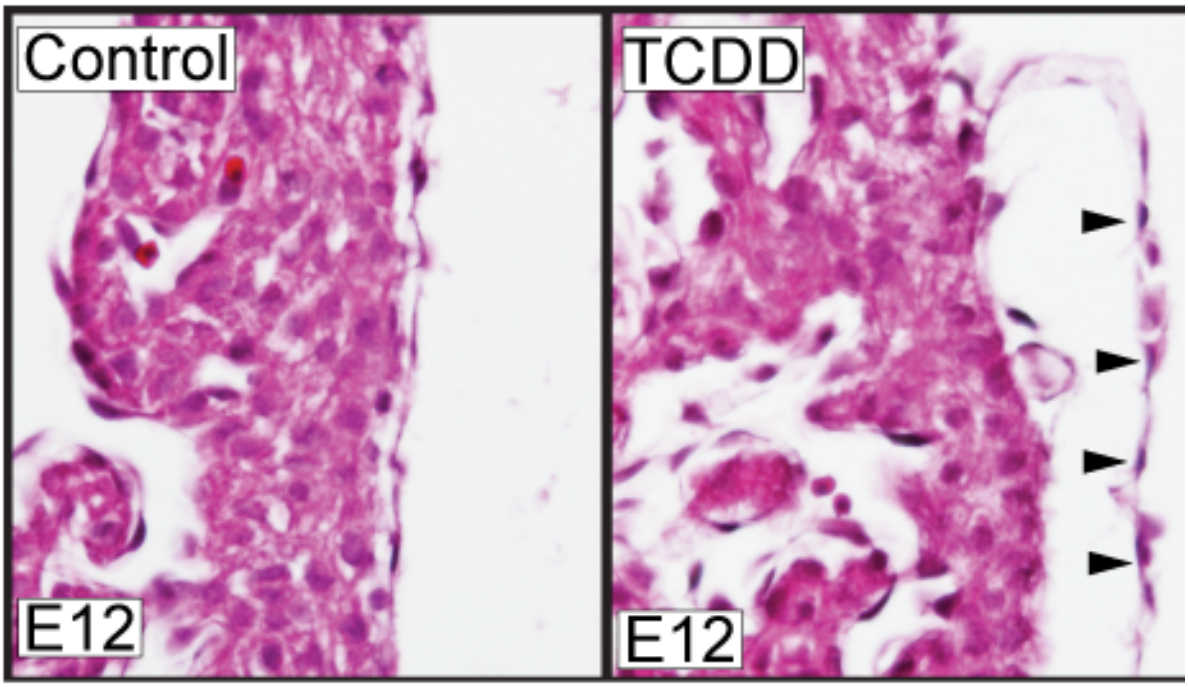

Figure 1. TCDD exposure causes epicardium detachment from the underlying myocardium in developing mice. Murine dams were exposed to vehicle control (corn oil) or TCDD (5 ug/g) at E7 and embryos were collected at E12 for sectional hematoxylin and eosin staining (n=3/ group). Shown are representative sections of control and TCDD hearts at the epicardium. Black arrows denote epicardial cells and their detachment from myocardium.

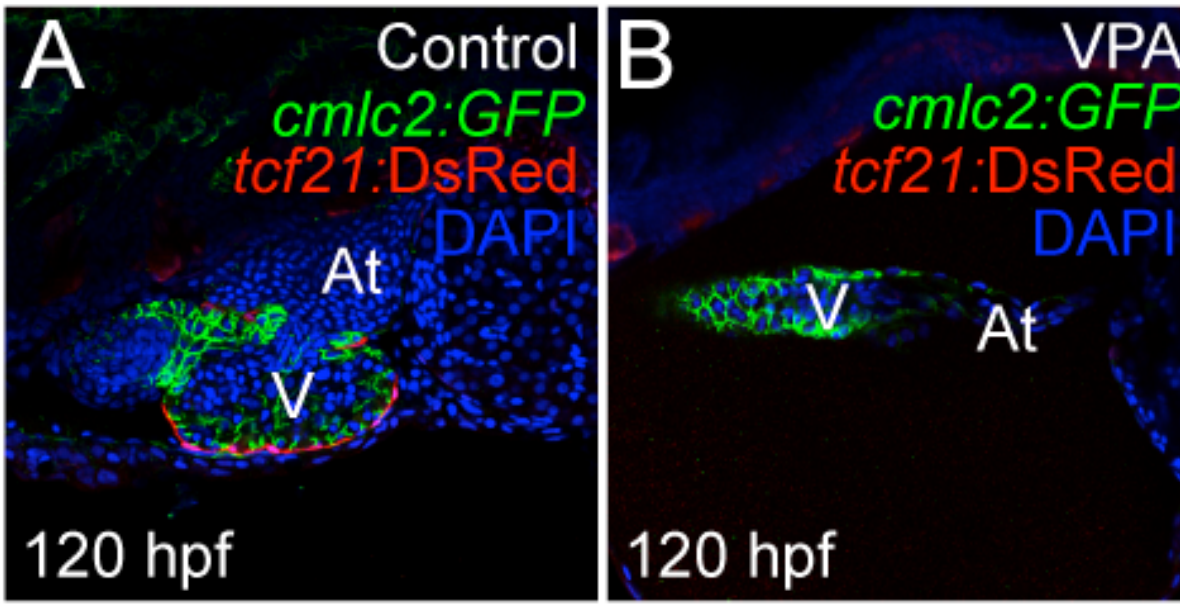

Figure 2. VPA exposed zebrafish larvae lack epicardium. Embryos from a zebrafish epicardial reporter line (*tcf21:DsRed*; (Kikuchi et al., 2011a) were exposed to VPA (0.06 mM; B), or vehicle (EtOH, 0.06mM; A) shortly following fertilization. The control is shown at left, while the VPA heart is shown at right. The presence or absence of epicardium was assessed with immunohistochemistry at 120 hours post fertilization using an antibody against *DsRed*, expressed in epicardial cells (Red). Cell nuclei are stained with DAPI shown as blue. Cytoplasmic *cmlc2:GFP* shown as green outlines the cardiomyocytes. Representative single plane confocal microscopy images (n=6/group) are shown with anterior to the left (V = ventricle, At = atrium).

CHAPTER II

TCDD Inhibits Heart Regeneration in Adult Zebrafish

Peter Hofsteen[§], Vatsal Mehta[§], Min-Sik Kim, Richard E. Peterson,

and Warren Heideman

Toxicological Sciences (2013) **132(1)**, 211-221.

[§] Authors contributed equally

ABSTRACT

Normal adult zebrafish can completely regenerate lost myocardium following partial amputation of the ventricle apex. We report that 2,3,7,8-tetrachlorodibenzo-*p*-dioxin (TCDD) significantly impairs this regeneration. Adult male zebrafish were injected with vehicle (control) or TCDD (70 ng/g, ip) one day prior to partial amputation of the ventricle apex. Gross observation and histological analysis of the amputated heart at 21 days post amputation (dpa) revealed that TCDD-exposed fish had not progressed beyond the initial clot formation stage, while the vehicle control fish showed substantial recovery and almost complete resolution of the formed clot. In contrast, hearts that were not surgically wounded showed no signs of TCDD-toxicity. Striking features in the TCDD-exposed hearts were the absence of the normal sheath of new tissue enveloping the wound, and the absence of intense cell proliferation at the site of the wound. In addition, the patterns of collagen deposition at the wound site were different between the TCDD and vehicle groups. Because the receptor for TCDD is the AHR ligand-activated transcriptional regulator, we examined the effects of TCDD exposure on gene expression in the ventricle using DNA microarrays. Samples were collected just prior to amputation and at 6 h and 7 d post amputation. TCDD-pretreated hearts had dysregulated expression of genes involved in heart function, tissue regeneration, cell growth, and extracellular matrix. Because embryonic, but not adult, hearts are major targets for TCDD-induced cardiotoxicity, we speculate that the need for embryonic-like cells in regeneration is connected with the effects of TCDD in inhibiting the response to wounding.

INTRODUCTION

The heart is a target for 2,3,7,8-tetrachlorodibenzo-*p*-dioxin (TCDD) toxicity in a number of vertebrate species, including humans (Dalton et al., 2001; Pesatori et al., 1998), non-human primates (Allen et al., 1977), rodents (Thackaberry et al., 2005), birds (Ivnitski et al., 2001) and fish (Carney et al., 2006a; Peterson et al., 1993). In zebrafish (*Danio rerio*), TCDD exposure during the first few days of development causes pericardial edema, decreased cardiomyocyte number, cardiac valve malformation, reduced cardiac output, altered looping, and ventricular standstill (Antkiewicz et al., 2005; Carney et al., 2006a; Henry et al., 1997; Mehta et al., 2008). While the newly formed zebrafish heart is exquisitely sensitive to TCDD toxicity, this sensitivity disappears with development, until at the end of the larval stage the heart is no longer sensitive to a lethal TCDD exposure (Lanham et al., 2012).

In addition to being a model system for studying cardiotoxicity, the zebrafish heart has been the subject of intense interest because of its ability to regenerate myocardium after surgical removal of part of the ventricle (Chablais et al., 2011; Poss et al., 2002; Wang et al., 2011). Damage of human ventricular myocardium is common in response to myocardial infarction; however, unlike adult zebrafish, humans are unable to regenerate the damaged cardiac muscle.

Following partial surgical amputation of a portion of the adult zebrafish ventricle, a fibrin-rich blood clot is formed. Shortly thereafter, cells proliferate and migrate towards the wound site to form a cluster of cardiac progenitor cells (Jopling et al., 2010; Kikuchi et al., 2011; Kikuchi et al., 2010; Lepilina et al., 2006; Poss et al.,

2002; Schnabel et al., 2011). The regenerating tissue goes through a process of sealing the wound, recruitment of cells, differentiation, and organization to eventually form new contractile myocardium that can hardly be distinguished from the original.

During zebrafish heart regeneration, the regenerating heart is sometimes said to become “embryonic-like” because genes normally expressed during heart development are found expressed in cells along the outer most layer of the heart, the epicardium (Lepilina et al., 2006; Poss et al., 2002). Among these genes is *raldh2*, encoding a key enzyme in the synthesis of retinoic acid (RA). The expression of *raldh2* is thought to provide a source of RA that assists cardiomyocyte proliferation (Kikuchi et al., 2011; Lepilina et al., 2006).

Knowing that TCDD is toxic to embryonic but not adult hearts, and that the response to wounding in the adult heart involves the dedifferentiation of cells to an embryonic-like state, we wondered if TCDD exposure would have an impact on the ventricular response to surgical resection. This idea is strengthened by the knowledge that TCDD exposure blocks regeneration of the rat liver (Bauman et al., 1995; Mitchell et al., 2006), and the zebrafish fin (Zodrow and Tanguay, 2003). Here we report that pre-exposure to TCDD does indeed inhibit regeneration of the heart muscle. TCDD prevents the intense proliferation of cells around the wound site and also alters the pattern of gene expression induced by wounding at the ventricle. We speculate that TCDD exposure inhibits a process that is important for progenitor cells needed for both early heart development and regeneration.

MATERIALS and METHODS

Zebrafish. Adult male zebrafish (AB strain) were housed in 38 L glass aquaria with recirculating reverse osmosis water, supplemented with Instant Ocean salts (60 mg/L; Aquarium Systems, Mentor, OH). Density of fish in the aquaria did not exceed 20 fish / tank. Water was filtered through biofilter media, activated charcoal, sterilized by ultraviolet light, and maintained at 25-27 °C with a 14h / 10h light / dark cycle. Fish were fed TetraMin Tropical flakes (Tetra Holding, Blacksburg, VA) and powdered brine shrimp flakes (Aquatic Eco-Systems Inc., Apopka, FL) twice daily. Fish were anesthetized by waterborne exposure to tricaine (160 mg/L; MS 222, Sigma) or euthanized by tricaine overdose.

TCDD treatment. TCDD dosing solutions were prepared as previously described (Walker and Peterson, 1991; Zodrow and Tanguay, 2003). Briefly, TCDD (>99% purity, Chemsyn, Lenexa, KS) dissolved in 1,4-dioxane was added to chicken egg yolk phosphatidylcholine (PC; >99% purity, Avanti Polar Lipids, Alabaster, AL). The mixture was evaporated using Argon gas to dryness, resuspended in 0.9% NaCl, and sonicated to form liposomes. The mole fraction of TCDD to PC did not exceed 0.6 nmol TCDD/ 0.1 mmol PC. The same procedure was followed for formulating the PC liposomes without TCDD as the vehicle control. Liposomes were stored under argon at 4°C and used within 1 week. Adult male zebrafish were anesthetized, weighed, and placed in a wet sponge. TCDD (70 ng/g) or vehicle (3.5 μl/g PC) was administered via intra-peritoneal (i.p.) injection with a 30-gauge needle and a gas tight Luer tip 10 μL Hamilton syringe (Hamilton Company, Reno, Nevada) (Zodrow et al., 2004). The amount of TCDD emulsion injected was matched with the fish weight

to produce the 70 ng/g dose. For controls, the amount of emulsion was calculated by weight using the same method as for the TCDD-injected fish, but the emulsion injected contained no TCDD.

Since TCDD is known to inhibit adult zebrafish fin regeneration, we removed a small portion at the margin of the caudal fin and monitored fin regeneration as a positive control for TCDD effect. Signs of regeneration were visually observed and recorded as notebook entries: the vehicle control fish consistently showed signs of fin regeneration; all of the TCDD-treated fish showed the halted blastema at the wound site as previously reported (Zodrow and Tanguay, 2003).

Surgery. The surgical procedures followed the descriptions from Poss and colleagues (Poss et al., 2002). Adult zebrafish were anesthetized and placed ventral side up on a sponge. The heart was exposed using a lateral incision along the ventral chest cavity, the ventricle apex was grasped with forceps, and approximately 20% of the ventricle was snipped away from the apex. Hearts were blotted to stop bleeding and the fish were returned to a recovery tank. Gills were ventilated with fresh water to stimulate recovery, and once swimming normally, fish were returned to the home tank and monitored daily. Fish that did not promptly resume swimming were euthanized by an overdose of Tricaine. Sham controls were exposed to vehicle or TCDD, and a lateral incision along the ventral chest cavity was made to expose the heart, but the ventricle apex was not clipped. All procedures were approved by the University of Wisconsin Institutional Animal Care and Use Committee.

Heart Morphology examination. Hearts were collected at the indicated times by dissection of terminally anesthetized fish. Hearts were placed in phosphate buffered saline (PBS, Cellgro) and photographed with an Optronics MicroFire camera mounted onto a Leica MZ16 stereomicroscope. For 7, 14, 21 dpa vehicle hearts *n* is 10, 18, and 23 respectively for vehicle control and *n* = 11, 17, 16 respectively for TCDD-treated fish. Each experiment was repeated at least 4 times.

In some cases, hearts were fixed overnight in 4% paraformaldehyde (PFA) at 4°C, embedded in paraffin, cut at 10-µm sections, and stained with either H&E (n = 5) or acid fuchsin orange G (AFOG; n= 8) as previously described (Poss et al., 2002). Each experiment was repeated 3 times.

BrdU Staining. Zebrafish were anesthetized for IP injection of bromodeoxyuridine (BrdU; 12.5mg/ml Hanks buffer, 10 µl/fish) on 6 dpa. Hearts were collected at 7 dpa, placed in PBS and fixed overnight in 4% PFA. The following day fixed heart samples were rinsed in PBS containing 0.1% Tween-20 (PBST), embedded, and vibratome sectioned (Vezina et al., 2008). Sections were collagenase digested and stained with a mouse monoclonal anti BrdU IgG1 (Santa Cruz Biotechnology, Santa Cruz, CA) and Alexa fluor secondary antibody (Invitrogen, Carlsbad, CA). Heart sections were counterstained with rhodadmine phalloidin (Invitrogen) to outline cardiac cells (Beis et al., 2005). Sections (*n* = 6 individual fish for each treatment) were visualized using a Nikon C1 Laser Scanning Confocal microscope.

In-situ hybridization. Hearts were removed and fixed overnight in 4% PFA. The following day hearts were washed in PBS, dehydrated to methanol and stored at -20°C until needed. Prior to sectioning, hearts were rehydrated into PBS-Tween

(PBST; 0.1%), and infiltrated with 30% sucrose in PBST before embedding in Tissue-Tek® O.C.T. Compound for Cryostat Sectioning. Heart sections (10 μm) were stored on slides at -80°C until needed. *In situ* hybridization was conducted as previously described (Thisse et al., 1993).

Riboprobe synthesis and detection. A 572-bp *raldh2* fragment was amplified from embryonic zebrafish cDNA and subcloned into pCRII-TOPO (Invitrogen Corporation, Carlsbad, CA). Primers positions were + 505 to + 1076 of Reference Sequence ID NM_131850 and were: 5'- ttc acc ctc acc aga cat gag -3' and 5'-ctt tga ccc aac cac tga aca -3'. Constructs were confirmed by sequencing. An antisense RNA probe was made with T7 RNA polymerase using vector linearized using *BamHI*, and was labelled using digoxigenin-UTP for probing with anti-digoxigenin-AP Fab fragments (Roche Applied Science, Indianapolis, IN) with BM purple (Roche). Hybridization was carried out at 60°. Images were photographed with an Optronics MicroFire camera mounted onto a Leica MZ16 stereomicroscope.

Quantitative RT-PCR. RNA was isolated from ventricular tissue (RNeasy, QIAGEN, Valencia, CA) and cDNA was synthesized from RNA using oligo(dT) primers (SuperScript II RT cDNA synthesis kit; Invitrogen). The qRT-PCR was performed on a Lightcycler (Roche Molecular Biochemicals, Indianapolis, IN) with a FastStart SYBR Green I kit (Roche, Indianapolis, IN) and quantification was based on standard curve analysis. The *raldh2* signal from each sample was normalized to a parallel measurement of *b-actin* mRNA to produce a final measurement on an arbitrary scale. Significant differences (arbitrarily set at $p \leq 0.05$) between control and TCDD treatment groups were determined by either Levene's or Student's t-test

using Statistica 7.0 software (StatSoft, Inc., Tulsa, OK). Results are presented as the mean ± SEM, with n = 6 independent experiments isolating tissue samples, and triplicate qRT-PCR measurements for each tissue sample. The effectiveness and specificity of each gene-specific amplicon was confirmed by agarose gel electrophoresis. Oligonucleotides (IDT; Coralville, IA) for qRT-PCR were: *b-actin*: forward, 5'-aag cag gag tac gat gag tc-3'; reverse, 5'-tgg agt cct cag atg cat tg-3'; *raldh2*: forward, 5'-atc caa gaa gca gca gga aa-3'; reverse 5'-gag gtc cgt gtt cag tgg tt-3'.

Microarrays. Ventricle apex samples were collected and stored at -80° in RNAlater (QIAGEN, Valencia, CA). RNA was isolated using QIAGEN RNeasy Micro Kit (QIAGEN, Valencia, CA), and cRNA amplification and hybridization was conducted using an Affymetrix GeneChip® 3' IVT Express Kit (Affymetrix, Santa Clara, CA) according to the manufacturer's instructions. Two independent biological replicate experiments were run for each condition.

Analysis of microarray data was adapted from the methods of Gould *et al.* (2006). The raw data (.CEL files) were normalized by RMA algorithm using the ExpressionFileCreator module of GenePattern software. Differences in gene expression produced by partial amputation and TCDD exposure were determined using the comparative selection marker module of GenePattern. Cutoffs for statistical significance were a Benjamini-Hochberg corrected False Discovery Rate (FDR) ≤ 0.1 and a minimum fold change ≥ 2. To compare the change in gene expression induced by partial heart amputation in vehicle control or TCDD treatment groups, the log2 values were calculated and were compared to their respective

unamputated 0 hpa samples (e.g. vehicle 6 hpa to vehicle 0 hpa and TCDD 6 hpa to TCDD 0 hpa). The raw data is stored in the Gene Expression Omnibus (GEO) of the National Center for Biotechnology Information (NCBI; http://www.ncbi.nlm.nih.gov/geo/; series record #GSE33981).

RESULTS

TCDD inhibits heart ventricle regeneration

To test the hypothesis that TCDD inhibits regeneration of the adult zebrafish heart ventricle, we treated fish with TCDD or vehicle one day prior to surgery as described in the Methods. Most of our experiments with embryos have used waterborne exposures; however, a substantial body of work studying the effects of TCDD on fin regeneration has established a dosing regimen using TCDD in a phosphatidylcholine emulsion injected into the peritoneum of adult fish. This has the advantage of reproducible delivery of a known dose, and we followed this established protocol (Zodrow et al., 2004). For the surgery, a small thoracic incision was made and a small portion (~20%) of the ventricle at the apex was snipped away with scissors (Poss et al., 2002). After bleeding was controlled, each fish was returned to aquarium water for recovery and sacrificed later for heart collection.

Normal regeneration was characterized by the formation of a blood clot at the amputation plane. The clot was then encased by a pale-white sheet of regenerating tissue (Figure 1; vehicle). This sheet initially includes rapidly dividing epicardial cells. As time progresses a new heart field is thought to form in which dedifferentiated cardiomyocytes replace the lost muscle cells (Lepilina et al., 2006). By 21 dpa, the vehicle control heart had recovered to the point that it was nearly indistinguishable

from a normal unamputated heart. The blood clot formed in response to wounding had been largely resorbed.

In striking contrast, TCDD-treated hearts did not show signs of regeneration other than the formation of the blood clot that initially seals the wound. During the 3-week period following surgery, this clot did not regress and the normal encompassing white sheath of tissue did not form (Figure 1; TCDD). This result indicates that TCDD exposure inhibits myocardial regeneration.

We found no evidence that the failure to regenerate was due to overt cardiotoxicity. On the contrary, we were unable to detect any effect of TCDD on hearts from TCDD-exposed sham controls (Figure 2). In this case, the TCDD-treated hearts were indistinguishable from vehicle controls. The hearts appeared normal despite the fact that the fish were exposed to a high dose of TCDD. At 3-4 weeks post dosing these fish showed signs of toxicity such as hyper-pigmentation, fin degeneration, and wasting; nonetheless, the hearts in these fish remained normal in appearance. This is consistent with results with juvenile zebrafish in which the hearts remained normal a month after receiving what is ultimately a lethal dose of TCDD (Lanham et al., 2012). Therefore, we conclude that while the adult heart is normally insensitive to TCDD, the regenerative process is TCDD-sensitive.

We did notice that for both the amputated and sham operated hearts, the pericardium was affected by TCDD exposure. Upon dissection we found that the pericardial layer had become sticky, and compared to the vehicle control fish, there was very little fluid in the pericardium surrounding the heart.

To obtain a closer look at the effects of TCDD on heart regeneration we sectioned the hearts for H&E staining. Microscopic examination showed that both vehicle and TCDD-exposed hearts had similar trabeculation and structure in the area not affected by the wound (Figure 3). In contrast there were distinct differences at the wound sites. As before, hearts that were not wounded did not appear affected by TCDD (Figure 3).

The vehicle control hearts showed extensive regeneration at the wound site: minimal residual blood clot remained at the amputation plane, and distinct myocardial and epicardial layers had closed together to repair the wound (Figure 3). The TCDD-treated hearts showed a striking lack of repair. The remaining blood clot was especially evident.

At 21 dpa only 5% of the control fish had a prominent blood clot, while 69% of the TCDD-treated fish showed a prominent blood clot with no visible signs of resolution or tissue repair ($p<0.02$). None of the TCDD-treated hearts had undergone the degree of clot resolution typical in the control hearts.

TCDD reduces cell proliferation

Zebrafish heart regeneration involves migration and intense proliferation of cells around the wound site (Poss et al., 2002). Because TCDD produces such a distinct halt in heart ventricle regeneration, we expected that this increased proliferation of cells needed to repair the wound might also be blocked. To test this, we used BrdU incorporation to measure cardiomyocyte proliferation in amputated hearts at 7 dpa. As expected, cells in the control hearts displayed extensive BrdU incorporation, concentrated at the margin of the wound, with a few BrdU-positive

cells scattered in the unwounded region of the heart (Figure 4). In contrast, TCDD hearts lacked BrdU-positive cells concentrated at the wound site.

We consistently observed small groups or individual cells proliferating at the surface of the heart away from the site of the wound. These can be seen in Figure 4 as individual BrdU-positive cells along the left edge of the TCDD-exposed heart. These cells did not appear to be affected by TCDD, and were observed at roughly equal frequency in TCDD and DMSO control hearts. We also sometimes observed small groups of proliferating cells at the edge of the wound in TCDD-treated hearts; however, this was inconsistent and not unambiguously linked to the region of the wound. For example the cluster of BrdU-positive cells at the right of the TCDD panel in Figure 4 appears to be more closely associated with the atrium than the edge of the wound.

TCDD alters the pattern of collagen deposition at the wound

Collagen deposition is required for normal wound repair. The pattern of collagen can be observed by AFOG staining in which the collagen shows as blue, and fibrin attracts the orange-red dye. We found that the vehicle control and TCDD-exposed hearts showed very different AFOG staining patterns at the wound site at 21 dpa (Figure 5). The control heart showed a layer of blue, indicative of collagen matrix, across the regenerating wound. Between this layer and the regenerating heart cells were the remains of the original clot, mostly resorbed. The TCDD-exposed hearts consistently showed the massive original clot, apparently unresorbed, with collagen deposition throughout the clot, with concentrated

deposition in some regions of the clot. In contrast to the control, this staining did not reveal an organized sheet across the resorbing clot.

***Raldh2* is upregulated in TCDD-treated amputated hearts**

During zebrafish heart regeneration, the RA synthesis enzyme, *raldh2* is expressed in epicardial and endocardial cells shortly after heart amputation (Kikuchi et al., 2011; Lepilina et al., 2006). Thus, we wanted to determine whether TCDD misregulates *raldh2* expression as the heart responds to amputation. To do this we used *in situ* hybridization and qRT-PCR to measure *raldh2* expression in TCDD and vehicle control amputated hearts.

At 7 dpa *raldh2* expression was highest in regions at or near the amputation plane (Figure 6). In the TCDD samples, *raldh2* was expressed more broadly, especially along portion of the epicardium distant from the wound boundary. In the controls, *raldh2* was intensely expressed in cells at the wound plane, while in the TCDD-exposed hearts the expression was far less restricted, and the wound plane did not stand out as the region of highest expression.

Our *in situ* hybridization experiments consistently showed an overall pattern of increased *raldh2* expression in the TCDD samples compared to the vehicle controls. We used qRT-PCR to more precisely measure differences in *raldh2* abundance between TCDD-exposed and control ventricles. For these experiments we removed the ventricles and sectioned them with a scalpel along a plane running parallel to the original wound. This yielded two samples: the tissue immediately adjacent to the wound, including the wounded region itself (apex); and samples

comprising the remainder of the ventricle, farther away from the wound site (upper). TCDD increased *raldh2* expression in both samples (Figure 6B; p≤0.05).

The timing of TCDD exposure is critical in halting heart ventricle regeneration

TCDD must disrupt some process critical to heart regeneration. The persistence of the initial clot with little sign of wound resolution suggests that TCDD might alter events occurring early in the regenerative process. To better understand when TCDD acts, we exposed zebrafish to TCDD at -1, +1 and +4 days relative to the amputation event, with the day of amputation considered day 0. Hearts were then examined at 14 dpa for signs of regeneration (Figure 7).

As expected, fish exposed to TCDD at day -1 appeared similar to those shown in Figure 1. Control hearts displayed a pale sheet of cells surrounding the resolving blood clot, indicating regeneration. TCDD-treated hearts lacked this white epithelial-like layer and displayed a persistent blood clot.

When fish were exposed to TCDD at day +1 or +4, the hearts showed normal regeneration. These TCDD-exposed hearts displayed normal blood clot regression and presence of an encasing sheath. These results show that TCDD must be present prior to +1 dpa to halt regeneration of the heart ventricle. These results suggest that TCDD does not block the progression of heart ventricle regeneration, but instead inhibits a process needed to set regeneration into motion.

Transcript changes in TCDD-treated zebrafish hearts

Because TCDD activates the AHR/ARNT transcription factor, we suspect that TCDD acts by altering the abundance of specific transcripts. We used microarray experiments to identify transcripts altered by amputation in control and TCDD-

treated heart tissue. For these experiments, we collected mRNA from ventricles dissected to capture tissue towards the apex, representing the site of the wound. For our comparisons we collected samples from ventricles at several different time points. In each case, the fish were injected with either TCDD or the vehicle as a control. Using the time of amputation as time = 0, the injections were at day -1.

The first set of samples collected were the ventricle apexes from TCDD and vehicle-treated fish at 0 hours post amputation (hpa). These fish were injected the day before and were not amputated, but instead were sham operated immediately before heart tissue collection. We collected these 0 hpa samples to understand how TCDD injection altered the state of the tissue before it was wounded.

The second set of samples collected were from fish treated as described above with either TCDD or vehicle at -1 dpa, amputated at time 0, and collected 6 hours after amputation (6 hpa). These were collected to assess mRNA changes soon after amputation.

The final set was at 7 dpa. These fish were treated as above and at 7 dpa, hearts were removed and ventricle tissue was collected for RNA isolation. These samples were used to assess transcriptome differences between cells in a regenerating heart and those in one prevented from healing by TCDD.

Our general approach in making comparisons was to use filters described in the Methods to identify altered transcripts. Our arbitrary cutoffs were a Benjamini-Hochberg corrected False Discovery Rate of ≤ 0.1 and a minimum fold-change ≥ 2. Several types of comparisons were made. One of these was comparing the transcripts between TCDD-treated and vehicle control samples collected at time 0.

This shows the effect of TCDD on the state of the ventricle at the time of amputation. Data from this comparison is shown in Supplemental Table S1. Comparison of the 0 hpa transcripts from the vehicle and TCDD-treated hearts shows how TCDD affected the transcriptional state of the cells prior to amputation. We found that exposure to TCDD induced 22 genes by ≥ 2 fold. Interestingly, no genes were significantly repressed following TCDD treatment. As would be expected, genes normally induced by TCDD including *cyp1a, cyp1c1, tiparp* and *ahr2* were induced. The remaining genes were generally regulators of transcription, but did not share any noticeable common function.

We also compared how TCDD altered the transcriptional response to amputation. Transcripts from control and TCDD amputated hearts were compared with their respective 0 hpa baseline samples. At 6 hpa, amputation altered 652 transcripts in the control ventricles, and 718 in the TCDD-treated ventricles. Taken together this produced a total of 817 transcripts in two sets overlapping by 553 transcripts. These transcripts and their responses to amputation are presented in Supplemental Table S2.

Figure 8A provides a graphical view of the 6 hpa results. This figure plots the total of 817 transcripts changed 2-fold or more by amputation in either the control or TCDD samples. In this figure each of the transcripts is represented by a small square. The position on the X-axis represents the fold-change produced by amputation in the vehicle control samples. The position on the Y-axis represents how the transcript was affected by amputation in the TCDD-treated hearts. Fold-change is plotted on a log2 scale, and in both cases the 6 hpa samples were compared to their respective

0 hpa baselines. Since each point represents a transcript that was altered by at least 2-fold in at least one of the conditions, there is an empty square in the middle of the plot, delineating absolute value 1. This represents the log2 value of a 2-fold change.

Most of the transcripts fall close to a diagonal line passing through the origin with a slope of 1. For these transcripts, the fold-change caused by amputation in the control was roughly equal to the fold change in the TCDD-treated samples.

The two diagonal lines on the plot have slopes of 0.5 and 2. Points falling between these lines have X and Y values that are within 2-fold of each other: their responses under the 2 conditions might be considered similar. Points above or below these lines have X and Y values that differ from each other by more than 2-fold. We considered these to be altered by TCDD. Of the 817 transcripts on the plot, 26 were expressed at least 2-fold more in the presence of TCDD than in the control, and 80 were expressed at least 2-fold less in the TCDD group than in the control. These transcripts are listed in Supplemental Table S3. The genes induced more in amputation when TCDD are associated with a range of biological processes, with signal transduction being perhaps the most represented. Among the genes whose response to amputation was dampened by TCDD, we found that cell adhesion, basement membrane production, and metalloproteinases were well represented. In addition both *gata1* and *gata5* were downregulated. These latter genes are involved in cell fate determination in heart and blood.

By 7 dpa, the pattern of TCDD effects on transcript abundance was more complex, perhaps reflecting responses in TCDD-exposed tissue failing to undergo

normal wound regeneration. A total of 731 transcripts were altered by at least 2-fold by amputation in the control hearts, while 753 transcripts were altered in the TCDD group, for a total of 914 transcripts changed by amputation with 570 transcripts overlapping between the groups. These genes are listed with their fold responses in Supplementary Table S4.

Figure 8B is a plot of the 7 dpa data following the methods used for the 6 hpa data in Figure 8A. This compares the responses for all 914 transcripts altered by amputation in either the TCDD or control samples at 7 dpa. We found 106 of the transcripts were expressed at least 2-fold more in the presence of TCDD than in the control samples, and 69 transcripts expressed at least 2-fold less in the TCDD group than in the controls. Among the induced genes were a wide variety of genes, but those involved in cell adhesion and production of connective fibers are well represented, with keratins and *epcam* near the top of the list. The list of genes repressed more in the TCDD samples contains genes associated with immune function and blood clotting (Supplementary Table S5).

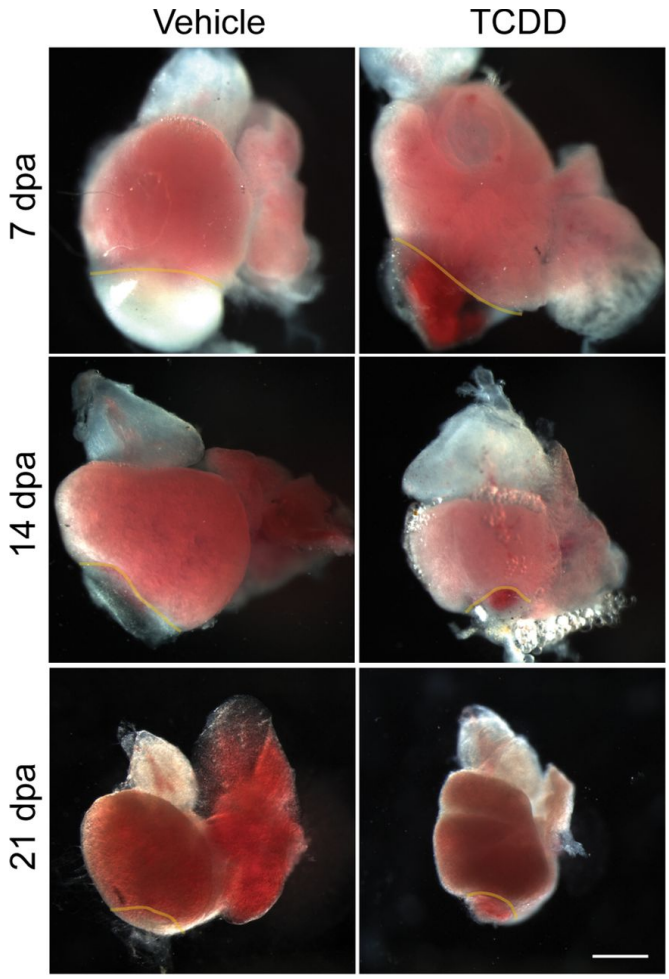

Figure 1. Exposure to TCDD inhibits the regenerative response in the adult zebrafish heart ventricle. Adult male zebrafish were exposed to TCDD or vehicle and the ventricle was amputated the following day as described in the Methods. Hearts were removed at 7, 14, and 21 dpa and photographed. In all cases, the atrium is positioned right of the ventricle, while the bulbus arteriosus is positioned above the ventricle. The translucent yellow line indicates the approximate position of the original amputation plane. The scale bar corresponds to 50 μm. dpa = days post amputation.

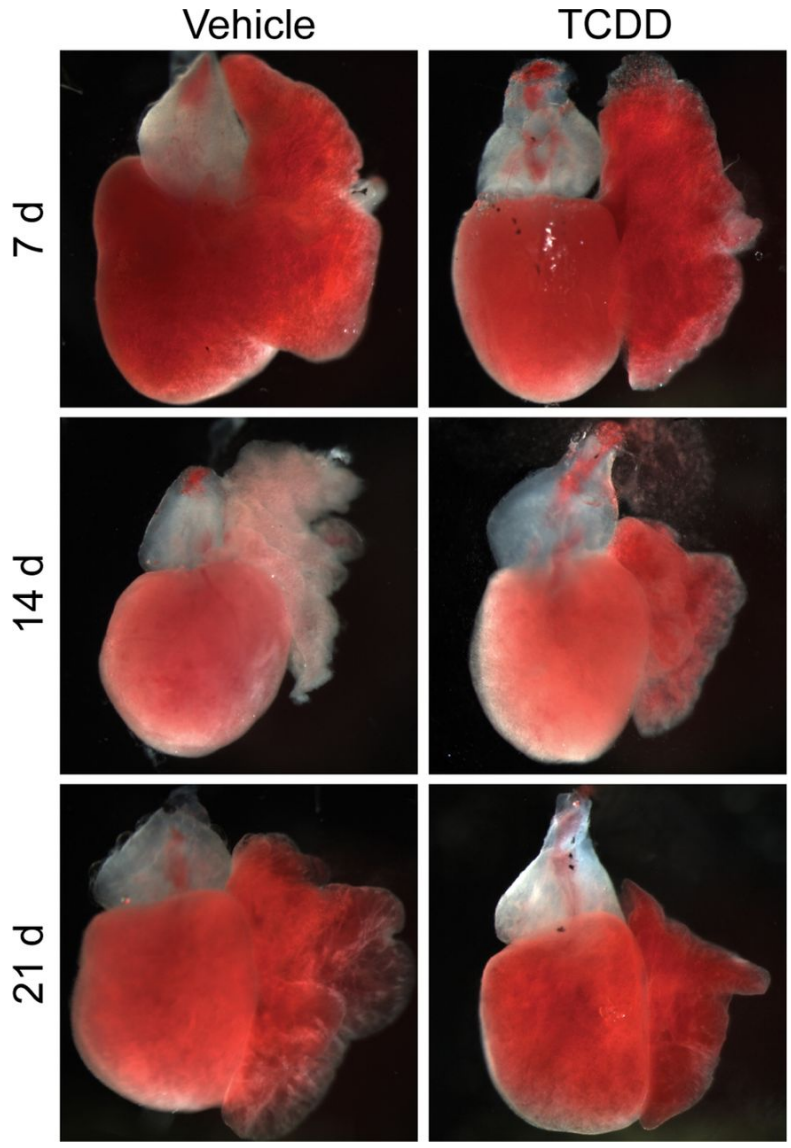

Figure 2. TCDD exposure has no apparent effect on unwounded hearts. Sham operated adult male zebrafish were exposed to TCDD or vehicle just as described in Figure 1 and collected at 7, 14, and 21 days. The scale bar corresponds to 50 μm. d= days post dose.

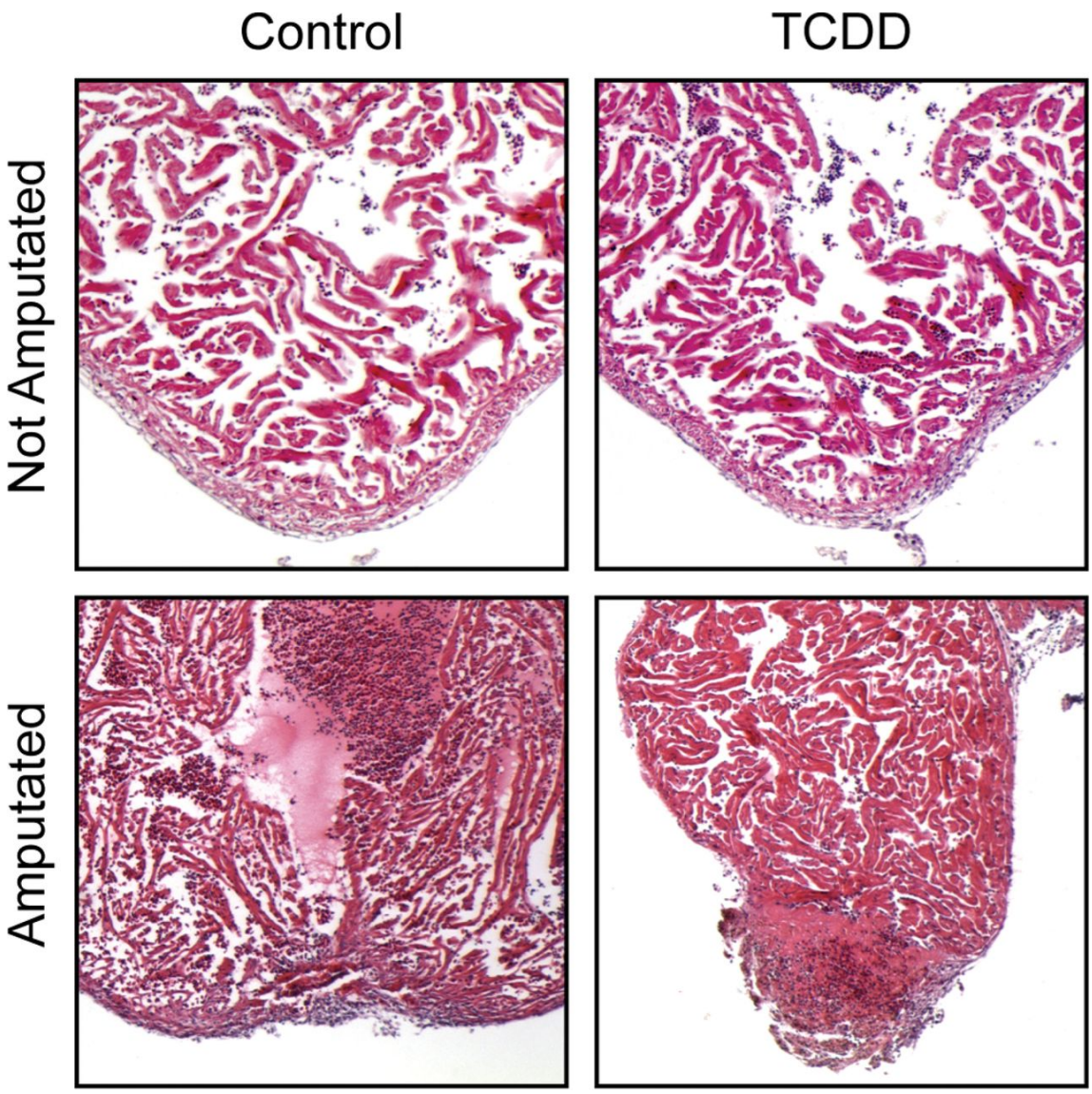

Figure 3. Histological examination of TCDD-exposed wounded hearts. Adult male zebrafish were exposed to TCDD or vehicle just as described in Figure 1 and Figure 2 to produce TCDD- and vehicle-exposed amputated and unamputated hearts that were collected for fixation and H&E staining at 21 days. Representative sections focused on the ventricle apex are shown.

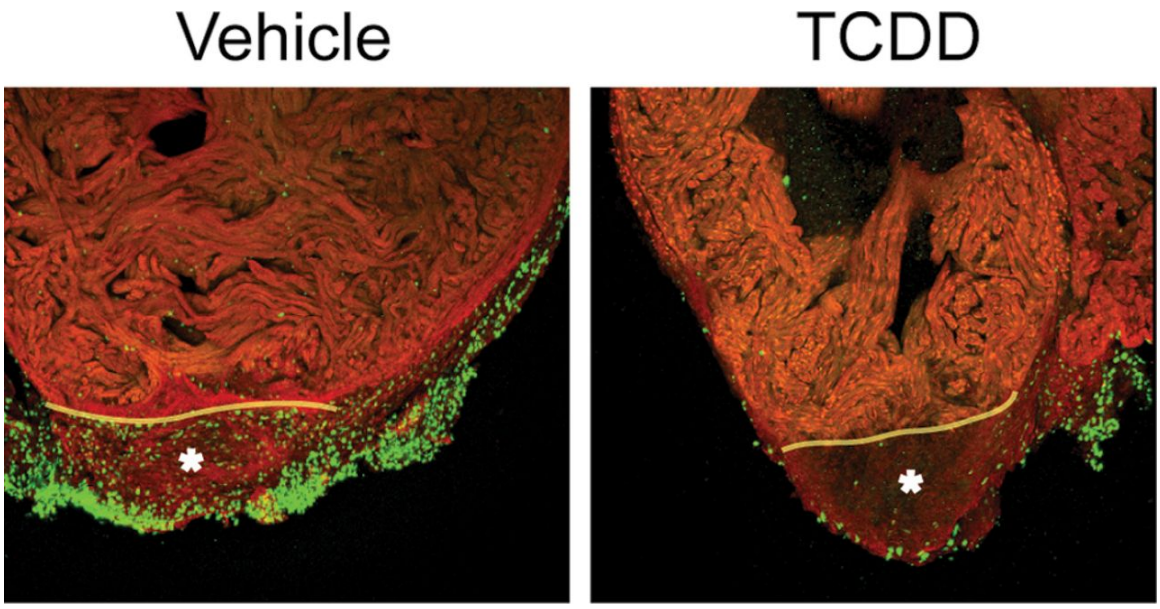

Figure 4. Exposure to TCDD decreases cell proliferation in amputated hearts. Adult male zebrafish were exposed to TCDD or vehicle and the ventricle was amputated the following day as described in Figure 1. Fish were then exposed to BrdU, and collected for sectioning at 7 dpa as described in the Methods. Confocal images are shown of sections stained with phalloidin in red and BrdU in green. The asterisk indicates residual clot, and the original wound plane is indicated as a faint yellow line. Scale bar corresponds to 20 μm.

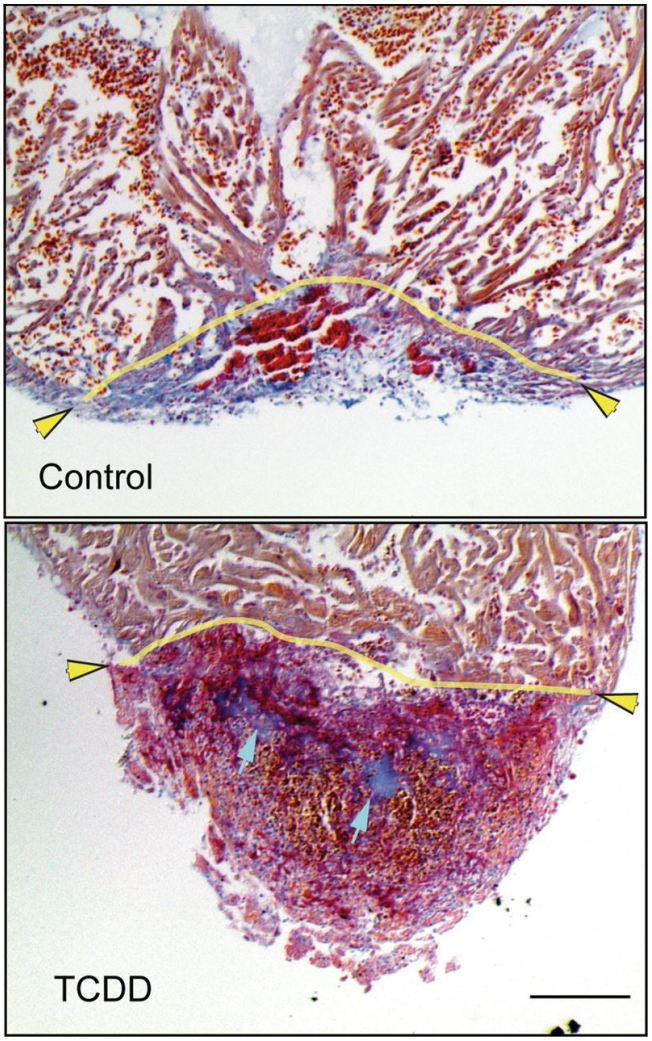

Figure 5. TCDD and collagen deposition. Adult male zebrafish were exposed to TCDD or vehicle and the ventricle was amputated the following day as described in Figure 1, and hearts were removed at 21 dpa. Images show paraffin sections (10 μm) after AFOG staining. Fibrin is stained orange red, collagen shows as blue. The overall abundance of collagen stain does not appear to be significantly altered between treatment groups. The yellow arrows and lines indicate approximate amputation planes. Blue arrowheads point to intense regions of collagen staining. Scale bar corresponds to 20 μm.

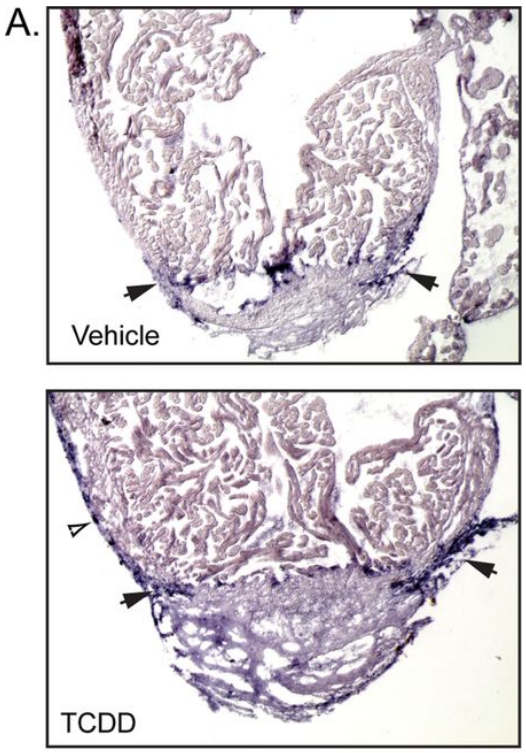
A.
Vehicle
TCDD

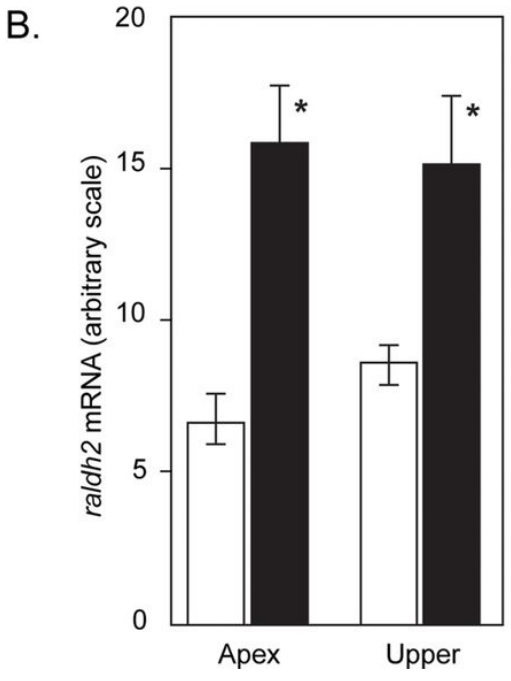
B.
20
15
10
5
0
raldh2 mRNA (arbitrary scale)
*
*
Apex
Upper

Figure 6. TCDD exposure increases *raldh2* expression in amputated ventricles. Adult male zebrafish were exposed to TCDD or vehicle and the ventricle was amputated the following day as described in Figure 1, and the hearts were collected at 7 dpa. A) Cryostat sections showing *in situ* hybridization with a *raldh2* probe stained as dark purple. Dark arrows point to hybridization signal at the amputation plane. Unfilled arrow shows example of increased hybridization at ventricle surface. B) Results from qRT-PCR measurements of *raldh2* mRNA. After removal, the ventricle was sliced parallel to the amputation plane to yield a ventricle sample containing the original wounded tissue (apex) and the upper region of ventricle not initially wounded in the surgery (upper). Results are presented as the mean ± SEM, with n = 6 independent experiments sampling tissues and 3 technical replicate qRT-PCR measurements for each sample. The *raldh2* signal from each sample was normalized to a parallel measurement of *b-actin* mRNA to produce a final measurement on an arbitrary scale.

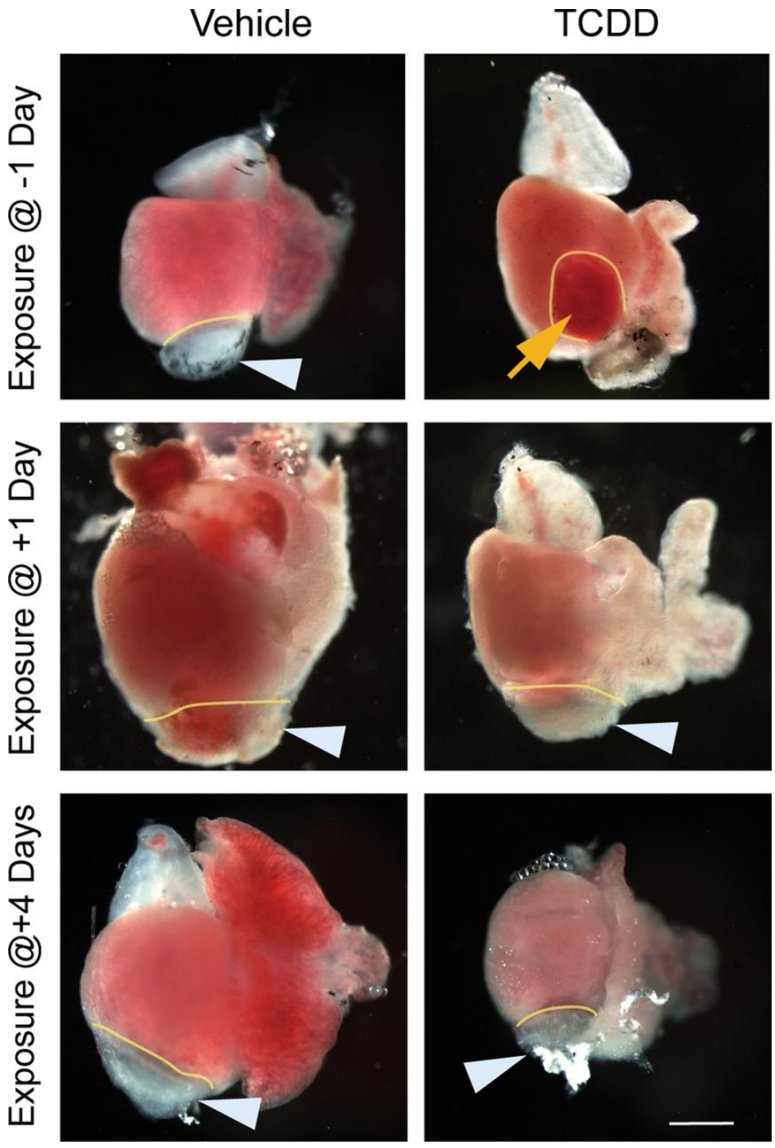

Figure 7. Timing of TCDD exposure is critical for the effect on heart ventricle regeneration. Adult zebrafish were exposed TCDD or vehicle at -1, +1 or +4 dpa as described in the Methods and hearts were collected at 14 dpa for gross examination as in Figure 1. The yellow line denotes the amputation plane. The white arrows indicate normal regeneration of the heart ventricle; the yellow arrow indicates a clot and no regeneration occurring. The scale bar corresponds to 50 μm.

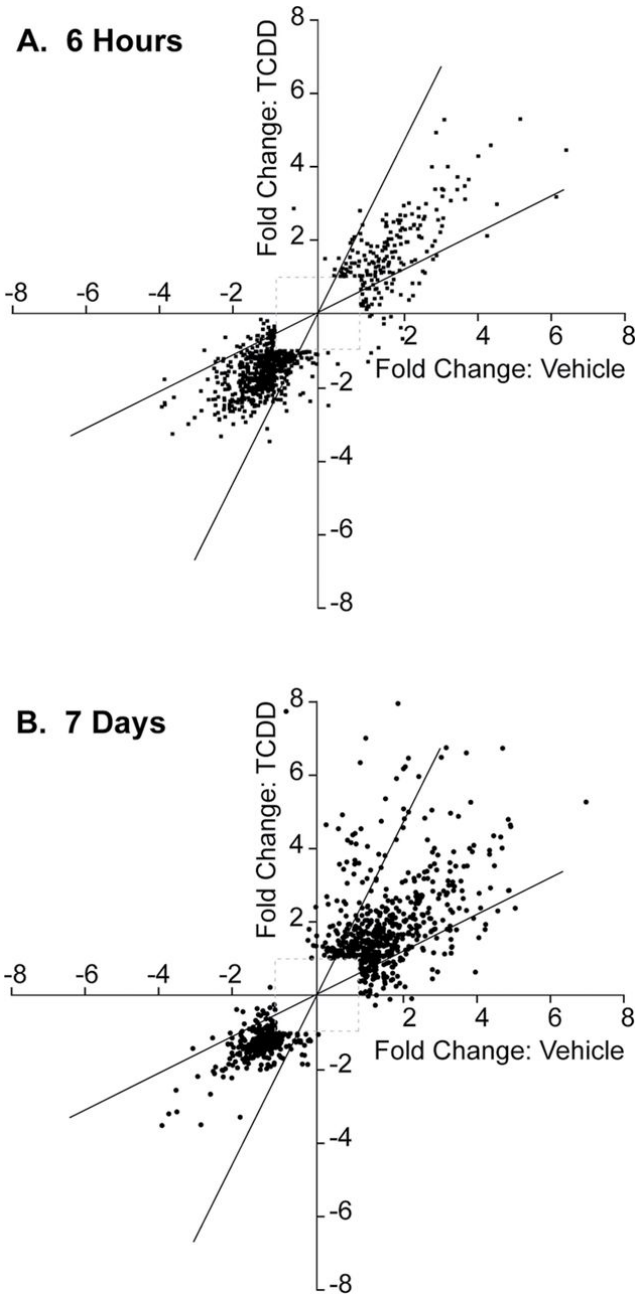
A. 6 Hours
Fold Change: TCDD
Fold Change: Vehicle
8
6
4
2
-2
-4
-6
-8
-8
-6
-4
-2
2
4
6
8
B. 7 Days
Fold Change: TCDD
Fold Change: Vehicle

Figure 8. Effect of TCDD on transcriptional response to amputation. Adult male zebrafish were exposed to TCDD or vehicle and the ventricle was amputated the following day as described in Figure 1. Ventricles were collected for RNA extraction and microarray analysis at 6 hours and 7 days post amputation as described in the Methods. Two biological replicates were run for each point, and each array was hybridized with RNA pooled from 10 hearts (2 biological replicates, with 3 technical replicate for each). A) A set of 817 transcripts altered at least 2 fold by amputation at 6 hpa were selected as described in the Methods. Each of these transcripts is represented as a small square on the plot. Each axis represents the fold-change in expression between the respective amputated sample and the unamputated control, i.e. TCDD 6 hpa vs. TCDD 0 hpa and vehicle 6 hpa *vs*. vehicle 0 hpa. For each point, the X-axis position reflects fold-change in response to amputation in vehicle, while the Y-axis position indicates the fold-change in the TCDD-exposed samples. Points falling between the diagonal lines had X and Y values that varied from each other by less than 2-fold, indicating a similar response to amputation between the TCDD and vehicle samples. Points above or below the diagonal lines had X and Y values that differed by at least 2-fold, indicating a change in response to amputation induced by TCDD. B) A set of 914 transcripts altered at least 2 fold by amputation at 7 dpa were selected as described in the Methods, and plotted as described above.

DISCUSSION

TCDD did not prevent the initial clot formation, but appeared to prevent any further steps in myocardial regeneration. In some cases, we scored TCDD-treated hearts as partially regenerated; however, in these cases the observed signs of repair were not robust, were associated with smaller initial wounds, and did not reflect the normal healing rate. It was not likely that hearts would ever completely regenerate. Indeed, while the control fish recovered from amputation, the TCDD-treated fish did not, and began to die at around 1 month after surgery. In contrast, the dose of TCDD was not lethal, and produced no observable cardiotoxicity in fish without amputation.

A proliferative response is required for heart regeneration (Porrello et al., 2011; Poss et al., 2002). We found that in a normal heart the wound became surrounded by rapidly dividing cells. TCDD did not appear to prevent division of cells away from the wound site as evidenced by the few BrdU-positive cells found in both control and TCDD-exposed hearts at sites away from the wound. However, we saw no dramatic increase in proliferation at the wound site in the TCDD-treated hearts. It is noteworthy that in the embryonic heart, TCDD-exposure produces the down regulation of a large cluster of genes termed the cell cycle gene cluster (CCGC), while at the same time halting cell division in the developing heart (Carney et al., 2006b). It is clear that the normal division of cells needed to replace those lost in the amputated heart is blocked by TCDD.

The TCDD dose required to produce this effect is quite high compared to the short 1 h waterborne exposure at 1 ng/ml that is lethal to developing zebrafish

embryos. This is also true in experiments with fin regeneration. We speculate that because of the well-known hydrophobic nature of TCDD, injected TCDD rapidly associates with macromolecules and lipids throughout the tissues of the fish, especially near the injection site. The levels of circulating TCDD reaching the nuclei of cells within the heart may be significantly lower. We note that this dose of TCDD has been used to block fin regeneration, which is AHR-dependent, suggesting that despite the high doses the effect is mediated by normal AHR binding (Mathew et al., 2006). However, in the case of heart regeneration, we found that lower doses did not produce a consistent effect. We do not know whether this represents an intrinsic difference between the tissues, or perhaps some difference in distribution of TCDD.

The consequences of TCDD exposure on the heart vary with the circumstances

Ordinarily, TCDD exposure in juveniles or adults has no apparent effect on the zebrafish heart (Lanham et al., 2012). On the other hand, exposure of the developing embryonic heart to TCDD produces catastrophic failure (Antkiewicz et al., 2005; Carney et al., 2006b). Our results show that if the heart is wounded it returns to a TCDD-sensitive state. This is especially interesting in light of the idea that the response to wounding depends on the mobilization of cells that have embryonic properties (Choi and Poss, 2012; Lepilina et al., 2006).

One possible explanation for these results is that there is a single process that is being disrupted by TCDD exposure in both the embryonic and wounded adult hearts. If this is the case it could provide clues about both the cardiotoxicity of TCDD exposure and mechanisms needed for heart development and regeneration.

Window of TCDD sensitivity

The embryonic heart is most sensitive to TCDD exposure between approximately 2 and 5 days post fertilization. This coincides with the period during which the epicardial layer is forming around the new heart. The epicardium also plays a supportive role in recovery from wounding in the adult heart (Kikuchi et al., 2011; Lepilina et al., 2006). We found that exposure at 24 h following amputation was too late to produce an effect on heart regeneration, while exposure prior to surgery produced a profound effect. One possibility is that by 24 hpa, the process affected by TCDD has reached a stage at which it is completed or committed, and is no longer a target. For example, it may be that TCDD affects a process needed for cellular dedifferentiation in response to wounding. This process would be most critical in the hours after wounding, and once completed might no longer be affected. An alternative idea is that the molecular responses to TCDD activation of AHR in the target cell change after wounding. In this example, the initial response to TCDD-activated AHR changes. Yet another idea is that TCDD alters the starting condition of the heart so that it already has an intrinsically altered repertoire of possible responses to wounding. While we observed little if any overt toxicity in the unwounded heart, TCDD causes gene expression changes in the ventricle that occur prior to wounding. One of these changes may disable the wound repair response.

Because the unwounded heart shows no response to TCDD, we propose that our results are not due to some non-specific general cardiotoxicity induced by the high dose of TCDD. TCDD may be acting indirectly to prevent wound repair;

however, we do not think that TCDD is producing an environment in which the unwounded heart cannot function normally.

AHR and gene expression

AHR agonists such as TCDD are thought to transform the inactive AHR into a heterodimeric transcriptional regulator that binds DNA at specific sites called AHR response elements (AHREs). While this suggests that TCDD acts by altering gene expression, we don't know what genes are crucial in producing toxicity. This led us to microarray experiments.

In these experiments we compared the transcriptional response to amputation in TCDD-exposed and control hearts. Previous work has examined the gene expression changes induced in the heart by amputation, giving us the opportunity to compare our results with the control-amputated samples and the results published by (Sleep et al., 2010). After normalization, regression analysis showed no significant difference ($p \leq 0.05$, rsq=0.86) between our data sets for comparable samples (data not shown). This provides a degree of validation for both sets of array results.

TCDD exposure altered the transcriptome of the ventricle even prior to amputation. However the list of 22 genes induced at least 2-fold did not provide obvious paths towards explaining the effect on heart regeneration. Most of the affected genes are common to the well-characterized TCDD-inducible battery induced in many tissues. We did not observe a common trend in function between the remaining genes in this list except that many are thought to regulate transcription.

Out of the set of 817 transcripts altered by amputation in either the control or treated hearts at 6 hpa, 553 were common to both. Later after amputation (7 dpa), the transcriptome in TCDD-exposed ventricles diverged farther from that of the control ventricle. For example, a large group of amputation-altered genes had enhanced expression in the TCDD-exposed hearts when compared to the controls. Within this group were genes involved in ECM formation, cell-cell adhesion, and epithelial to mesencyhmal transition. This may reflect the hyper-expression of genes required for wound repair in response to the blockade itself. While we were able to detect changes in *raldh2* expression using *in situ* hybridization and qRT-PCR, the data for this gene did not pass the quality control and fold change filters in the microarray experiments, and was not counted as changed by TCDD. We speculate that TCDD does indeed alter *raldh2* expression, but this is not captured due to a poor signal for this particular transcript on the arrays.

Rather than producing a Venn diagram of overlapping sets, we chose to plot each transcript directly. This provided several advantages. First, the Venn diagram approach can separate transcripts that are not very different. For example a transcript altered by 2.1 fold in both control and TCDD falls into the common circle, while a transcript induced 2.1-fold by amputation in TCDD and 1.9-fold in the control would fall into a TCDD-specific group. Furthermore, transcripts meeting the criteria to be in the common group might be very different in actual response. For example, at 7 dpa the keratin gene *krt5* was induced 3.4-fold in the control, yet in the TCDD amputated sample the transcript was increased by168-fold: using simple grouping with a 2-fold cutoff, these would have been grouped together as not TCDD altered.

TCDD and wound healing in fin and heart

The discovery that TCDD inhibits the regeneration of fish fins produced a great deal of excitement. The effect of TCDD on wound healing in the zebrafish fin is relatively well characterized: it is known that TCDD arrests the expansion of the initial blastema, and work has been done characterizing the effects of TCDD on gene expression in the regenerating fin. In a superficial manner, our work shows similarities between the two systems. In both cases the presence of TCDD blocks cell proliferation and tissue regeneration. Beyond that, the responses appear to diverge. While TCDD can stop the advancing blastema at the site of fin regeneration several days after the initial damage, in the heart, TCDD is ineffective in blocking regeneration if administered a day following the surgery. Furthermore, while there are regenerating progenitor cells in the regenerating heart, it is not clear that a blastema exists.

Finally, when we compared our results with those from Andreason *et al* (2006) we found little overlap between the genes affected by TCDD in the heart and those affected in the regenerating fin. The lack of concordance can in part be attributed to differences in the methods of data comparison, but only to a limited extent. We chose to compare the amputated tissue to 0 hpa samples of the same treatment, i.e. TCDD 6 hpa to TCDD 0 hpa and 6 hpa PC control to 0 hpa PC control. We might also have compared between TCDD and PC samples at equivalent time points, or chosen a single sample such as 0 hpa PC control as the baseline for all comparisons. We have tried all of these types of comparisons with our data, and the major change in outcome is the appearance of genes from the AHR battery such as

cyp1a. Our decision to compare genes affected by amputation to unamputated controls in the same treatment group removes genes such as *cyp1a*, that are well known targets for TCDD induction: this battery of genes is already induced in the 0hpa TCDD-treated baseline samples, and is therefore filtered out with our approach. These genes did not change appreciably in response to amputation. We compared our lists of genes affected by TCDD at 6 hpa with the 36 genes affected in the fin at 1 dpa and found no overlapping genes. Comparison of genes affected in the heart at 7 dpa with the 142 genes affected in the fin at 5 dpa produced an overlap of 8 genes: induced, *timp2, ccl1, ass1, and btbd6a*; repressed, *cxcl12a*, si:ch1073-459j12.1, *f13a1*, and si:ch211-237l4.5.

However, whenever we compare any heart tissue treated with TCDD with any PC control heart sample we find that genes in the AHR battery appear; this is amputation-independent. In order to better compare our results with those of Andreasen *et al* we have reanalyzed our data using the 0 hpa PC control as the baseline for comparisons. This is as close as we can come to their approach, since our time points differ. The lists from Andreasen *et al* and from our work are shown compared in Supplemental Table S6. As indicated above, there were few overlapping transcripts, especially at the earliest time points, 6 hpa (heart) and 24 hpa (fin). At later time points, 7dpa (heart) and 5dpa (fin) the most interesting similarities were enzymes such as metalloproteinases needed for basement membrane remodeling and formation. In particular, the transcripts for *sox9b* and R-spondin 1 affected by TCDD in the amputated fin were not affected by TCDD in our

experiments. We speculate that these results reflect fundamental differences between the two regeneration processes.

Conclusion

The ability of the zebrafish heart to regenerate tissue after wounding is of great interest. It is remarkable that the zebrafish heart, while so sensitive to TCDD during a short period of development should become almost immune to TCDD after the end of larval development, and then again become sensitive when the heart is wounded. Understanding these phenomena will provide helpful clues to unraveling both the mystery the regeneration of the heart ventricle and the cardiotoxicity of AHR agonists.

Funding: Supported by the National Institutes of Health (NIH) grant R01 ES012716 from the National Institute of Environmental Health Sciences (NIEHS) (W.H. and R.E.P.) and the University of Wisconsin Sea Grant Institute, National Sea Grant College Program, National Oceanic and Atmospheric Administration, U.S. Department of Commerce grant number NA 16RG2257, Sea Grant Project R/BT-25 (W.H. and R.E.P.).

Acknowledgments: We thank Dr. Robert Tanguay and Dr. Eric Andreasen for discussions on preparation and administration of TCDD dosing solutions and Dr. Francisco J. Pelegri. We also thank two anonymous reviewers for excellent critiques and advice. We thank Dr. Gilbert Weidinger for the AFOG protocol, and Dorothy Nesbit for technical assistance with the real time PCR and fish facility maintenance. We thank Dr. Chad Vezina, E. Piaf, A. Yauch, Joni Mitchell, and laboratory members for helpful discussions.

The contents are solely the responsibility of the authors and do not necessarily represent the official view of the National Institute of Environmental Health Sciences, National Institutes of Health. The funders had no role in study design, data collection and analysis, decision to publish, or preparation of the manuscript.

REFERENCES

Allen, J.R., Barsotti, D.A., Van Miller, J.P., Abrahamson, L.J., and Lalich, J.J. (1977). Morphological changes in monkeys consuming a diet containing low levels of 2,3,7,8-tetrachlorodibenzo-p-dioxin. Food Cosmet Toxicol *15*, 401-410.

Andreasen, E.A., Mathew, L.K., and Tanguay, R.L. (2006). Regenerative growth is impacted by TCDD: gene expression analysis reveals extracellular matrix modulation. Toxicol Sci *92*, 254-269.

Antkiewicz, D.S., Burns, C.G., Carney, S.A., Peterson, R.E., and Heideman, W. (2005). Heart malformation is an early response to TCDD in embryonic zebrafish. Toxicol Sci *84*, 368-377.

Bauman, J.W., Goldsworthy, T.L., Dunn, C.S., and Fox, T.R. (1995). Inhibitory effects of 2,3,7,8-tetrachlorodibenzo-p-dioxin on rat hepatocyte proliferation induced by 2/3 partial hepatectomy. Cell Prolif *28*, 437-451.

Beis, D., Bartman, T., Jin, S.W., Scott, I.C., D'Amico, L.A., Ober, E.A., Verkade, H., Frantsve, J., Field, H.A., Wehman, A.*, et al.* (2005). Genetic and cellular analyses of zebrafish atrioventricular cushion and valve development. Development *132*, 4193-4204.

Carney, S.A., Chen, J., Burns, C.G., Xiong, K.M., Peterson, R.E., and Heideman, W. (2006a). Aryl hydrocarbon receptor activation produces heart-specific transcriptional and toxic responses in developing zebrafish. Mol Pharmacol *70*, 549-561.

Carney, S.A., Prasch, A.L., Heideman, W., and Peterson, R.E. (2006b). Understanding dioxin developmental toxicity using the zebrafish model. Birth Defects Res A Clin Mol Teratol *76*, 7-18.

Chablais, F., Veit, J., Rainer, G., and Jazwinska, A. (2011). The zebrafish heart regenerates after cryoinjury-induced myocardial infarction. BMC Dev Biol *11*, 21.

Choi, W.Y., and Poss, K.D. (2012). Cardiac regeneration. Curr Top Dev Biol *100*, 319-344.

Dalton, T.P., Kerzee, J.K., Wang, B., Miller, M., Dieter, M.Z., Lorenz, J.N., Shertzer, H.G., Nerbert, D.W., and Puga, A. (2001). Dioxin exposure is an environmental risk factor for ischemic heart disease. Cardiovasc Toxicol *1*, 285-298.

Gould, J., Getz, G., Monti, S., Reich, M., and Mesirov, J.P. (2006). Comparative gene marker selection suite. Bioinformatics *22*, 1924-1925.

Henry, T.R., Spitsbergen, J.M., Hornung, M.W., Abnet, C.C., and Peterson, R.E. (1997). Early life stage toxicity of 2,3,7,8-tetrachlorodibenzo-p-dioxin in zebrafish (Danio rerio). Toxicol Appl Pharmacol *142*, 56-68.

Ivnitski, I., Elmaoued, R., and Walker, M.K. (2001). 2,3,7,8-tetrachlorodibenzo-p-dioxin (TCDD) inhibition of coronary development is preceded by a decrease in myocyte proliferation and an increase in cardiac apoptosis. Teratol *64*, 201-212.

Jopling, C., Sleep, E., Raya, M., Marti, M., Raya, A., and Izpisua Belmonte, J.C. (2010). Zebrafish heart regeneration occurs by cardiomyocyte dedifferentiation and proliferation. Nature *464*, 606-609.

Kikuchi, K., Holdway, J.E., Major, R.J., Blum, N., Dahn, R.D., Begemann, G., and Poss, K.D. (2011). Retinoic acid production by endocardium and epicardium is an injury response essential for zebrafish heart regeneration. Dev Cell *20*, 397-404.

Kikuchi, K., Holdway, J.E., Werdich, A.A., Anderson, R.M., Fang, Y., Egnaczyk, G.F., Evans, T., Macrae, C.A., Stainier, D.Y., and Poss, K.D. (2010). Primary contribution to zebrafish heart regeneration by gata4(+) cardiomyocytes. Nature *464*, 601-605.

Lanham, K.A., Peterson, R.E., and Heideman, W. (2012). Sensitivity to Dioxin Decreases as Zebrafish Mature. Toxicol Sci.

Lepilina, A., Coon, A.N., Kikuchi, K., Holdway, J.E., Roberts, R.W., Burns, C.G., and Poss, K.D. (2006). A dynamic epicardial injury response supports progenitor cell activity during zebrafish heart regeneration. Cell *127*, 607-619.

Mathew, L.K., Andreasen, E.A., and Tanguay, R.L. (2006). Aryl hydrocarbon receptor activation inhibits regenerative growth. Mol Pharmacol *69*, 257-265.

Mehta, V., Peterson, R.E., and Heideman, W. (2008). 2,3,7,8-Tetrachlorodibenzo-p-dioxin exposure prevents cardiac valve formation in developing zebrafish. Toxicol Sci *104*, 303-311.

Mitchell, K.A., Lockhart, C.A., Huang, G., and Elferink, C.J. (2006). Sustained aryl hydrocarbon receptor activity attenuates liver regeneration. Mol Pharmacol *70*, 163-170.

Pesatori, A.C., Zocchetti, C., Guercilena, S., Consonni, D., Turrini, D., and Bertazzi, P.A. (1998). Dioxin exposure and non-malignant health effects: a mortality study. Occup Environ Med *55*, 126-131.

Peterson, R.E., Theobald, M.G., and Kimmel, G.L. (1993). Developmental and reproductive toxicity of dioxins and related compounds: cross-species comparisons. Crit Rev Toxicol *23*, 283-335.

Porrello, E.R., Mahmoud, A.I., Simpson, E., Hill, J.A., Richardson, J.A., Olson, E.N., and Sadek, H.A. (2011). Transient regenerative potential of the neonatal mouse heart. Science *331*, 1078-1080.

Poss, K.D., Wilson, L.G., and Keating, M.T. (2002). Heart regeneration in zebrafish. Science *298*, 2188-2190.

Schnabel, K., Wu, C.C., Kurth, T., and Weidinger, G. (2011). Regeneration of cryoinjury induced necrotic heart lesions in zebrafish is associated with epicardial activation and cardiomyocyte proliferation. PLoS One *6*, e18503.

Sleep, E., Boue, S., Jopling, C., Raya, M., Raya, A., and Izpisua Belmonte, J.C. (2010). Transcriptomics approach to investigate zebrafish heart regeneration. J Cardiovasc Med (Hagerstown) *11*, 369-380.

Thackaberry, E.A., Nunez, B.A., Ivnitski-Steele, I.D., Friggins, M., and Walker, M.K. (2005). Effect of 2,3,7,8-tetrachlorodibenzo-p-dioxin on murine heart development: alteration in fetal and postnatal cardiac growth, and postnatal cardiac chronotropy. Toxicol Sci *88*, 242-249.

Thisse, C., Thisse, B., Schilling, T.F., and Postlethwait, J.H. (1993). Structure of the zebrafish snail1 gene and its expression in wild-type, spadetail and no tail mutant embryos. Development *119*, 1203-1215.

Vezina, C.M., Allgeier, S.H., Moore, R.W., Lin, T.M., Bemis, J.C., Hardin, H.A., Gasiewicz, T.A., and Peterson, R.E. (2008). Dioxin causes ventral prostate agenesis by disrupting dorsoventral patterning in developing mouse prostate. Toxicol Sci *106*, 488-496.

Walker, M.K., and Peterson, R.E. (1991). Potencies of polychlorinated dibenzo-*p*-dioxin, dibenzofuran and biphenyl congeners, relative to 2,3,7,8-tetrachlorodibenzo-*p*-dioxin for producing early life stage mortality in rainbow trout (*Oncorhynchus mykiss*). Aquatic toxicology (Amsterdam, Netherlands) *21*, 219-238.

Wang, J., Panakova, D., Kikuchi, K., Holdway, J.E., Gemberling, M., Burris, J.S., Singh, S.P., Dickson, A.L., Lin, Y.F., Sabeh, M.K.*, et al.* (2011). The regenerative capacity of zebrafish reverses cardiac failure caused by genetic cardiomyocyte depletion. Development *138*, 3421-3430.

Zodrow, J.M., Stegeman, J.J., and Tanguay, R.L. (2004). Histological analysis of acute toxicity of 2,3,7,8-tetrachlorodibenzo-p-dioxin (TCDD) in zebrafish. Aquatic toxicology (Amsterdam, Netherlands) *66*, 25-38.

Zodrow, J.M., and Tanguay, R.L. (2003). 2,3,7,8-tetrachlorodibenzo-p-dioxin inhibits zebrafish caudal fin regeneration. Toxicol Sci *76*, 151-161.

CHAPTER III

Dioxin inhibits zebrafish epicardium and proepicardium development

Jessica Plavicki, Peter Hofsteen, Richard E. Peterson,

and Warren Heideman

Toxicological Sciences (2013) **131(2)**, 558-567.

ABSTRACT

Embryonic exposure to the environmental contaminant and aryl hydrocarbon receptor agonist, 2,3,7,8-tetrachlorodibenzo-*p*-dioxin (TCDD, dioxin) disrupts cardiac development and function in fish, birds, and mammals. In zebrafish, the temporal window of sensitivity to the cardiotoxic effects of TCDD coincides with epicardium formation. We hypothesized that this TCDD-induced heart failure results from disruption of epicardial development. To determine whether embryonic TCDD exposure inhibits epicardium and proepicardium (PE) development in zebrafish, we used histology and fluorescence immunocytochemistry to examine the epicardium formation in fish exposed to TCDD. TCDD exposure prevented epicardium formation. Using live imaging and *in situ* hybridization, we found that TCDD exposure blocked the formation of the PE cluster. *In situ* hybridization experiments showed that TCDD exposure also prevented the expression of the PE marker *tcf21* at the site where the PE normally forms. TCDD also inhibited expansion of the epicardial layer across the developing heart: exposure after PE formation was completed prevented further expansion of the epicardium. However, TCDD exposure did not affect epicardial cells already present. Because TCDD blocks epicardium formation, but is not directly toxic to the epicardium once complete, we propose that inhibition of epicardium formation can account for the window of sensitivity to TCDD cardiotoxicity in developing zebrafish. Epicardium development is crucial to heart development. Loss of this layer during development may account for most if not all of the TCDD-induced cardiotoxicity in zebrafish.

INTRODUCTION

Zebrafish are an established model for studying cardiovascular development and disease. Developing zebrafish hearts are exquisitely sensitive to cardiotoxicity induced by the environmental contaminant 2,3,7,8-tetrachlorodibenzo-*p*-dioxin (TCDD, dioxin). Heart malformations caused by TCDD exposure in zebrafish include valve malformation, reduced heart size, and impaired development of the bulbus arteriosus (Antkiewicz et al., 2005; Grimes et al., 2008; Heideman et al., 2005; Mehta et al., 2008). TCDD exposure produces decreased cardiac output, reduced end diastolic volume, and decreased peripheral blood flow. This ultimately leads to heart failure, which includes ventricular standstill and total loss of circulation (Antkiewicz et al., 2005; Belair et al., 2001; Henry et al., 1997). One of the most interesting features of TCDD-induced cardiotoxicity is the fact that zebrafish carrying a lethal body burden of TCDD develop normal appearing hearts through heart tube formation and looping, with a functional circulation. It is only at approximately 48 hpf that the signs of TCDD toxicity become manifest. At this stage, the TCDD-exposed heart begins a process of unlooping, myocyte proliferation halts, cardiac output fails, the ventricle stops beating, valves are malformed, and the fish succumb with massive pericardial and yolk sac edema. Later in development, at between the 2nd and 3rd week of life, the zebrafish heart returns to a state of resistance to TCDD-induced cardiotoxicity (Lanham et al., 2012). It is known that cardiotoxicity is mediated by the receptor for TCDD, Ahr2 (Prasch et al., 2003). However, the mechanism underlying toxicity remains unknown, and in particular the basis for the developmental window of sensitivity remains a mystery.

Studies of the developing zebrafish heart initially identified only two cell layers, the myocardial layer, and the endothelium lining the heart chambers, continuous with the vascular endothelium. However, recently Serluca (2008) showed that zebrafish develop an epicardium, which can first be observed during the third day after fertilization. The epicardium is derived from a transient cluster of cells termed the proepicardium (PE) that initially forms at the venous pole, or inflow tract, during heart development. PE cells migrate to the myocardium and spread out to form the epicardium, a simple squamous epithelium (Manner et al., 2001; Martinsen, 2005; Munoz-Chapuli et al., 2002; Schlueter and Brand, 2012). A subset of epicardial cells undergo epithelial to mesenchymal transition and contribute to the development of coronary vasculature smooth muscle, and become perivascular and intermyocardial fibroblasts (Vincent and Buckingham, 2010). Epicardial derived cells (EPDC) are also involved in valve development, cardiomyocyte alignment and proliferation and maturation of the cardiac conduction system (Gittenberger-de Groot et al., 2012; Lie-Venema et al., 2007; Munoz-Chapuli et al., 2002).

We noted that the onset of sensitivity to TCDD cardiotoxicity in zebrafish coincides with the beginning of PE formation (Antkiewicz et al., 2005; Serluca, 2008). Cardiotoxicity begins at approximately 48 hpf, while the PE can first be clearly distinguished at approximately 50 hpf (Liu and Stainier, 2010; Serluca, 2008). Over the next few days the epicardial cells migrate and envelope the zebrafish heart. TCDD cardiotoxicity begins to decline at about 5 dpf, a time that roughly coincides with completion of the initial epicardial cell layer. Over the next two weeks the

epicardium becomes thicker as epicardium formation is completed, while TCDD sensitivity at the heart disappears (Lanham et al., 2012).

Because TCDD does not appear to interfere with initial heart formation, we hypothesized that TCDD inhibits a process that does not occur until after the heart chambers had formed. The timing of TCDD sensitivity suggested epicardium formation as a possible target. In addition, mutations that block epicardium formation produce cardiac malformations similar to those caused by TCDD (Gittenberger-de Groot et al., 2012; Lie-Venema et al., 2007; Olivey and Svensson, 2010; Ratajska et al., 2010; Serluca, 2008).

Here we report that TCDD exposure prevents PE formation, and subsequent epicardium development. If the PE is allowed to form prior to TCDD exposure, TCDD halts further epicardial development, but does not alter epicardial cells already present. Thus, TCDD has profound effects on the epicardium, which appear to be limited to the process of epicardium formation. This provides a model explaining the temporal pattern of sensitivity to TCDD-induced cardiotoxicity observed in the developing zebrafish.

MATERIALS and METHODS

Zebrafish Strains and exposure. Adult zebrafish (*Danio rerio*) lines were maintained and zebrafish embryos were reared and housed according to procedures described by Westerfield (2000). The AB wild type line was used unless otherwise indicated. Transgenic lines, *pard3:EGFP* (Poon et al., 2010), *tcf21:DsRed* fish

(Kikuchi et al., 2011), *ahr2*^{hu3335} (Goodale et al., 2012) were kindly provided by Drs. Vladamir Korzh, Kenneth Poss and Robert Tanguay, respectively. All procedures involving animals were approved by the Animal Care and Use Committee of the University of Wisconsin-Madison, and adhered to the National Institutes of Health's "Guide for the Care and Use of Laboratory Animals."

TCDD (>99% purity; Chemsyn) was used as a 1 mg/ml stock solution in dimethyl sulfoxide (DMSO). Fish were exposed to TCDD (1ng/ml) or vehicle (0.1% DMSO) for 1 h in glass scintillation vials with gentle rocking (Antkiewicz et al., 2005). Ten embryos or larvae were present per ml of dosing solution and each group of fish in a vial was considered n=1 for statistics.

Control and TCDD exposed embryos were dosed for 1 h beginning at 4 hpf with either waterborne TCDD (1 ng/ml) or an equivalent volume of 0.1% DMSO (control) and raised in 175 mmol/L mannitol in embryo water. This concentration was previously determined to prevent pericardial edema while allowing development of the embryo (Hill et al., 2004). The mannitol solution was replaced daily and embryos were collected at 120 hpf.

Histology. Larvae were fixed in 4% paraformaldehyde overnight at 4°C, dehydrated in a graded ethanol series, embedded in paraffin, sectioned (4 ìm) and stained with hematoxylin and eosin (King Heiden et al., 2009). Sections were imaged using a Zeiss Axiocam digital camera mounted on a Zeiss Axioplan microscope.

Immunohistochemistry. Antibody staining was performed as previously described (Dong et al., 2007). The antibody against *activated leukocyte cell adhesion*

molecule (ALCAM) was used at a 1:50 dilution in phosphate buffered saline with 4% bovine albumin serum and 0.3% Triton (PBT). Secondary anti mouse antibodies (Alexa 488, Alexa 568; Invitrogen) were used at 1:200 dilution in PBT. Embryos were mounted in Vectashield or Vectashield with DAPI (Vector Laboratories). Confocal images were collected on an Olympus Fluoview FV1000 microscope. Brightest point projections were made using Olympus Fluoview software and images were processed using Adobe Photoshop.

PE Imaging and Scoring. Live embryos (50 and 72 hpf) were imaged in 3% methylcellulose using a Nikon TE300 inverted microscope attached to a Princeton Instruments Micromax CCD camera. Ten second videos showing the presumptive PE site were captured for each embryo using MotionScope software and analyzed using Metamorph software. Scores for PE development were assigned by an experimenter blinded to the treatment groups using a 0-3 scale (0 = PE clearly absent; 1 = slight evidence / very small PE; 2 = defined cluster, but smaller than normal; 3 = clearly present, normal PE). A two-tailed Student's t-test assuming equal variance was used to determine statistical significance ($p<0.01$).

***In situ* Hybridization.** Whole mount in situ hybridization was preformed as previously described with minor modifications (Mehta et al., 2008). The *tcf21* probe was kindly provided by Dr. Fabrizio C. Serluca. Riboprobes were labeled with digoxigenin-UTP and visualized using anti-digoxigenin-AP Fab fragments (Roche) with BM purple (Roche). Hybridization was carried out at 60°C. Embryos were cleared in a 70% glycerol solution in PBS and imaged using an Olympus DP72 digital camera on an Olympus S2X16 microscope.

Epicardial development. Individual fish carrying the *pard3:EGFP* reporter were exposed to TCDD at the indicated time, collected at 120 hpf, and fixed for confocal microscopy as described above. Individual fish were assessed for epicardium formation on the ventricle and the atrium. A chamber was scored as positive for epicardium formation if any *EGFP*-positive cell was detected overlying the myocardium. Between 45 and 54 fish were examined for each point, yielding an n=45-54. Incidence data was analyzed using a Fisher's Exact Test to determine statistical significance ($p<0.001$).

RESULTS

Embryonic TCDD exposure prevents epicardium formation in zebrafish

We exposed newly fertilized eggs to TCDD as described in the Methods and collected larvae at 120 hpf to assess epicardium formation. H&E staining clearly showed oblong epicardial cells in control hearts, and a consistent absence of these cells in TCDD exposed hearts (Figure 1A and 1B). The inset in Figure 1A shows the appearance of flattened cells creating a layer on the outside of the myocardium. The TCDD-exposed heart lacks these cells.

We used epicardial-specific reporter lines to follow epicardium development. Embryos carrying a *pard3:EGFP* reporter (Poon et al., 2010) were exposed to TCDD or vehicle as above and hearts were examined using confocal microscopy at 120 hpf. While epicardial cells expressing *pard3:EGFP* were consistently found on the ventricles in control hearts (Figure 2A), we saw no EGFP epicardial cells in the

TCDD-exposed hearts (Figure 2B). Optical cross sections allowed a precise evaluation of the position of the *pard3:EGFP*-positive cells relative to the myocardium. In the control hearts, EGFP-positive cells clearly covered the myocardium (Figure 2C); in the TCDD-exposed hearts EGFP-positive cells were not detected on the myocardium (Figure 2D).

We also examined a *tcf21*-DsRed transgenic line expressing DsRed in epicardial cells (Kikuchi et al., 2011). As with the *pard3:EGFP* experiment, in 120 hpf fish the DsRed signal clearly showed epicardial cells surrounding the control ventricle (Figure 3A), but not the ventricle in fish exposed to TCDD immediately after fertilization (Figure 3B). Taken together, the histological and reporter studies show that early exposure to TCDD prevents formation of the epicardium.

AHR2 mediates loss of epicardium.

TCDD-induced cardiotoxicity has been shown to be dependent on the receptor for TCDD, Ahr2. MO knockdown of either Ahr2 or its dimerization partner Arnt1 is sufficient to protect zebrafish from developmental cardiotoxicity (Prasch et al., 2006; Prasch et al., 2003). To determine whether TCDD activation of AHR2 mediates the loss of epicardium, we used a mutant lacking Ahr2 function (Goodale et al., 2012). Eggs were exposed to either DMSO as a vehicle control or to TCDD immediately after fertilization as described in the Methods. At 120 hpf the fish were harvested and examined by confocal microscopy using antibodies against ALCAM to visualize the excitable myocardial cells. The DAPI staining showing cell nuclei allows visualization of epicardial cells on the outer surface of the myocardial layer

(Figure 4). As expected, TCDD had no apparent impact on epicardial coverage in these mutants.

Loss of the epicardium is not a secondary effect of pericardial edema.

TCDD exposure alters heart shape and produces acute pericardial edema, beginning at approximately 72 hpf. This change in geometry alters the intra-pericardial space, changing the environment in which the PE and epicardium are forming. Therefore, it is possible that the loss of epicardium was secondary to TCDD-induced pericardial edema. We used mannitol in the water as an osmotic support to prevent the TCDD pericardial edema produced (Hill et al., 2004). While mannitol prevented TCDD-induced pericardial edema, the epicardium still failed to form in *pard3:EGFP* reporter embryos exposed to TCDD, while it clearly formed in the vehicle control larvae (Figure 5). We conclude that the loss of the epicardium was not secondary to pericardial edema.

TCDD exposure blocks proepicardium (PE) development in zebrafish.

TCDD is not readily metabolized nor excreted and the half life in adult trout is measured in months (Brambilla et al., 2007); consequently we expect that our initial exposure at fertilization produces a persistent TCDD body burden in the developing fish lacking mature metabolism and excretion organs. Therefore, our first experiments do not point to disruption of any a specific step in epicardium development. We first examined PE formation.

In zebrafish, the PE is first visible by brightfield microscopy around 50 hpf and increases in size from 50 to 72 hpf (Liu and Stainier, 2010; Serluca, 2008). This can

be seen in the control images in Figure 6A and 6B. PE development was significantly impaired in TCDD exposed fish at 50 hpf (Figure 6C). While the PE is visible at 50 hpf, it is more distinct at 72 hpf. Exposure to TCDD retards growth, therefore the loss of PE formation at 50 hpf might have been due to a developmental delay. We also examined PE formation in exposed and control embryos at 72 hpf. Even as late as 72 hpf, TCDD inhibited formation of the PE, indicating that the loss of the PE could not be explained by simple delay in formation (Figure 5D).

Because the PE is a small cluster of cells among other groups of cells, positive identification is difficult. To be certain that we were correctly identifying the PE, we scored PE formation in live fish, taking advantage of the fact that the real PE clusters remain relatively stationary, attached to the pericardium, while other cells move with the beat of the heart. We used video microscopy to allow observers, blind to the treatment groups, to score PE formation in treated and control fish as described in the Methods. The results of these experiments at both 50 and 72 hpf show a significant loss of PE formation in TCDD-exposed fish (Figure 7).

Loss of PE marker *tcf21*

The PE is formed as a small cluster of cells that form in preparation for migration to the heart. TCDD might simply block the motility of these cells, producing a small region of PE-destined cells with failed adhesive properties, unable to form a cluster. If this were the case, we would expect to find a group of cells on the pericardial surface expressing PE marker genes. To test this, we used *in situ* hybridization to determine whether the PE marker gene *tcf21* was still expressed in

this region (Figure 8). While we were clearly able to discern the dot of *tcf21* marking the PE in the control fish, TCDD exposure prevented the expression of *tcf21* in this presumptive region of PE formation. This suggests that TCDD prevented not only the migration of cells to form the PE structure, but also prevented the formation of the group of cells expressing this PE marker.

Timing of TCDD exposure differentially affects epicardial development

The PE loss can readily explain the absence of an epicardium in larvae exposed to TCDD at the time of fertilization. However, does TCDD also affect the epicardium itself?

We tested this by delaying TCDD exposure until after the PE had formed. Zebrafish carrying the *pard3:EGFP* reporter were exposed to TCDD prior to or during PE formation at 24, and 48 hpf, and after initial epicardium establishment at 72, or 96 hpf. All samples were collected at 120 hpf for examination of the epicardium by confocal microscopy (Figure 9). The control shows the normal development of the epicardium across both ventricle and atrium at 120 hpf. As expected, embryos exposed at 24 and 48 hpf, prior to PE formation, had no epicardium at 120 hpf.

Complete epicardial formation was also inhibited in hearts in which TCDD exposure was delayed until the PE had completely formed: exposure at 72 hpf produced hearts with epicardial cells covering the ventricle, but not the atrium; exposure at 96 hpf produced hearts with ventricular epicardium, but few if any

epicardial cells on the atrium. These results show that even after the PE has formed, exposure to TCDD inhibits the normal advance of the epicardial layer.

As with PE formation, we developed a numerical system to score the progression of the epicardial layer in hearts exposed to TCDD at the different times in the above experiments. Fish (approximately 50 individuals per point) were exposed at 24, 48, 72, and 96 hpf as described above and collected for examination at 120 hpf. Fish were scored for epicardial cells at the atrium and ventricle separately and were scored positive if even a single epicardial was found on the chamber. The incidence of epicardium cells found on the ventricle (squares) or the atrium (circles) is plotted on the Y-axis in Figure 10.

All control fish exposed to vehicle at any of the time points showed both ventricular and atrial coverage by epicardial cells. TCDD exposure at 72 hpf had little effect on the incidence of epicardial cells on the ventricle, probably due to the fact that epicardium formation has begun on the ventricle by about 72 hpf. However, epicardium coverage of the atrium was completely prevented. Even when exposure was delayed to 96 hpf, we found a significant inhibition of atrial coverage. These results show that TCDD exposure blocks epicardial expansion from the ventricle to the atrium, while apparently not reversing already formed epicardium.

To determine whether TCDD could affect the epicardium after it had been formed, we delayed TCDD exposure until 120 hpf, a point when epicardial cells have covered both atrium and ventricle, and collected hearts two days later at 168 hpf. H&E sections showed no difference in epicardium coverage between the exposed

and control samples indicating that while epicardium progenitors building the layer are sensitive, the established epicardium as formed is not a TCDD target (Figure 11).

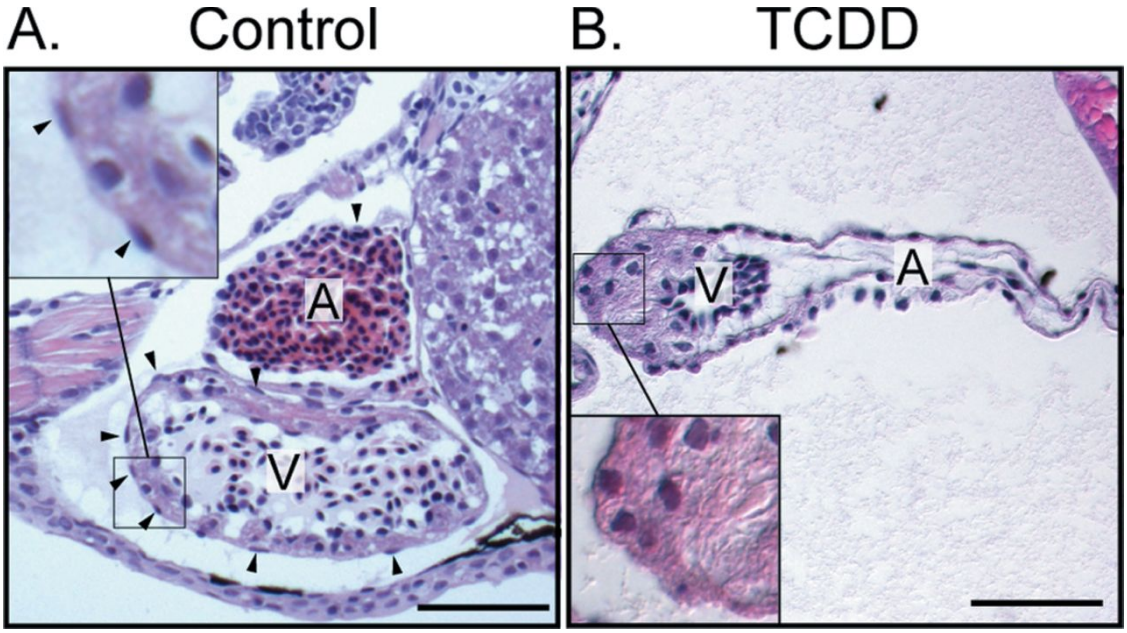

Figure 1. TCDD exposure prevents epicardium formation in zebrafish. Zebrafish were exposed to vehicle (panel A) or TCDD (panel B) immediately following fertilization as described in the Methods and collected at 120 hpf. H&E stained sagital sections show atrium and ventricle from lateral view, with anterior to the left. A = Atrium; V = Ventricle. Scale bars: 50 m. Vehicle control hearts are on the left and corresponding TCDD-exposed hearts are shown at right. Insets show the flattened epicardial cells in the control ventricle, and the corresponding region lacking epicardial cells in the TCDD-exposed heart. Arrowheads indicate epicardial cells.

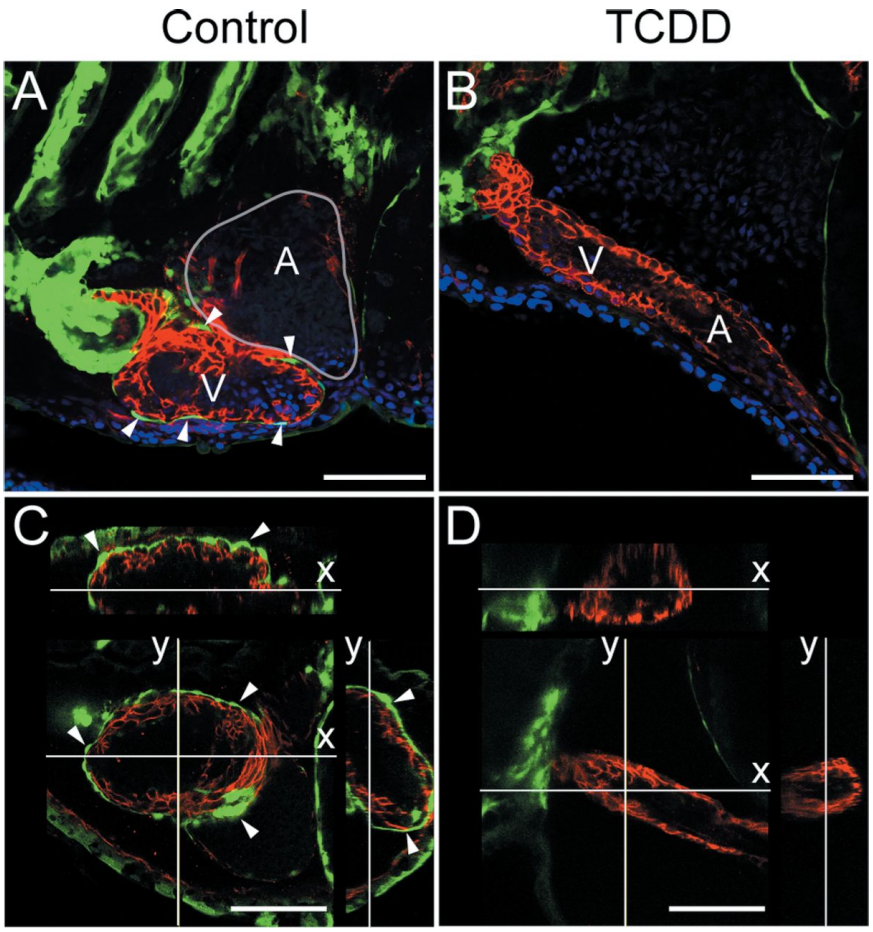

Figure 2. Loss of *pard3* reporter expression in TCDD exposed hearts. Zebrafish were exposed to TCDD as in Figure 1. A and B) Fish were collected at 120 hpf and lateral confocal images of *pard3:EGFP* control and exposed hearts are shown. ALCAM is counterstained as red, and EGFP is indicated as green. DAPI staining shows nuclei in outer pericardium as blue. White arrowheads indicate GFP-positive epicardial cells. C and D). X and Y orthogonal optical slices through z-stacks (z-step=0.52 m) showing ventricle lumen. White arrowheads indicate GFP-positive epicardial cells.

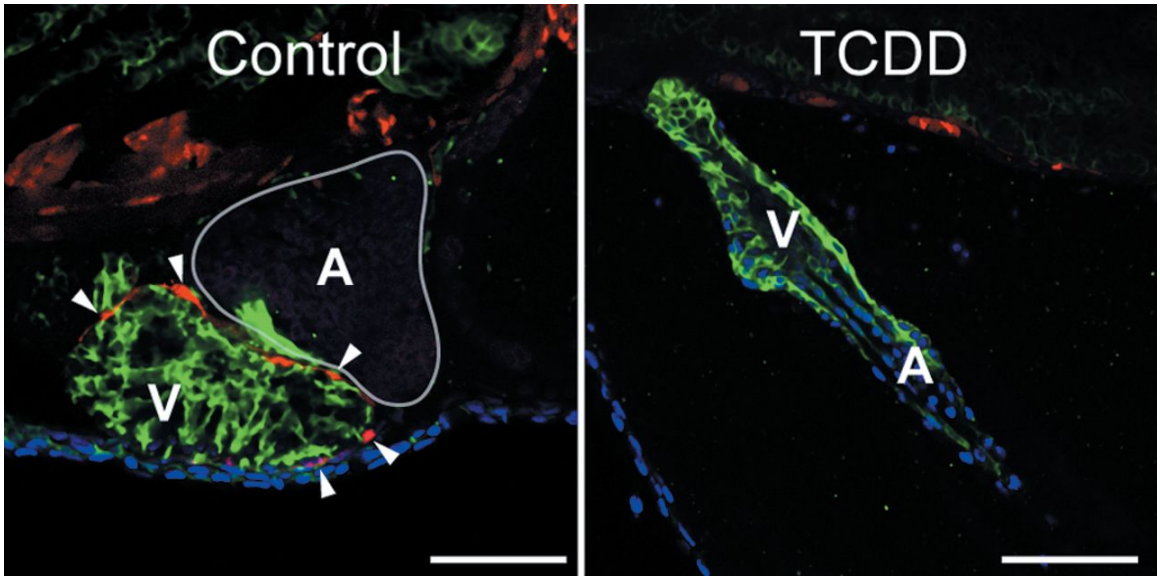

Figure 3. Expression of the *tcf21* epicardium marker is lost in TCDD-exposed hearts. Zebrafish were exposed to TCDD immediately after fertilization and collected at 120 hpf as in the figures above. Confocal images show lateral views of hearts from the *tcf21:DsRed* transgenic line. Red indicates *tcf21* expression; ALCAM expression is shown as green. DAPI in blue shows cell nuclei, generally at the pericardial surface. White arrowheads indicate DsRed-positive epicardial cells.

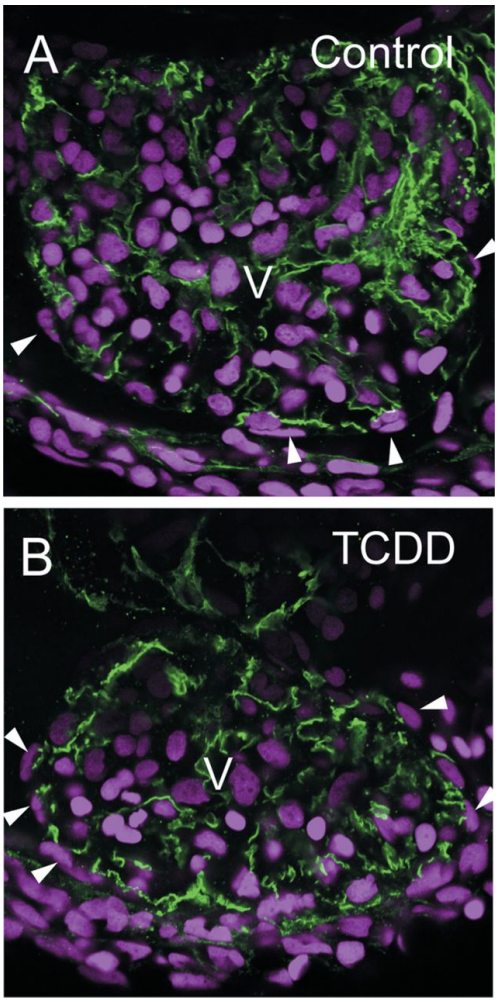

Figure 4. TCDD has no effect on epicardium formation in *ahr2*-/- mutants. Zebrafish homozygous for loss of functional *ahr2* were exposed to TCDD immediately after fertilization and collected at 120 hpf as in the figures above. Confocal images show lateral views of hearts. ALCAM expression is shown as green, and delineates the cytoplasm in myocardial cells. DAPI shows cell nuclei in blue. White arrowheads indicate flattened cells lying on the surface of the heart, outside of the myocardial layer. The ventricle center is labelled as V, and rounded erythrocyte nuclei are prominent within the ventricles.

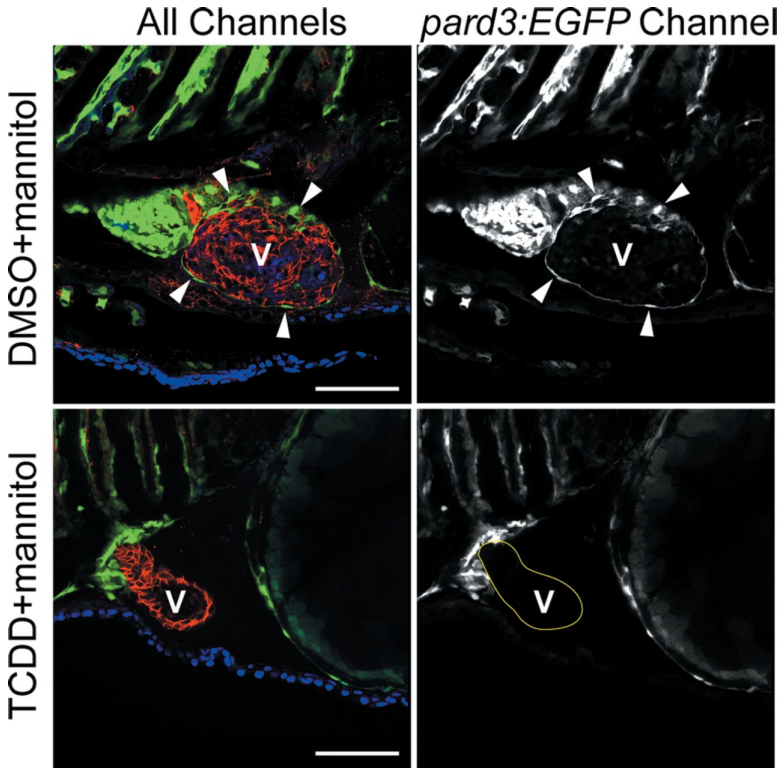

Figure 5. TCDD-induced pericardial edema is not linked to the loss of epicardium in TCDD exposed larvae. Zebrafish carrying the *pard3:EGFP* reporter were exposed to TCDD or vehicle immediately following fertilization and moved into water with 175 mM mannitol added as an osmotic support. Samples were collected at 120 hpf for confocal microscopy as described in the Methods. Ventral views are shown with the anterior to the left. The left column of images shows all 3 channels of fluorescence together. ALCAM is counterstained as red, and EGFP is indicated as green. DAPI staining shows nuclei in outer pericardium as blue. White arrowheads indicate GFP-positive epicardial cells. The column of images at right shows the *pard3 :EGFP* signal alone as white. Arrowheads show examples of *pard3:EGFP*-positive cells. A indicates atrium; V indicates ventricle. Scale bars: 50 m.

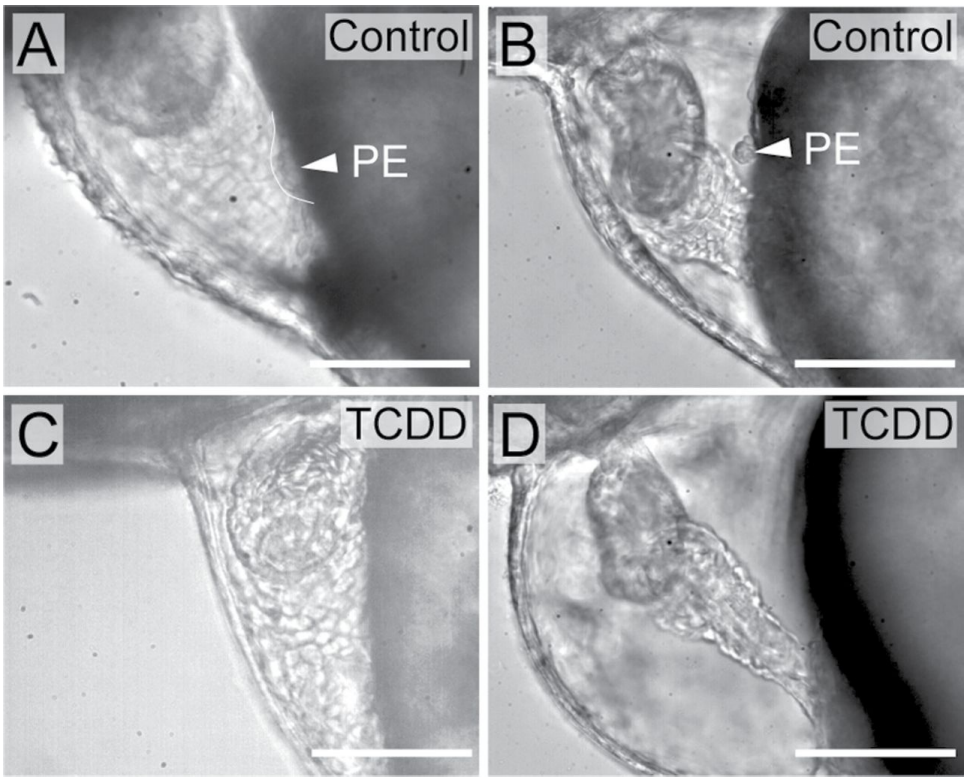

Figure 6. TCDD exposure blocks PE development in zebrafish. Zebrafish were exposed to TCDD or vehicle immediately following fertilization as described in the Methods. A-D) Lateral views of hearts at 50 and 72 hpf are shown; anterior is to left in all panels. Vehicle control hearts are on the left and corresponding TCDD-exposed hearts are shown at right. White arrowhead indicates the PE. Scale bars: 50 m. A) Vehicle control heart at 50 hpf. B) TCDD-exposed heart at 50 hpf. C) Vehicle control heart at 72 hpf. D) TCDD-exposed heart at 72 hpf.

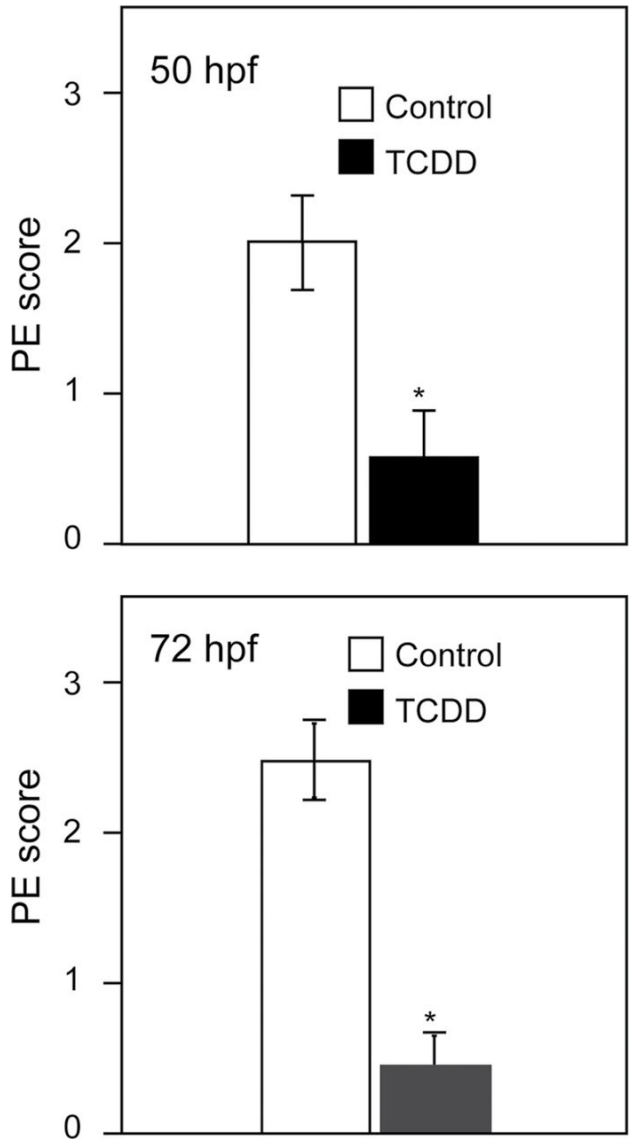

Figure 7. Scoring of PE formation. Graphs show incidence of PE formation at 50 and 72 hpf respectively. Scoring is described in detail in Supplemental Methods. Briefly, embryos were scored using the following scale: 0, no PE; 1, slight evidence of PE; 2=moderate evidence for PE; 3=normal PE in full view. Experimenters were blind to the treatment groups scored. Asterisk indicates difference from control $p<0.01$; Student's t-Test.

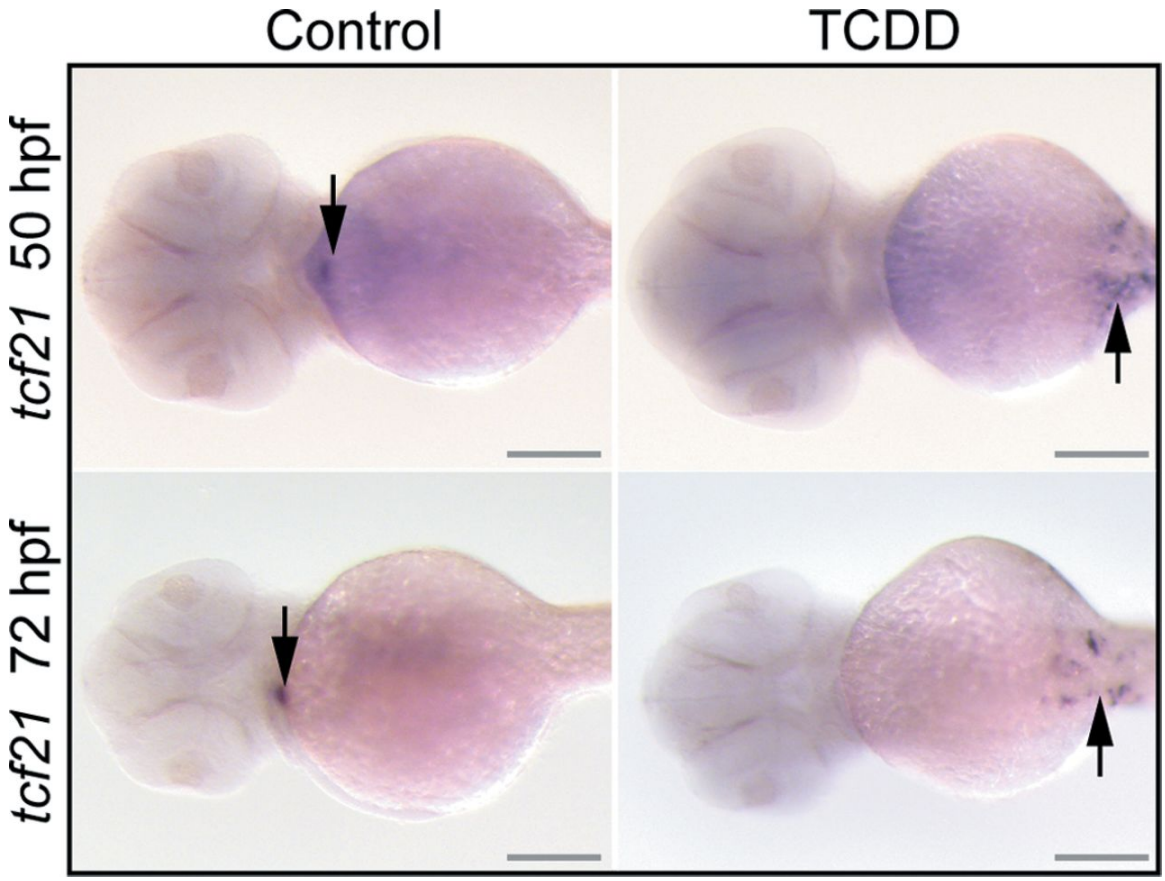

Figure 8. TCDD alteration of PE and epicardium-specific marker. Zebrafish embryos were exposed to TCDD or vehicle at 24 hpf as described in the Methods. Vehicle control hearts are on the left and corresponding TCDD-exposed hearts are shown at right. Fish were collected for *in situ* hybridization probing for *tcf21* at either 50 or 72 hpf as indicated, and ventral views are shown with anterior end to the left. Arrows indicate regions of hybridization. Scale bars: 100 m. A) TCDD- and vehicle-exposed fish collected at 50 and 72 hpf as indicated.

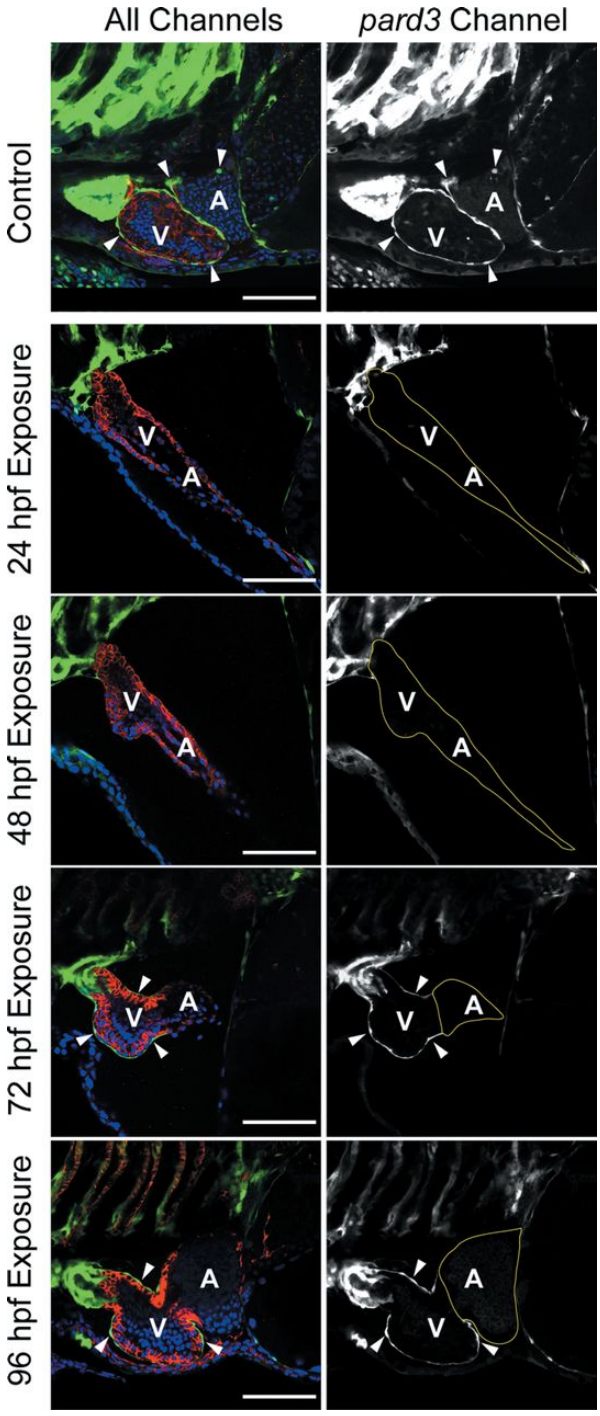
All Channels
pard3 Channel
Control
24 hpf Exposure
48 hpf Exposure
72 hpf Exposure
96 hpf Exposure
A
V

Figure 9. TCDD after PE formation halts further epicardium progression. Zebrafish carrying the *pard3:EGFP* reporter were exposed to TCDD at the indicated times. Samples were collected at 120 hpf for confocal microscopy as described in the Methods. The left column of images shows all 3 channels of fluorescence together. ALCAM is counterstained as red, and EGFP is indicated as green. DAPI staining shows nuclei in outer pericardium as blue. White arrowheads indicate GFP-positive epicardial cells. The column of images at right shows the *pard3:EGFP* signal alone as white. The control was not exposed to TCDD and demonstrates normal epicardium formation at 120 hpf. Scale bars: 50 m.

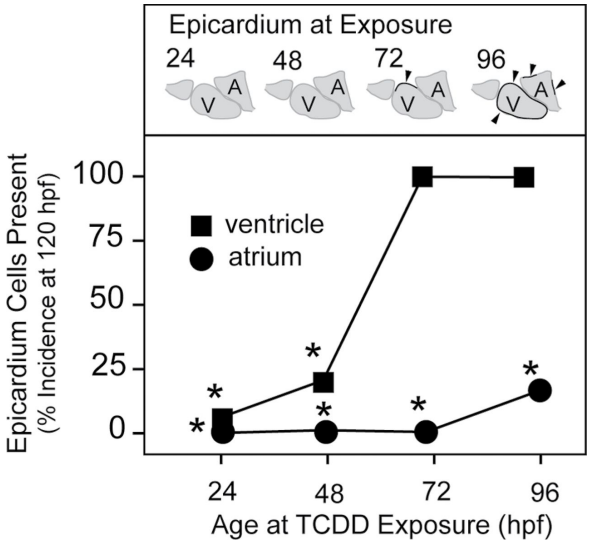

Figure 10. TCDD exposure during epicardial expansion halts further epicardium development. Zebrafish carrying the *pard3:EGFP* reporter were exposed to TCDD at the times indicated on the X-axis and collected at 120 hpf for staining and confocal microscopy. The control was exposed to the DMSO vehicle alone. Incidence of the appearance of GFP-positive cells on either ventricle or atrium in the confocal images was counted at 120 hpf. The schematic figures above each time point represent the normal course of epicardium formation. Chambers with at least 1 *EGFP*-positive cell were scored as positive. If no cells were observed the chamber was scored as negative. For these experiments n=1 was an individual fish, and the n for each treatment ranged from 45 - 54. The values shown are the percentages of positive scoring individuals in the treatment group. Scoring the percentage of individuals with an all or none response produces no error bars. Instead, Fisher's Exact Test was used and asterisks indicate difference from control at $p<0.001$.

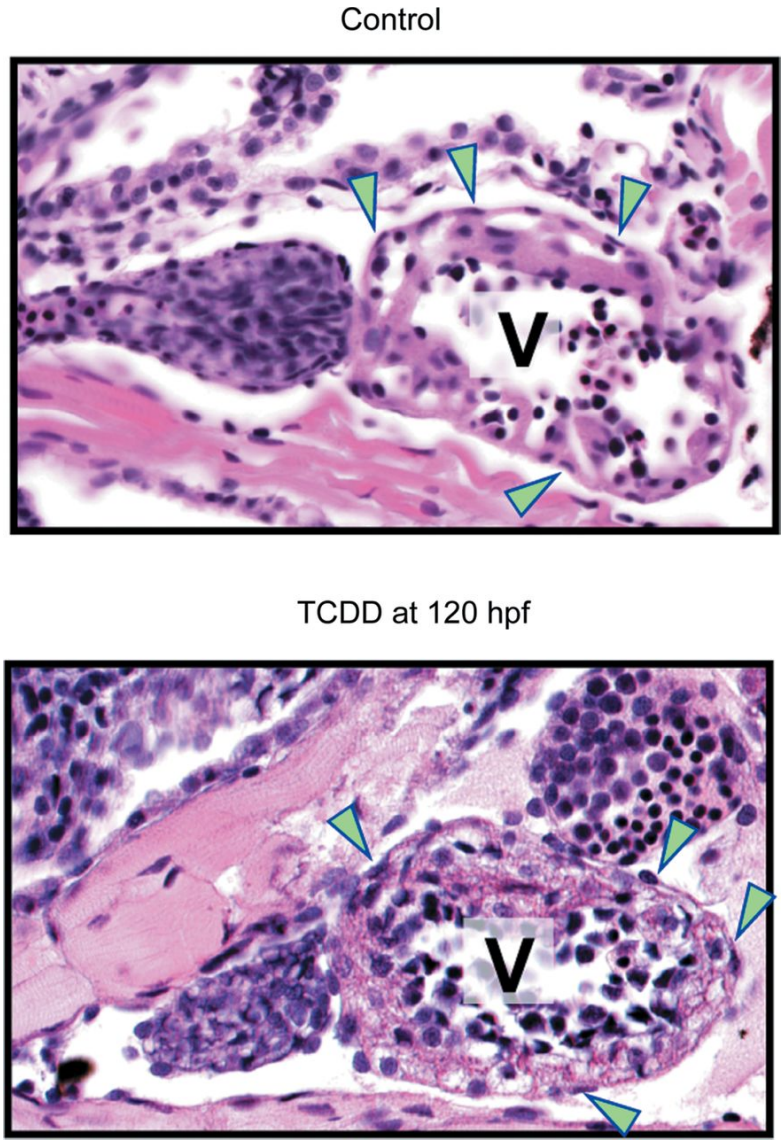

Figure 11. TCDD does not remove formed epicardium. The panels show H&E sections of 168 hpf larval hearts treated with DMSO (control) or TCDD at 120 hpf. Arrowheads indicate epicardial cells. In all panels ventral views are shown with the anterior to the left. A indicates atrium; V indicates ventricle.

DISCUSSION

Epicardium development involves specification of the PE, translocation of PE cells to the myocardium, and migration of epicardial cells across the heart chambers to form an epicardial sheet (Carmona et al., 2010; Manner et al., 2001; Ratajska et al., 2008). TCDD inhibited PE formation and disrupted the expression of PE markers. Ahr2 is required for the known cardiotoxic effects of TCDD in zebrafish embryos, and not surprisingly we also found this true for the effects on PE and epicardial development: in *ahr2* null mutants, the epicardium developed normally despite the presence of TCDD.

Pericardial Edema

An obvious effect of TCDD exposure is pronounced pericardial edema. This is thought to be secondary to heart failure and circulation loss (Incardona et al., 2005; Incardona et al., 2004). We have previously shown that relief of the pericardial edema with mannitol added as an osmotic support does not alter the course of heart failure, unlooping, and arrest induced by TCDD (Hill et al., 2004). We considered the possibility that pericardial edema could alter the concentrations of factors in the fluid surrounding the heart, as well as the spatial relationships between tissues. This could conceivably alter epicardium formation. However, we have ruled this out with experiments in which the pericardial edema in TCDD exposed embryos was prevented using mannitol as an osmotic support.

TCDD exposure and PE development

We found that TCDD produced a significant loss of PE formation in the developing zebrafish. We should note that our scoring system was set up to address problems in conclusively identifying the zebrafish PE. In contrast to species such as the chicken, it can be difficult to identify the PE with certainty, especially at early time points. The PE is a small cluster of perhaps a dozen cells. With many other groups of cells in the region, we found that the most effective method of scoring is to do so with live fish. In live fish, attachment of the PE to the pericardium distinguishes the more stable PE from groups of cells associated with the beating heart.

Even with this system and a trained eye, we found that the PE is variable in size. Often identification was easy and certain: these were scored as 3s. However, in other cases the PEs in control fish were smaller and harder to identify with complete certainty. These groups of cells were scored as 2s. With this variation in size, the converse situation was sometimes encountered as well: in some cases it was not possible to state with certainty that a clump of a few cells was not a small PE. These groups were scored as 1. It is noteworthy that by 72 hpf no control fish was scored below 2 and no TCDD treated fish was scored higher than 1. We presume that all of the control fish indeed had PEs, and speculate that the TCDD-exposed fish did not all score as zeros because of false positives.

One gene expressed in PE and epicardial cells is *tcf21*. It is not known exactly what role *tcf21* plays in epicardial formation; however, it is associated with the PE and then the epicardial cells as they form. We consistently observed a loss

of the PE structure. The *in situ* hybridization experiments reinforce the idea that the PE fails to form in the TCDD-exposed fish.

It seems unlikely that TCDD directly affects the genes marking the epicardium such as *pard3* or *tcf21*, since once formed the epicardial cells continue to express these mRNAs in the presence of TCDD. Rather, TCDD appears to prevent these progenitor cells from properly forming, thereby indirectly blocking expression of these and possibly many other as yet undiscovered genes marking epicardium progenitors.

While *tcf21* expression was absent at the presumptive site of PE formation in TCDD exposed fish, it was ectopically expressed elsewhere. Previous work has shown increased and delocalized expression of genes such as *bmp4*, *noggin*, and *flk1* in TCDD exposed zebrafish hearts, indicating a failure to maintain normal specification of gene expression (Mehta et al., 2008). How this occurs remains an important unanswered question.

TCDD exposure and heart disease

Early embryonic exposure to TCDD disrupts cardiovascular development and function in a wide range of vertebrate species including fish, birds, and mammals. In humans, epidemiological studies have correlated long-term TCDD exposure with ischemic heart disease (Bertazzi et al., 1998; Flesch-Janys et al., 1995; Puga, 2011) and, interestingly, sectioned and stained heart samples from patients with this disease lack epicardial cells (Di Meglio et al., 2010). In zebrafish, an established model for studying cardiovascular development and disease, TCDD exposure

results in valve malformation (Mehta et al., 2008), reduced heart size (Antkiewicz et al., 2005), and impaired development of the bulbus arteriosus (Grimes et al., 2008; Mehta et al., 2008). TCDD-exposed zebrafish larvae have decreased cardiac output, reduced end diastolic volume, and decreased peripheral blood flow (Antkiewicz et al., 2005; Belair et al., 2001; Carney et al., 2006). Heart failure steadily worsens to ventricular standstill and total loss of circulation (Antkiewicz et al., 2005). The pericardial and yolk sac edema that ensues is thought to be secondary to circulation failure (Incardona et al., 2004).

We propose that much of these effects seen in the exposed zebrafish heart can be accounted for by the failure of the epicardial layer to form and mature; however, this must at present remain a working model because while the epicardium is assumed to be necessary for heart formation, the exact consequences of epicardium loss are difficult to define. Most of what is known about the loss of epicardium is based on mutations or other gene alterations that cause epicardium loss. For example, in the mouse *tcf21* null embryos (E9.5) have defects in PE migration, epicardial adhesion, and spreading. This partial loss of epicardium is accompanied by thinning of the myocardium and impaired atrioventricular valve formation (Mahtab et al., 2008). Loss of the *wt1* gene in the mouse is embryonic lethal. In addition to epicardium defects, cardiac abnormalities such as thinning of the myocardial wall, pericardial edema and pericardial hemorrhage were observed in these *wt1* mutant mice. The function of *wt1* conserved in zebrafish, and MO knockdown of *wt1* expression causes a loss of the PE followed by the heart

elongation and pericardial edema. These cardiac defects have all have been reported for zebrafish exposed to TCDD.

It is clear that *bmp4* is critical in PE and cardiac development. In zebrafish, *tcf21* and *tbx18* expression are lost in *bmp4* and type I BMP receptor (*acvrl1*) mutants. Liu and Stanier (2010) went on to block BMP signalling using a heat shock-inducible dominant negative BMP receptor construct. Heat shock at 36 hpf produced significant reduction in *tcf21* and *tbx18* expression at the region of the presumptive PE. Perhaps more informative for our purposes, Liu and Stainier also found that the T-box transcription factor Tbx5a plays a role in heart development that appears to become critical around the time of PE formation. The *tbx5a* gene was originally discovered as the *heartstrings* mutation (Garrity et al., 2002). As with TCDD-exposed hearts, the hearts in zebrafish lacking *tbx5a* develop relatively normally until about the time of PE formation. At this stage, the PE and epicardial markers *tbx18* and *tcf21* are markedly reduced. After this, the heart deteriorates to become string-like. Heat-shock expression of a dominant negative *tbx5a* at 10 hpf, long before PE formation, produces more dramatic effects than expression at 24 hpf, indicating that *tbx5a* is important in some early process needed later for PE and epicardium specification (Liu and Stainier, 2010).

Two congruent temporal windows for TCDD sensitivity

One of the most puzzling and interesting aspects of TCDD cardiotoxicity in zebrafish has been the narrow temporal window of sensitivity. When zebrafish are exposed to TCDD immediately after fertilization, the hearts form and develop normally, such that at 48 hpf, they are practically indistinguishable from normal

control hearts. Blood flow is normal and chamber formation and looping proceeds, despite the presence of both TCDD and the AHR. However, after 48 hpf the exposed hearts deteriorate: looping is reversed, chamber morphology is altered, valve cushions fail to form, and with massive pericardial edema, circulation ceases. Remarkably, this sensitivity to TCDD drops off noticeably at around 120 hpf, and cardiotoxic effects entirely disappear after the second week of life (Lanham et al., 2012).

As closely as we can determine, this temporal window of TCDD sensitivity matches the time course of epicardium formation. However, the exact time course of epicardium formation has not been well defined. The PE is first visible at around 50 hpf, but an indistinct cluster of cells beginning to form a PE would be hard to identify, so the exact beginning of PE formation must remain an estimate. We find that the epicardium covers the ventricle first, and then spreads onto the atrium at around 120 hpf. After that time there is an apparent maturation of the epicardium all over the surface of the heart as it begins to contribute to heart formation. This coincides with the gradual complete loss of TCDD-sensitivity at the heart.

It is noteworthy that TCDD does not appear to affect epicardial cells after they have formed. Therefore, if the epicardium formation is the target for TCDD cardiotoxicity, one would expect to see a loss of cardiotoxicity once the epicardial layer had been established. To the extent to which we can determine, this is the case. We propose that inhibition of epicardium formation can account for the window of sensitivity to TCDD cardiotoxicity in developing zebrafish. Because epicardium development is crucial to so many aspects of heart development, this

toxic effect, inhibiting the development of a specific set of cells, may account for most of the TCDD-induced cardiotoxicity in developing zebrafish.

It is important perhaps not to oversimplify our interpretation. Replication of epicardial cells has been observed in adult zebrafish during periods of growth (Wills et al., 2008). While we observed no overt toxicity in the adult heart (Lanham et al., 2012), subtle changes due to altered epicardial cell growth might not have been observed.

ACKNOWLEDGEMENTS

We thank Dorothy Nesbit, B. David Campbell, and Rickie L. Jones for assistance in the lab.

SOURCES OF FUNDING

Supported by the National Institutes of Health (NIH) grant R01 ES012716 from the National Institute of Environmental Health Sciences (NIEHS) (W.H. and R.E.P.) and the University of Wisconsin Sea Grant Institute, National Sea Grant College Program, National Oceanic and Atmospheric Administration, U.S. Department of Commerce grant number NA 16RG2257, Sea Grant Project Numbers R/BT-22 and R/BT-25 (W.H. and R.E.P.). The contents are solely the responsibility of the authors and do not necessarily represent the official view of the NIEHS, NIH.

The funders had no role in study design, data collection and analysis, decision to publish, or preparation of the manuscript.

REFERENCES

Antkiewicz, D.S., Burns, C.G., Carney, S.A., Peterson, R.E., and Heideman, W. (2005). Heart malformation is an early response to TCDD in embryonic zebrafish. Toxicol Sci *84*, 368-377.

Belair, C.D., Peterson, R.E., and Heideman, W. (2001). Disruption of erythropoiesis by dioxin in the zebrafish. Dev Dyn *222*, 581-594.

Bertazzi, P.A., Bernucci, I., Brambilla, G., Consonni, D., and Pesatori, A.C. (1998). The Seveso studies on early and long-term effects of dioxin exposure: a review. Environ Health Perspect *106 Suppl 2*, 625-633.

Brambilla, G., Dellatte, E., Fochi, I., Iacovella, N., Miniero, R., and di Domenico, A. (2007). Depletion of selected polychlorinated biphenyl, dibenzodioxin, and dibenzofuran congeners in farmed rainbow trout (Oncorhynchus mykiss): a hint for safer fish farming. Chemosphere *66*, 1019-1030.

Carmona, R., Guadix, J.A., Cano, E., Ruiz-Villalba, A., Portillo-Sanchez, V., Perez-Pomares, J.M., and Munoz-Chapuli, R. (2010). The embryonic epicardium: an essential element of cardiac development. J Cell Mol Med *14*, 2066-2072.

Carney, S.A., Chen, J., Burns, C.G., Xiong, K.M., Peterson, R.E., and Heideman, W. (2006). Aryl hydrocarbon receptor activation produces heart-specific transcriptional and toxic responses in developing zebrafish. Mol Pharmacol *70*, 549-561.

Di Meglio, F., Castaldo, C., Nurzynska, D., Romano, V., Miraglia, R., and Montagnani, S. (2010). Epicardial cells are missing from the surface of hearts with ischemic cardiomyopathy: a useful clue about the self-renewal potential of the adult human heart? Int J Cardiol *145*, e44-46.

Dong, P.D., Munson, C.A., Norton, W., Crosnier, C., Pan, X., Gong, Z., Neumann, C.J., and Stainier, D.Y. (2007). Fgf10 regulates hepatopancreatic ductal system patterning and differentiation. Nat Genet *39*, 397-402.

Flesch-Janys, D., Berger, J., Gurn, P., Manz, A., Nagel, S., Waltsgott, H., and Dwyer, J.H. (1995). Exposure to polychlorinated dioxins and furans (PCDD/F) and mortality in a cohort of workers from a herbicide-producing plant in Hamburg, Federal Republic of Germany. Am J Epidemiol *142*, 1165-1175.

Garrity, D.M., Childs, S., and Fishman, M. (2002). The *heartstrings* mutation in zebrafish causes heart/fin Tbx5 deficiency syndrome. Dev *129*, 4635-4645.

Gittenberger-de Groot, A.C., Winter, E.M., Bartelings, M.M., Jose Goumans, M., Deruiter, M.C., and Poelmann, R.E. (2012). The arterial and cardiac epicardium in development, disease and repair. Differentiation; research in biological diversity.

Goodale, B.C., La Du, J.K., Bisson, W.H., Janszen, D.B., Waters, K.M., and Tanguay, R.L. (2012). AHR2 mutant reveals functional diversity of aryl hydrocarbon receptors in zebrafish. PLoS One *7*, e29346.

Grimes, A.C., Erwin, K.N., Stadt, H.A., Hunter, G.L., Gefroh, H.A., Tsai, H.J., and Kirby, M.L. (2008). PCB126 exposure disrupts zebrafish ventricular and branchial but not early neural crest development. Toxicol Sci *106*, 193-205.

Heideman, W., Antkiewicz, D.S., Carney, S.A., and Peterson, R.E. (2005). Zebrafish and cardiac toxicology. Cardiovasc Toxicol *5*, 203-214.

Henry, T.R., Spitsbergen, J.M., Hornung, M.W., Abnet, C.C., and Peterson, R.E. (1997). Early life stage toxicity of 2,3,7,8-tetrachlorodibenzo-p-dioxin in zebrafish (Danio rerio). Toxicol Appl Pharmacol *142*, 56-68.

Hill, A.J., Bello, S.M., Prasch, A.L., Peterson, R.E., and Heideman, W. (2004). Water Permeability and TCDD-Induced Edema in Zebrafish Early Life Stages. Toxicol Sci.

Incardona, J.P., Carls, M.G., Teraoka, H., Sloan, C.A., Collier, T.K., and Scholz, N.L. (2005). Aryl hydrocarbon receptor-independent toxicity of weathered crude oil during fish development. Environ Health Perspect *113*, 1755-1762.

Incardona, J.P., Collier, T.K., and Scholz, N.L. (2004). Defects in cardiac function precede morphological abnormalities in fish embryos exposed to polycyclic aromatic hydrocarbons. Toxicol Appl Pharmacol *196*, 191-205.

Kikuchi, K., Gupta, V., Wang, J., Holdway, J.E., Wills, A.A., Fang, Y., and Poss, K.D. (2011). tcf21+ epicardial cells adopt non-myocardial fates during zebrafish heart development and regeneration. Development *138*, 2895-2902.

King Heiden, T.C., Spitsbergen, J., Heideman, W., and Peterson, R.E. (2009). Persistent adverse effects on health and reproduction caused by exposure of zebrafish to 2,3,7,8-tetrachlorodibenzo-p-dioxin during early development and gonad differentiation. Toxicol Sci *109*, 75-87.

Lanham, K.A., Peterson, R.E., and Heideman, W. (2012). Sensitivity to Dioxin Decreases as Zebrafish Mature. Toxicol Sci.

Lie-Venema, H., van den Akker, N.M., Bax, N.A., Winter, E.M., Maas, S., Kekarainen, T., Hoeben, R.C., deRuiter, M.C., Poelmann, R.E., and Gittenberger-de Groot, A.C. (2007). Origin, fate, and function of epicardium-derived cells (EPDCs) in normal and abnormal cardiac development. TheScientificWorldJournal *7*, 1777-1798.

Liu, J., and Stainier, D.Y. (2010). Tbx5 and Bmp signaling are essential for proepicardium specification in zebrafish. Circ Res *106*, 1818-1828.

Manner, J., Perez-Pomares, J.M., Macias, D., and Munoz-Chapuli, R. (2001). The origin, formation and developmental significance of the epicardium: a review. Cells Tissues Organs *169*, 89-103.

Martinsen, B.J. (2005). Reference guide to the stages of chick heart embryology. Dev Dyn *233*, 1217-1237.

Mehta, V., Peterson, R.E., and Heideman, W. (2008). 2,3,7,8-Tetrachlorodibenzo-p-dioxin exposure prevents cardiac valve formation in developing zebrafish. Toxicol Sci *104*, 303-311.

Munoz-Chapuli, R., Macias, D., Gonzalez-Iriarte, M., Carmona, R., Atencia, G., and Perez-Pomares, J.M. (2002). The epicardium and epicardial-derived cells: multiple functions in cardiac development. Rev Esp Cardiol *55*, 1070-1082.

Olivey, H.E., and Svensson, E.C. (2010). Epicardial-myocardial signaling directing coronary vasculogenesis. Circ Res *106*, 818-832.

Poon, K.L., Liebling, M., Kondrychyn, I., Garcia-Lecea, M., and Korzh, V. (2010). Zebrafish cardiac enhancer trap lines: new tools for in vivo studies of cardiovascular development and disease. Dev Dyn *239*, 914-926.

Prasch, A.L., Tanguay, R.L., Mehta, V., Heideman, W., and Peterson, R.E. (2006). Identification of zebrafish ARNT1 homologs: 2,3,7,8-tetrachlorodibenzo-p-dioxin toxicity in the developing zebrafish requires ARNT1. Mol Pharmacol *69*, 776-787.

Prasch, A.L., Teraoka, H., Carney, S.A., Dong, W., Hiraga, T., Stegeman, J.J., Heideman, W., and Peterson, R.E. (2003). Aryl hydrocarbon receptor 2 mediates 2,3,7,8-tetrachlorodibenzo-p-dioxin developmental toxicity in zebrafish. Toxicol Sci *76*, 138-150.

Puga, A. (2011). Perspectives on the potential involvement of the AH receptor-dioxin axis in cardiovascular disease. Toxicol Sci *120*, 256-261.

Ratajska, A., Czarnowska, E., and Ciszek, B. (2008). Embryonic development of the proepicardium and coronary vessels. Int J Dev Biol *52*, 229-236.

Ratajska, A., Kolodzinska, A., Ciszek, B., and Wasiutynski, A. (2010). [Relationship between heart development and pathogenesis of congenital heart defects in current literature]. Kardiol Pol *68 Suppl 5*, S418-427.

Schlueter, J., and Brand, T. (2012). Epicardial Progenitor Cells in Cardiac Development and Regeneration. J Cardiovasc Transl Res.

Serluca, F.C. (2008). Development of the proepicardial organ in the zebrafish. Dev Biol *315*, 18-27.

Vincent, S.D., and Buckingham, M.E. (2010). How to make a heart: the origin and regulation of cardiac progenitor cells. Curr Top Dev Biol *90*, 1-41.

Westerfield, M. (2000). The Zebrafish Book. A Guide for the Laboratory Use of Zebrafish (Danio rerio), 4th edn (Eugene, OR, Univ. of Oregon Press).

Wills, A.A., Holdway, J.E., Major, R.J., and Poss, K.D. (2008). Regulated addition of new myocardial and epicardial cells fosters homeostatic cardiac growth and maintenance in adult zebrafish. Development *135*, 183-192.

CHAPTER IV

S*ox9b* is Required for Epicardium Formation and Plays a Role in TCDD-Induced Heart Malformation in Zebrafish

Peter Hofsteen, Jessica Plavicki, Shaina D. Johnson,

Richard E. Peterson, and Warren Heideman

Molecular Pharmacology (2013) Sep **84(3)** 353-60

ABSTRACT

Activation of the transcription factor AHR by 2,3,7,8-tetrachlorodibenzo-*p*-dioxin (TCDD) prevents the formation of the epicardium and leads to severe heart malformations in developing zebrafish (*Danio rerio*). The downstream genes that cause heart malformation are not known. Because TCDD causes craniofacial malformations in zebrafish by downregulating the *sox9b* gene, we hypothesized that cardiotoxicity might also result from *sox9b* downregulation. We found that *sox9b* is expressed in the developing zebrafish heart ventricle and that TCDD exposure markedly reduces this expression. Furthermore, we found that manipulation of *sox9b* expression could phenocopy many but not all of the effects of TCDD at the heart. Loss of *sox9b* prevented the formation of epicardium progenitors comprising the proepicardium on the pericardial wall, and prevented the formation and migration of the epicardial layer around the heart. Zebrafish lacking *sox9b* showed pericardial edema, an elongated heart and reduced blood circulation. Fish lacking *sox9b* failed to form valve cushions and leaflets. *Sox9b* is one of two mammalian *Sox9* homologs, *sox9b* and *sox9a.* Knock down of *sox9a* expression did not cause cardiac malformations, or defects in epicardium development. We conclude that the decrease in *sox9b* expression in the heart caused by TCDD plays a role in many of the observed signs of cardiotoxicity. We find that while *sox9b* is expressed in myocardial cells, it is not normally expressed in the affected epicardial cells or progenitors. We therefore speculate that *sox9b* is involved in signals between the cardiomyocytes and the nascent epicardial cells.

INTRODUCTION

The zebrafish (*Danio rerio*) has been used as a model for studying the toxicity of 2,3,7,8-tetrachlorodibenzo-p-dioxin (TCDD) (Henry et al., 1997). By using zebrafish, it has been possible to determine that TCDD exposure during development causes heart failure and circulation collapse (Antkiewicz et al., 2005; Belair et al., 2001; Heideman et al., 2005). Interestingly, it is only during heart development that fish are sensitive to TCDD cardiotoxic effects: TCDD does not appear to harm the juvenile or adult heart (Hofsteen et al., 2013; Lanham et al., 2012).

In zebrafish, TCDD-induced heart malformation is associated with the loss of epicardium and the proepicardium (PE) (Plavicki et al., 2013). During the period before 48 hours post fertilization (hpf), TCDD exposure has no discernible effect on development of the zebrafish heart. However, after 48 hpf, TCDD-exposed hearts begin to deteriorate and unloop. The manifestation of cardiotoxicity corresponds to the timing of epicardium formation (Plavicki et al., 2013). The epicardium and epicardium derived progenitor cells are thought to play a critical role in cardiomyocyte proliferation, valve development, heart looping, generation of fibroblasts, cardiac morphogenesis, development of the coronary vasculature, and adult cardiac regeneration (Lepilina et al., 2006; Lie-Venema et al., 2007; Olivey and Svensson, 2010; Svensson, 2010). TCDD-induced epicardium failure accounts for most if not all of the observed cardiotoxicity.

TCDD-induced toxicity in zebrafish is mediated through the aryl hydrocarbon receptor (AHR) (Prasch et al., 2003). AHR is a ligand-activated transcription factor

belonging to the basic helix-loop-helix per-ARNT-Sim (PAS) family of DNA-binding proteins (Schmidt and Bradfield, 1996). TCDD-activation of AHR leads to altered gene expression. While identification of DNA sequence motifs recognized by AHR allows us to better understand the activation of genes encoding cytochrome P-450s and other AHR-battery genes (Chang and Puga, 1998), it has remained difficult to link AHR regulation of a specific target gene with toxic responses. A recent study showed that TCDD-induced jaw malformation in developing zebrafish is caused by downregulation of *sox9b* (Xiong et al., 2008).

Sox9b is a critical chondrogenic transcription factor, derived from an ancestral genome duplication in teleost fish that produced two *sox9* homologs in zebrafish: *sox9a* and *sox9b* (Yan et al., 2005). In humans, *SOX9* mutations cause campomelic dysplasia, producing defects in long bones, jaw, palate, axial skeleton, heart development, and reproductive systems. It is particularly interesting that campomelic dysplasia patients suffer from a defect in heart development known as the Teratology of Fallot (Houston et al., 1983). The discovery that TCDD downregulates *sox9b* and the similarity between known developmental effects of *sox9b* mutation and TCDD developmental toxicity ed us to the question: might TCDD-induced heart malformation in zebrafish larvae be caused by downregulation of *sox9b*?

Here we report that *sox9b* is expressed in the developing zebrafish heart, and that this expression is reduced by TCDD. We also show that loss of *sox9b* causes cardiac malformation, pericardial edema, and decreased circulation. Furthermore, *sox9b* is required for PE, epicardium, and valve formation.

MATERIALS and METHODS

Zebrafish husbandry. Lines used were: AB wild type, *sox9b*^{b971} (Yan et al., 2005), *pard3:EGFP (ET(Krt4:EGFP)*^{spe27}) (Poon et al., 2010), *tcf21:DsRed (Tg(tcf21:DsRed2)*^{pd32}) (Kikuchi et al., 2011), *sox9b:EGFP* (Tg(*-2450/0sox9b:EGFP*)) (manuscript in preparation), Tg(*cmlc2:GFP*) and Tg(*flk:GFP*) (Cross et al., 2003). All embryos were housed in water buffered with Instant Ocean salts (60 mg/L; Aquarium Systems, Mentor, OH) at 27 °C with a 14h/10h light/dark cycle. All procedures involving zebrafish were approved by the Animal Care and Use Committee of the University of Wisconsin-Madison, and adhered to the National Institutes of Health's "Guide for the Care and Use of Laboratory Animals".

TCDD exposure. Embryos were collected at 2-4 hpf and exposed to TCDD (1ng/ml; 99% purity; Chemsyn, Lenexa, KS) or dimethyl sulfoxide (DMSO) vehicle (0.1%) with gentle rocking for 1 h in glass scintillation vials (10 embryos per ml) as described (Carney et al., 2006a). After the exposure, embryos were rinsed with water and returned to culture vessels.

Heart extraction and quantitative PCR. Hearts were extracted from 72 hpf *cmlc2:GFP* embryos using shearing as previously described (Burns and MacRae, 2006; Carney et al., 2006a). Three independent replicate experiments were conducted, with each replicate using total RNA from 200 hearts for both TCDD and controls. The RNA was extracted using a QIAGEN RNeasy Minikit following the manufacture's protocol, and cDNA was synthesized using oligo(dT) primers and a Superscript II RT cDNA synthesis kit (Invitrogen).

The qRT-PCR was performed as described previously using a Light Cycler (Roche Applied Science Indianapolis, IN) and SYBR green (Carney et al., 2006a). Standard curves were made using serial dilutions of *sox9b* and *b-actin* plasmid DNA. Primers were: *β-actin*: forward, 5' -aag cag gag tac gat gag tc- 3'; reverse, 5' -tgg agt cct cag atg cat tg- 3' and *sox9b*: forward primer, 5' -tga cga gtt gtt ctc cag ag- 3'; reverse primer, 5' -agg cca cac gtc tat aac cc- 3'. *Sox9b* mRNA levels were normalized to *β-actin* to generate a relative expression ratio. Statistical analysis was performed using Minitab 12. Significance was determined using one-way ANOVA followed by Fisher's least significant difference test ($p<0.05$).

Pericardial edema and heart length. Larvae were mounted in 3% methylcellulose and imaged laterally at 8.5X on a Leica MZ16 stereomicroscope using a 1.5x lens. Pericardial area and heart length were measured using NIH Image J 1.44 software (http://rsb.info.nih.gov/nih-image/). Boundaries of the pericardial area were traced and the computer determined pericardial area. Length of the heart was measured with a segmented line that started at the beginning of the inflow tract, travelled across the atrium to the atrioventricular (AV) junction, and then continued straight across the ventricle to the outflow attachment. The computer then calculated the length of this line. Three replicate experiments (n=3) were conducted using groups of control or TCDD-treated fish with 50-100 fish per group. Statistical analysis was performed using Minitab 12. Significance was determined using t-tests followed by Fisher's least significant difference test and Levine's test ($p<0.05$).

Red blood cell perfusion rate. Red blood cell (RBC) perfusion rates were measured at 96 hpf as previously described (Carney et al., 2006b; Prasch et al.,

2003). Larvae were mounted in 3% methylcellulose and 10 second videos of the caudal end of the tail were taken using a MotionScope camera (RedLake) mounted on a Nikon TE300 inverted microscope. For each fish, the number of RBCs moving through a reference point in each of the four most caudal intersegmental vessels was measured, and the average was calculated (1 fish = 1n; n=10). Statistical analysis was performed using Minitab 12. Significance was determined using one-way ANOVA followed by Fisher's least significant difference test and Levine's test ($p<0.05$).

Histology. Zebrafish were fixed in 4% paraformaldehyde at 4°C overnight, dehydrated to ethanol, embedded in paraffin and sectioned (8 μm). Fish sections were stained with hematoxylin and eosin (King Heiden et al., 2009), and imaged using a Zeiss Axiocam digital camera mounted on a Zeiss Axioplan microscope.

***In situ* hybridization**. Whole mount *in situ* hybridization was conducted as previously described (Plavicki et al., 2013). A 560 base pair fragment of *sox9b* was amplified from embryonic zebrafish cDNA and subcloned into a pCRII-TOPO vector (invitrogen Corporation, Carlsbad, CA). Primers used were: 5'-gtg cag taa agc gca tct gaa-3' and 5'-gcg caa gta tgt gtg tgt gtg-3'. Synthesis of the *sox9b* probe, restriction enzyme used, and detection were conducted as previously described (Hofsteen et al., 2013).

Immunohistochemistry and confocal microscopy. Antibody staining was performed as previously described (Dong et al., 2007). The antibody against activated leukocyte cell adhesion molecule (ALCAM) was used at a 1:50 dilution in phosphate buffered saline with 4% bovine serum albumin and 0.3% Triton (PBT).

The antibody against DsRed (Anaspec, Fremont, CA) was used at a 1:200 dilution in PBT. Secondary antibodies (Alexa 488, Alexa 568; Invitrogen) were used at 1:100 dilution in PBT. Confocal images were collected on an Olympus Fluoview FV1000 microscope.

Proepicardium imaging. Live embryos were imaged in 3% methylcellulose using a Nikon TE300 inverted microscope attached to a Princeton Instruments Micromax CCD camera. Ten second videos showing the presumptive PE site were captured for each embryo using MotionScope software and analyzed using Metamorph software. This technique allowed us to differentiate the PE from surrounding tissue due to the PE remaining relatively stationary while adhered to the pericardium adjacent to the AV junction.

Morpholinos. All morpholino oligonucleotides (MOs) were from Gene Tools, LLC and used as previously reported (Antkiewicz et al., 2006; Prasch et al., 2003; Xiong et al., 2008). MOs were fluorescein tagged at the 3' ends to monitor injection success. The MO sequences were: sox9a, 5’ AAT GAA TTA CTC ACC TCC AAA GTT T 3’; sox9b, 5’ TGC AGT AAT TTA CCG GAG TGT TCT C 3’ (Yan et al., 2005). The standard Gene Tools Control MO (5’-CCT CTT ACC TCA GTT ACA ATT TAT A-3’) was used to control for non-specific responses. All zebrafish were injected at the 1-4 cell stage with 3 nl of 1 or 2 nM solution containing the MO with Fast Green (40 mg/ml) to allow visualization of the injected liquid with a dissecting microscope. Injected embryos were examined during blastula formation using epifluorescence microscopy for incorporation of the fluorescent MO into cells.

***Sox9b* mRNA injection.** Wild type (AB) embryos were injected with *sox9b* mRNA (200 pg) at the 1-4 cell stage. Shortly following mRNA injection, fish were exposed to either DMSO as a control (*n=46)* or TCDD (*n=73*) as described above. As a control, a subset of fish were exposed to DMSO (*n=50*) or TCDD (*n=50*) in parallel but were not injected. Fish were raised in 0.003% phenylthiouracil in the water to inhibit pigment formation and were analyzed for PE formation at 72 hpf as previously described. *Sox9b* mRNA was synthesized as described (Xiong et al., 2008). Briefly, a pCMV-Sport6ccd vector (Open Biosystems, Huntsville, AL) containing full-length *sox9b* was digested with *Not1* and the *sox9b* mRNA was synthesized with SP6 polymerase following manufacturer's instructions (SP6 mMessage mMachine Kit; Ambion, Austin, TX).

RESULTS

Zebrafish *sox9b* is expressed in the developing heart ventricle

We first sought to determine if *sox9b* was expressed in the developing zebrafish heart. *In situ* hybridization experiments showed a specific signal in the developing heart at 72 hpf, which became even more distinct at 96 hpf (Figure 1A and B). A *sox9b:EGFP* reporter line (*-2450/0sox9b:EGFP,* manuscript in preparation) showed a more distinct signal, allowing individual cells to be identified (Figure 1C and D). In these experiments, it was apparent that *sox9b* is expressed in myocardial cells, especially in the ventricle. The *in situ* hybridization and reporter expression patterns showed consistent evidence for *sox9b* expression in the zebrafish heart during the period of sensitivity to TCDD-induced cardiotoxicity.

TCDD and s*ox9b* expression in the larval heart

To determine if TCDD affects the expression of *sox9b* in the larval heart, we exposed the *sox9b:EGFP* reporter line to TCDD at fertilization and assessed *sox9b* expression in the heart at 72 hpf. Compared to the control, we consistently observed a noticeable decrease in the GFP signal in TCDD-exposed hearts (Figure 2A and B).

To directly measure downregulation of *sox9b* mRNA, fish were treated as before and hearts were isolated at 72 hpf for mRNA extraction and quantitative RT-PCR. TCDD caused an approximately 2-fold downregulation of *sox9b* mRNA in the TCDD-exposed hearts relative to the control hearts (Figure 2C). We conclude that TCDD downregulates *sox9b* in the developing zebrafish heart.

Loss of *sox9b* impairs heart development.

If *sox9b* downregulation by TCDD causes heart malformation, then other means of decreasing *sox9b* expression should also produce heart malformation. To test this, we examined developing hearts in *sox9b* deletion mutants. In these experiments, we crossed heterozygous *sox9b*^{b971} zebrafish, and examined cardiac function in the homozygous *sox9b*^{b971} null offspring. The hallmark phenotype identifying *sox9b*^{b971} null homozygotes is a pronounced curlydown or “corkscrew” tail. We therefore examined heart development in the ~25% offspring with this phenotype.

By 72 hpf, homozygous *sox9b*^{b971} nulls showed clear signs of heart malformation and pericardial edema (data not shown), that became more pronounced at 96 hpf (Figure 3). The pericardial edema observed in the *sox9b*^{b971} null homozygotes was very similar to that produced by TCDD. Furthermore, the

larval hearts showed an unlooping defect and heart elongation that resembled the response to TCDD. While both *sox9b*^{b971} nulls and TCDD-treated wild type fish had unlooped and elongated hearts, the heart chambers of the *sox9b*^{b971} null fish appeared more functional. The atrium in the TCDD-treated hearts was uniformly string-like with little apparent lumen, and a constricted ventricle. In contrast, loss of *sox9b* produced elongated chambers with open lumens.

Hallmark characteristics of TCDD-induced heart malformation include an unlooped extended heart and pronounced pericardial edema, or effusion (Antkiewicz et al., 2005; Antkiewicz et al., 2006). These phenotypes can be compared quantitatively by measuring pericardial area and heart length from the sinus venosus (SV) to the bulbous arteriosus (BA), producing the SV-BA distance at 96 hpf. In our measurements, the pericardial edema in both *sox9b* null and TCDD-treated larvae were significantly different from control, but not from each other (Table 1). The SV-BA distance in homozygous *sox9b*^{b971} null mutant heart was significantly longer than wild type hearts; however, the length in TCDD-exposed hearts was greater (Table 1), consistent with the more elongated appearance of the TCDD-treated heart in Figure 3.

We compared the effect of TCDD exposure and *sox9b* loss on red blood cell (RBC) flow, using video capture microscopy to follow RBC movement at a set of intersegmental vessels in the tail. At 96 hpf, we found that loss of *sox9b* caused an approximately 2-fold decrease in the RBC perfusion rate relative to wild type controls (Table 1). However, the decrease in RBC perfusion rate of *sox9b* null larvae did not

approach the complete halt of RBC movement in the tail of TCDD-exposed larvae (Antkiewicz et al., 2005; Belair et al., 2001).

We also used MOs to specifically block *sox9b* mRNA maturation and subsequent Sox9b protein production (Yan et al., 2005). We found that injection of the *sox9b* MOs phenocopied the curled tail and cardiac malformations observed in the homozygous *sox9b*^{b971} null mutants. This response was dose dependent: injection of the 1 nM stock produced mild pericardial edema and heart defects, without consistently producing the curly tail phenotype that characterizes complete loss of function (Figure 4). Injection of the 2 nM stock produced more severe cardiac defects ranging from that seen in Figure 4C to that shown in Figure 4D. With this higher dose, the curly tail phenotype was always evident. The control MO did not produce this phenotype at any concentration tested.

Overall, loss of *sox9b* produced substantial cardiac malformation with pronounced pericardial edema. This substantially overlapped the cardiotoxic effects of TCDD.

Loss of *sox9b* prevents zebrafish epicardium development

Zebrafish embryos exposed to TCDD do not form the cluster of epicardial progenitor cells comprising the PE, or the epicardial layer surrounding the heart (Plavicki et al., 2013). We examined hearts from homozygous *sox9b*^{b971} mutants at 120 hpf, a time when the epicardium should envelop the ventricle. H&E sections showed normal epicardial cells, identified as flat, oblong cells on the periphery of myocardium in the wild type sections (Figure 5). In contrast, these cells were not visible in sections from the *sox9b*^{b971} mutants.

We confirmed this finding by injecting the *sox9b*-specific MO into zebrafish lines carrying reporters marking epicardial cells. In the *tcf21:DsRed* reporter line (Kikuchi et al., 2011), epicardial cells are marked with a DsRed+ signal. In the *pard3:EGFP* line, the GFP is expressed in the epicardium (Poon et al., 2010). Epicardial cells marked with DsRed or GFP were consistently observed in the control MO fish, lying along the outermost layer of the heart ventricle to form a sheath of epithelial cells (Figure 5C, and E). However, the *sox9b* morphants, displaying the hallmark curly tail, lacked expression of either epicardial marker at 96 hpf (Figure 5D and F). We conclude that knockdown of *sox9b* prevents formation of the epicardium.

S*ox9b* is required for PE formation

We used video microscopy to identify the PE cluster forming at the region of the pericardium adjacent to the AV junction, where the PE forms (Liu and Stainier, 2010; Serluca, 2008). This allowed us to visualize the difference between the PE cluster, held stationary against the pericardial wall, and other clumps of cells associated with the moving heart. By 72 hpf the PE was clearly visible in the control fish, but not in fish failing to express *sox9b* (Figure 6). We were unable to find signs of PE formation in any homozygous *sox9b*^{b971} null mutants (Figure 6B), nor in fish injected with the *sox9b* MO (Figure 6C).

***Sox9b* is expressed in zebrafish myocardial cells**

We crossed the *sox9b* GFP reporter line with the *tcf21* reporter line to determine where *sox9b* is expressed during heart and epicardium development. We examined these fish at 3, 7 and 21 days post fertilization (Figure 7). The

development of the epicardium was clearly marked by DsRed fluorescence. However, the GFP signal from the *sox9b* reporter, while clearly evident in the myocardial cells, did not overlap the DsRed signal from the PE and epicardial cells.

Endocardial valve cushions do not form in *sox9b* morphants

After formation of the epicardial layer, epicardial derived cells migrate into the underlying myocardium and assist development of the cardiac valves (Lie-Venema et al., 2008; Lie-Venema et al., 2007). Given that TCDD prevents formation of the valve cushions (Mehta et al., 2008), and reduced levels of *sox9b* prevent epicardium development, we hypothesized that *sox9b* may be needed for zebrafish valve development. During the normal progression of valve development, a ring of endothelial cells forms marking the presumptive valve sites at the AV junction and the outflow junction between the ventricle and bulbus arteriosus (Bartman et al., 2004; Keegan et al., 2002). These rings of endothelial cells thicken to form cushions that mature into valve leaflets at the AV junction and outflow tract. We used a cardiac endothelial cell reporter line (*flk1:GFP*) to follow valve development. For these images, the cell adhesion molecule was visualized in red by immunostaining to show the surrounding heart cells. The formation of valve cushions and nascent valve leaflets at the AV junction can be seen at 96 hpf in the control heart shown in Figure 8, and more clearly at higher magnification in the panel at lower left. In contrast, the *sox9b* morphants lacked the cushion and leaflet, and had no accumulation of the GFP-labelled endothelial cells at the valve sites. Instead, the endothelial cells in the *sox9b*-deficient fish were distributed throughout the ventricle

and atrium. These results indicate that *sox9b* is necessary for valve cushion development.

Ectopic *sox9b* expression rescues PE formation in TCDD-treated embryos

The finding that loss of *sox9b* partially phenocopies TCDD toxicity suggests that TCDD causes cardiotoxicity by reducing *sox9b* expression. To test this we injected *sox9b* mRNA into embryos at the 1-4 cell stage and then treated the embryos with TCDD as described in the Methods. Expression of injected mRNA tends to follow a mosaic pattern, so not all of the injected embryos would be expected to express *sox9b* in the region of the heart, and might not be rescued. However, we found that a significant fraction of injected fish (19/73 = 26%) developed PEs, even in the presence of TCDD (Figure 9).

We found that while *sox9b* mRNA injection frequently restored PE formation, it never restored normal heart morphology, nor did we observe epicardial cell migration onto the heart. While rescue experiments are difficult to interpret this indicates that decreased *sox9b* produced by TCDD is responsible for the failure of PE formation.

Zebrafish *sox9a* morphants lack notable cardiac defects

Zebrafish have two copies of the mammalian *Sox9* gene, *sox9a* and *sox9b* (Chiang et al., 2001). It is not clear how much the functions of the two genes have diverged. Therefore, we injected *sox9a* MOs into the *pard3:EGFP* epicardial reporter line to determine whether loss of *sox9a* expression would also affect epicardium development.

The *sox9a* morphants exhibited the jaw phenotype reported by (Yan et al., 2005) (Figure S1), indicating that the *sox9a* MO had been effective in reducing *sox9a* expression. As with the previous work, we sometimes observed mild pericardial edema, the *sox9a* morphants did not have notable defects in the heart structure and in particular, the epicardium developed normally (Figure S1). These data indicate a divergent role between *sox9a* and *sox9b* during development of the zebrafish heart.

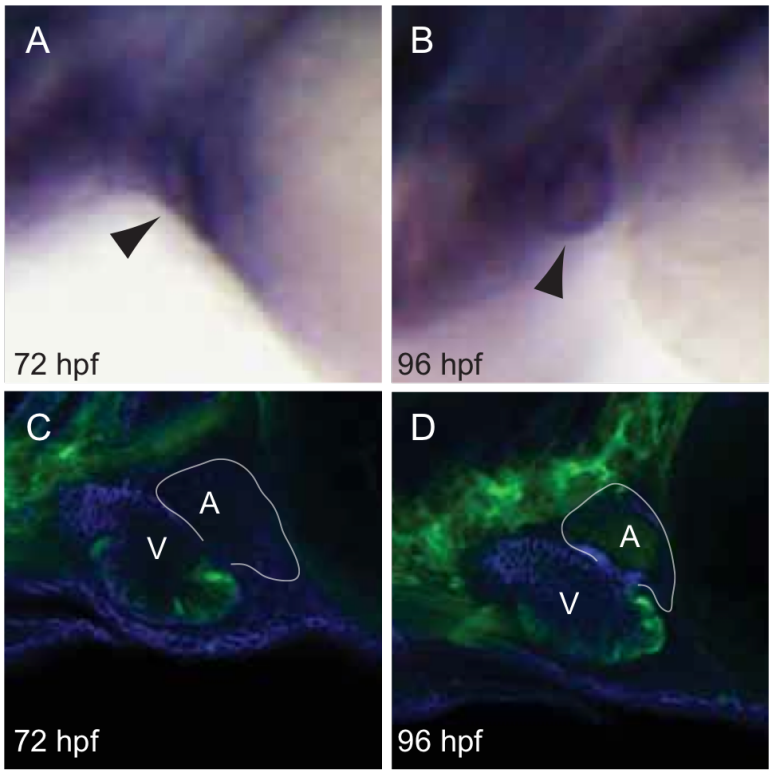

Figure 1. *Sox9b* is expressed in the zebrafish larval heart. Wild type AB zebrafish and carrying s*ox9b:EGFP* were collected at the indicated times for either *in situ* hybridization with a *sox9b* probe (A and B) or confocal microscopy (C and D). Lateral views are shown in all images, with head extending leftward, and the yolk sac to the right with n=6 fish examined per group. For the *in situ* images, the arrowheads point to the heart. For the confocal images, the white outline indicates the border of the atrium, indicated as A; the ventricle is indicated as V. The *sox9b*-GFP signal is shown in green. Blue indicates immunostaining for ALCAM.

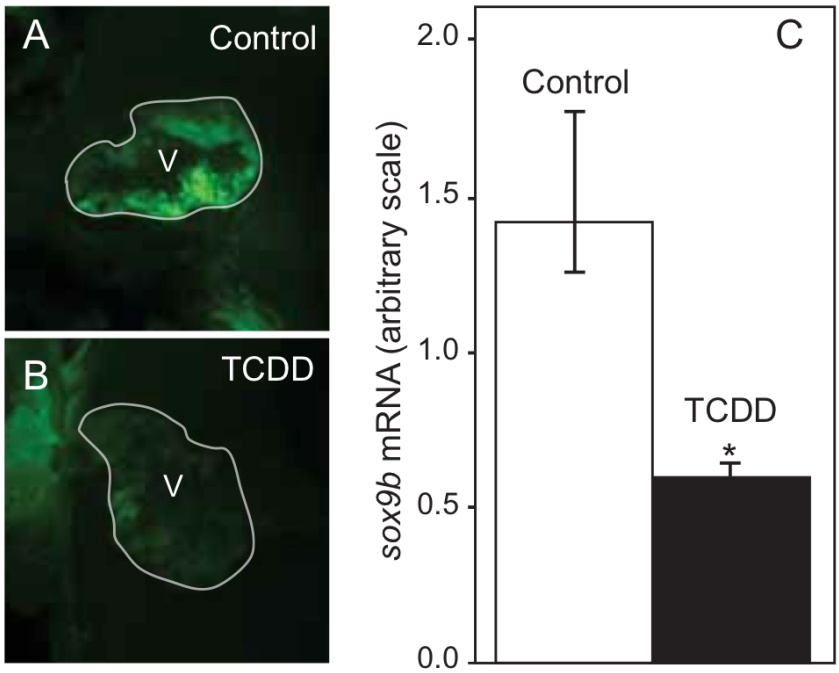

Figure 2. TCDD reduces *sox9b* expression in the zebrafish larval heart. Zebrafish embryos carrying the *sox9b:EGFP* reporter were exposed to TCDD as described in the Methods. Embryos were examined at 72 hpf using confocal microscopy and representative lateral images are shown (A) Control heart; (B) TCDD-treated. White outline denotes ventricle (V); anterior is to the left. (C) Hearts were isolated at 72 hpf for qRT-PCR measurement of *sox9b* expression, normalized to *β-actin* mRNA for each treatment group. Results are mean +/- SE, n=3 replicate experiments. Asterisk denotes significantly different from controls ($p<0.05$).

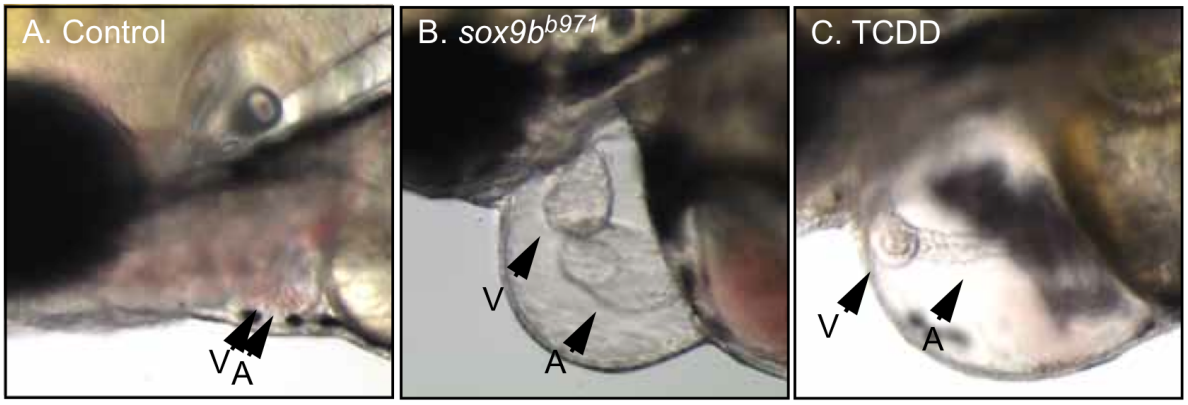

Figure 3. Loss of sox9b produces cardiac malformations that resemble those produced by TCDD. Representative brightfield photomicrographs of 96 hpf zebrafish. Lateral views are shown in all images, with head extending leftward, and the yolk sac to the right. Arrowheads denote location of the heart ventricle (V) and atrium (A). AB control and TCDD-treated fish are at left and right, respectively. The center panel shows a *sox9b*^{b971} homozygous mutant fish.

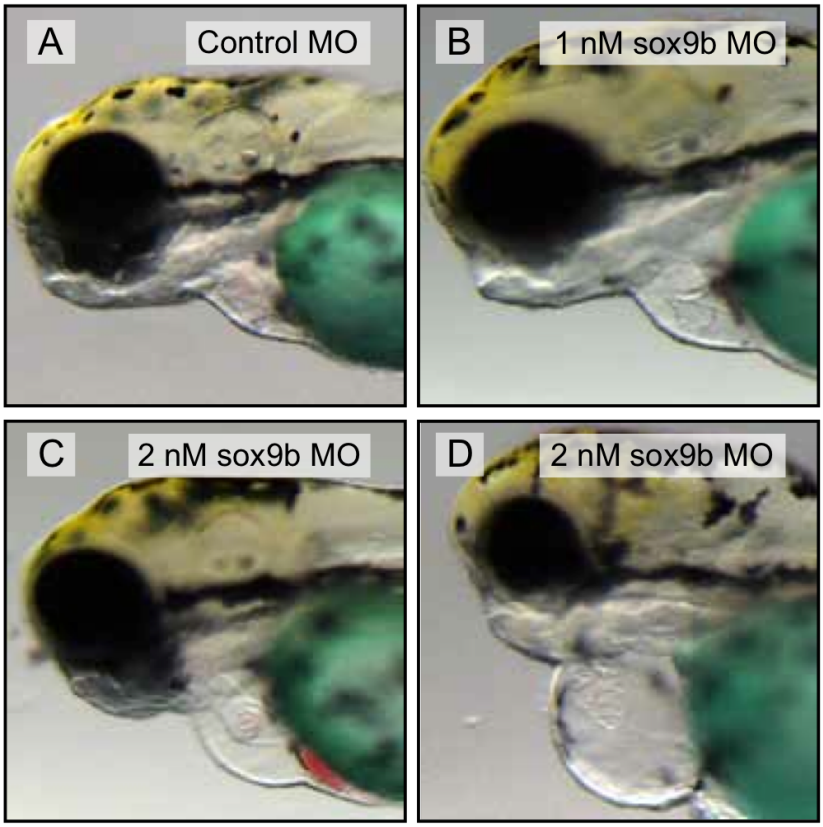

Figure 4. Graded doses of *sox9b* MO produce a range of cardiac malformation severity. Wild type zebrafish embryos were injected with control and sox9b MOs and collected at 96 hpf for brightfield microscopy. Representative brightfield lateral images are shown with anterior to the left. (A) Control MO; (B) sox9b MO (1 nM); (C and D) sox9b MO (2nM). The Fast Green used as part of the MO injection solution has colored the yolk green (n = 10 fish per treatment).

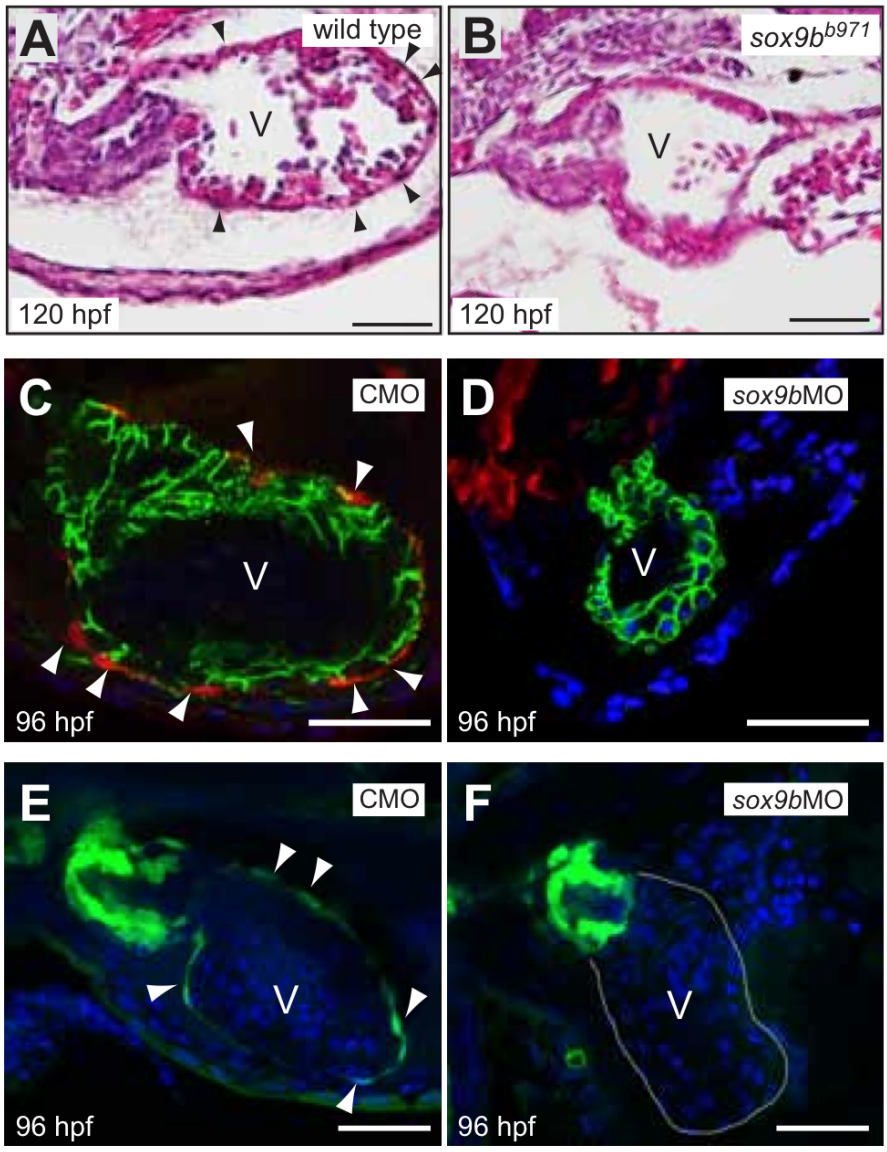
A
wild type
V
120 hpf
B
sox9b^b971
V
120 hpf
C
CMO
V
96 hpf
D
sox9bMO
V
96 hpf
E
CMO
V
96 hpf
F
sox9bMO
V
96 hpf

Figure 5. *Sox9b* is required for zebrafish epicardium development. (A and B) Brightfield images of hematoxylin and eosin stained hearts from representative wild type larva (A) and homozygous *sox9b*^{b971} null mutant larva (B) at 120 hpf. Black arrowheads indicate epicardial cells. (C and D) Embryos from the *tcf21:DsRed* reporter line marking epicardial cells were injected with the control or *sox9b* MO, and examined using confocal microscopy at 96 hpf for epicardium formation. Red indicates expression of *tcf21*, with white arrowheads indicating epicardial cells. Green indicates immunostaining for ALCAM, marking cell boundaries, and the blue is DAPI staining, revealing nuclei. (E and F) Eggs from the *pard3-GFP* reporter line marking epicardial cells were injected with the control or sox9b MO, and examined using confocal microscopy at 96 hpf for epicardium formation. Green indicates expression of *pard3* in epicardial cells which are indicated with white arrowheads. The blue is DAPI staining, revealing nuclei. For all panels representative images are shown with a minimum of n=6 per group. Scale bar = 50 μm.

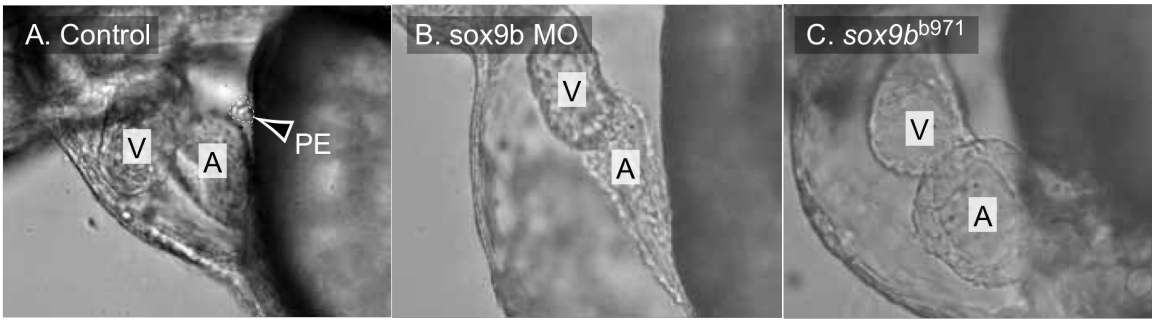

Figure 6. Formation of the proepicardium is dependent on *sox9b* expression. Representative lateral images of hearts within the pericardium of 72 hpf zebrafish. The left panel shows a wild type control; the middle panel shows a wild type zebrafish injected with sox9b MO; and the right panel shows a homozygous *sox9b*^{b971} mutant (n=10 per group; anterior to the left). Arrow and white outline indicate the "grape-like" PE in the wild type control, and not found in the others. The ventricles and atria are marked as V and A respectively.

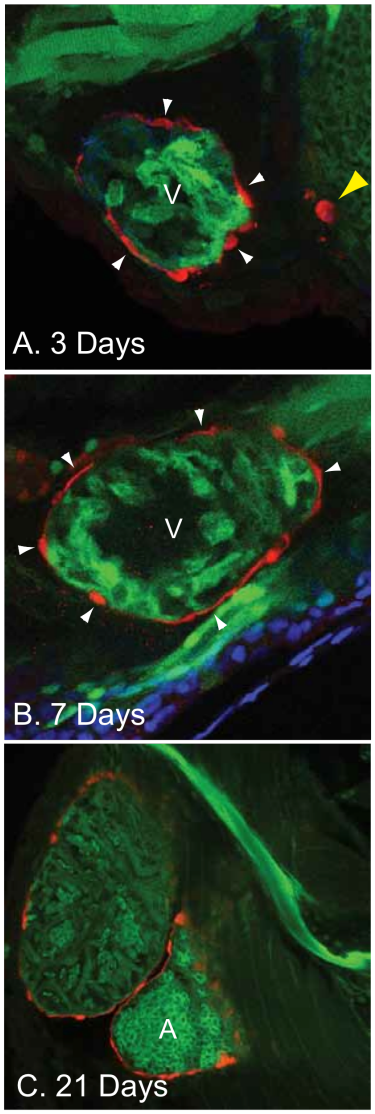

Figure 7. *Sox9b* is not expressed in proepicardial or epicardial cells. Representative ventral-lateral images of the zebrafish heart in reporter fish expressing both *sox9b:EGFP* and *tcf21:DsRed* with anterior to the left (n=minimum of 8 per group). The top panel shows the heart at 3 days post fertilization, the middle shows a heart at 7 days, and the bottom panel shows the heart at 3 weeks. The yellow arrowhead indicates the proepicardium, while white arrowheads denote epicardial cells.

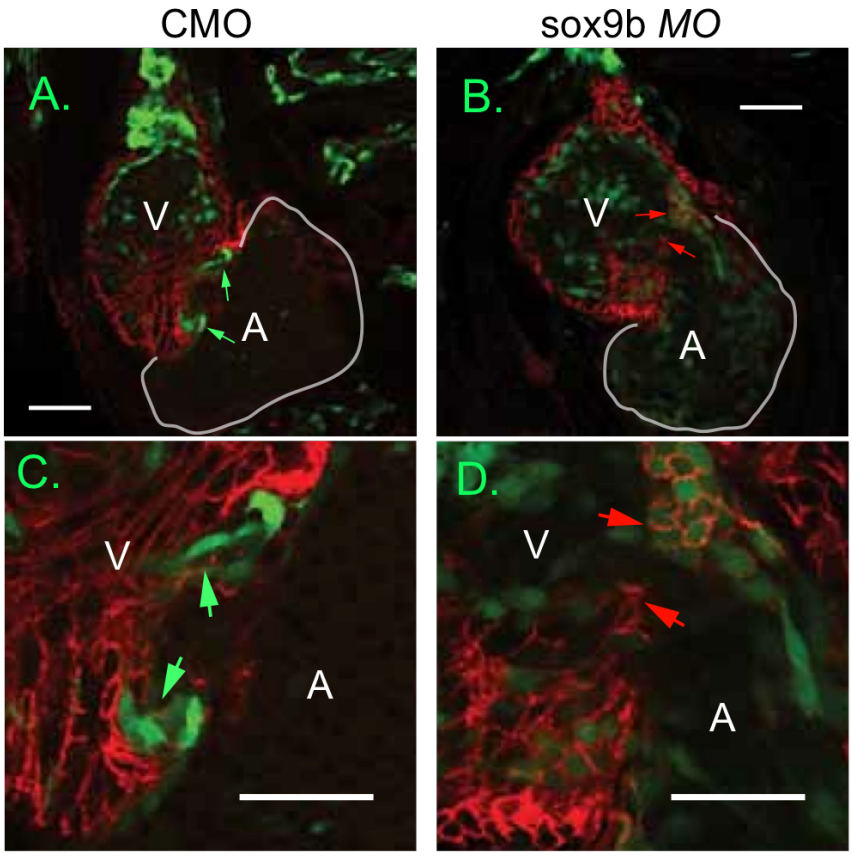

Figure 8. Endocardial valve cushions fail to form following loss of *sox9b*. Representative 96 hpf ventral images of *flk1:GFP* zebrafish that were injected with *sox9b* MO or control MO (n=5 per group). Samples were immunostained with ALCAM in red to show cell boundaries. The ventricles and atria are marked as V and A respectively. The green arrows indicate the valve cushions and nascent leaflets forming in the AV junction; the red arrows indicate the sites at the AV junction where valve cushions failed to form. Scale bar = 50 μm.

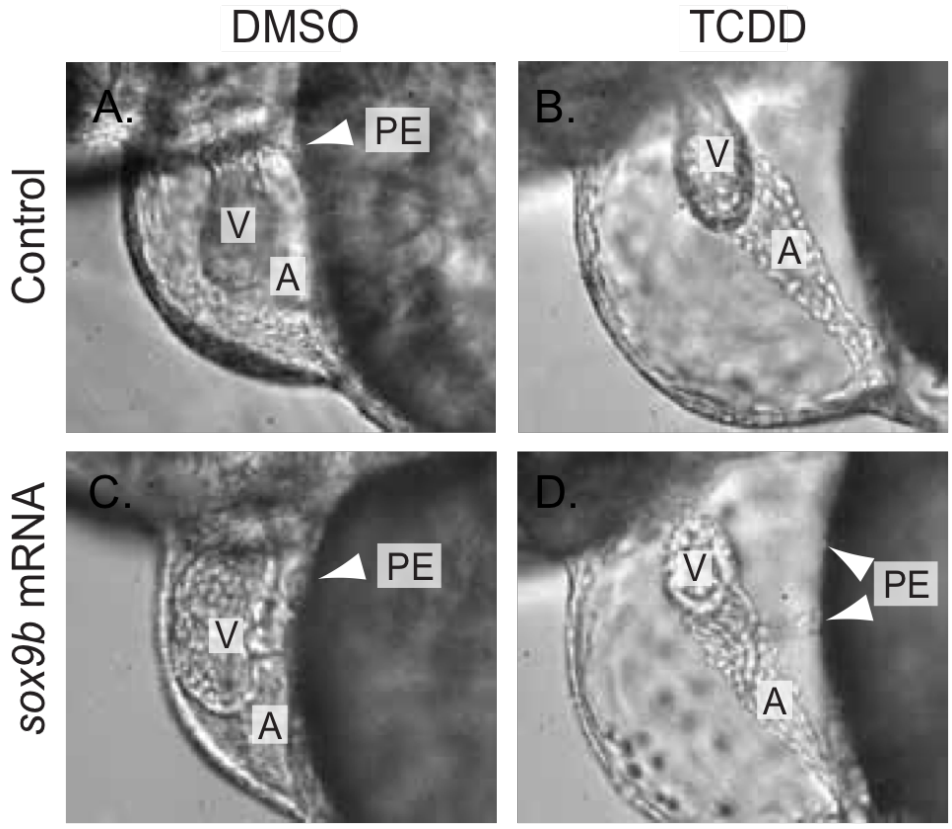

Figure 9. *Sox9b* mRNA injection can restore PE formation in fish treated with TCDD. Wild type (AB) embryos were injected with *sox9b* mRNA (200 pg) at the 1-4 cell stage, or left uninjected as controls. The embryos were then exposed to TCDD or vehicle (DMSO) as in previous experiments, as indicated. Images were collected with DIC microscopy at 72 hpf. The A, and V indicate the atrium and ventricle, respectively. Where present the PE is indicated by white arrowheads. Representative images are shown, with n= 46-73 individuals examined.

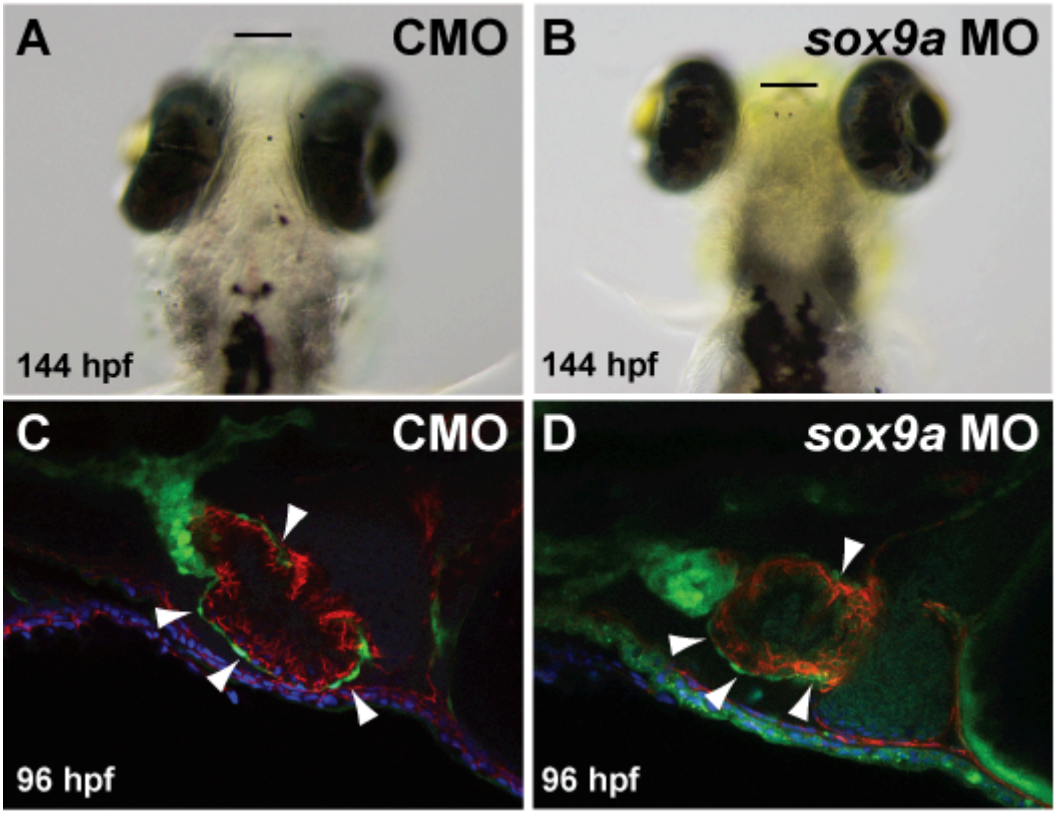

Figure S1. *Sox9a* is not required for zebrafish epicardium development. Transgenic *pard3:EGFP* fish were injected with *sox9a* MO or at the 1-4 cell stage. Shown are representative images of control MO (A, C) *sox9a* morphants (B, D) at 96 (confocal ventral-lateral anterior to the left; C, D) and 144 hpf (brightfield ventral anterior to the top; A, B). Black lines denote position of snout (A, B) and white arrowheads mark epicardial cells (C, D). Fish analyzed for epicardium development were counterstained with ALCAM in red and DAPI in blue (minimum n= 10 per group).

Table 1. Effect of *sox9b*-null mutation and TCDD treatment on pericardial area, heart length and blood flow.

Response	**Control**	***sox9b* null**	**TCDD**
Pericardial Area (μm^2)	44 ± 0.36	59 ± 4.0*	86 ± 1.0*
Heart Length (μm)	150 ± 5.8	220 ± 14.0*	320 ± 8.0 **
RBC Perfusion RBCs/10 sec)	63 ± 3	33 ± 7*	0**

Control, homozygous *sox9b*^{b971} deletion mutants, and TCDD-treated wild type fish were obtained by spawning and TCDD exposure as described in the Methods. Pericardial area, heart length, and blood flow rate were measured using videomicroscopy as described in the Methods. Results are presented as the mean ± the standard error of the mean. The single asterisk indicates significantly different from control; the double asterisk indicates significantly different from both control and the *sox9b* mutants ($P \leq 0.05$).

DISCUSSION

Sox9b and TCDD-induced heart malformation

As with the developing jaw, we found that TCDD downregulates *sox9b* in the embryonic zebrafish heart. From this, we hypothesized that the downregulation of *sox9b* expression might contribute to TCDD-induced heart malformation. We found that indeed, decreased *sox9b* expression largely phenocopied the cardiac malformations caused by TCDD. Loss of *sox9b* expression produced most, but not all, signs of TCDD-induced cardiotoxicity. Loss of *sox9b* expression was associated with pericardial edema, unlooping, loss of the PE, and failure to form the epicardium and endocardial cushions.

In previous work we used microarrays to search for AHR gene targets responsible for cardiotoxicity (Carney et al., 2006a). At the time, we were expecting to find genes upregulated by TCDD, and even though *sox9b* was found in the list of significantly altered genes presented in the supplementary data, it was downregulated by approximately 2-fold in the embryonic hearts examined in this experiment. It wasn't until we found a 14-fold downregulation of *sox9b* in the jaw that we began to consider genes downregulated by activated AHR as important (Xiong et al., 2008).

However, loss of *sox9b* did not produce the typical TCDD-induced compacted ventricle and elongated string-like atrium. Additionally, while TCDD treatment produced a complete halt in circulation, loss of *sox9b* slowed, but did not completely stop circulation. Homozygous *sox9b*^{b971} mutants are completely lacking *sox9b*, while TCDD produces an approximately 50% decrease in *sox9b* mRNA in the heart.

Therefore, we conclude that TCDD-induced downregulation of *sox9b* can account for some, but not all of the cardiotoxic effects of TCDD.

The overlap between the effects of TCDD and loss of *sox9b* suggested that downregulation of *sox9b* by TCDD exposure leads to some of the cardiotoxicity observed. Our attempts to rescue the cardiotoxicity by injection of extra *sox9b* mRNA sheds some light on this. The restoration of the PE in TCDD-treated fish by *sox9b* addition supports the idea that downregulation of *sox9b* plays a role in the loss of the PE and subsequent failure of epicardium formation. However, *sox9b* mRNA did not prevent other forms of TCDD cardiotoxicity.

Rescue experiments are generally difficult because it is unlikely that whatever manipulation is chosen will precisely reverse the loss of the biological molecule in question. For example, bulk injection of *sox9b* mRNA cannot be expected to undo cell-specific losses of endogenous *sox9b* mRNA caused by TCDD. The situation is even harder in cases such as ours, in which we already know that loss of *sox9b* cannot account for all of the cardiotoxicity produced by TCDD. In this case, complete rescue would be very surprising, while no rescue at all would not be unexpected: adding back *sox9b* cannot reverse *sox9b*-independent TCDD effects. Despite this perhaps pessimistic view, we observed some rescue. The failure to rescue heart malformation could be attributed to a number of factors including the possibility that the mRNA persisted only long enough to ensure PE specification but not for 3 days of heart development, the possibility that expression in the heart was somehow inadequate, and the simple possibility that the heart malformation is due to

some factor other than *sox9b* loss. More specific and sophisticated experiments will be needed to distinguish between these and other possibilities.

It is possible that TCDD affects both the heart and the vasculature to produce the observed circulation collapse. TCDD activates AHR in the vascular endothelium of fish, birds, and mammals, and suppresses vascular remodeling of the rat placenta, and coronary vasculogenesis in the chicken embryo (Ishimura et al., 2006; Ivnitski-Steele et al., 2005). In lake trout and zebrafish larvae TCDD induces cytochrome P4501A in the vascular endothelium (Andreasen et al., 2002; Cook et al., 2003). Furthermore, TCDD induces a rearrangement of the zebrafish proencephalic artery, and a reduction in mesencephalic blood flow (Kubota et al., 2011; Teraoka et al., 2010).

Sox9 and the vertebrate heart

In the mouse heart, *Sox9* has been implicated in endocardial cushion formation and valve leaflet remodeling (Akiyama et al., 2004; Lincoln et al., 2004; Montero et al., 2002). Furthermore, loss of *Sox9* expression in *Sox9$^{flox/flox}$:Tie2-cre* mice resulted in embryonic death between E11.5 and E14.5 days post conception (dpc). These mice exhibited pericardial edema and increased blood pooling (Lincoln et al., 2007). Akiyama and colleagues also documented embryonic death at E11.5 and 12 dpc in *Sox9*-null mutants. These S*ox9* null mice had severe blood vessel dilation, suggesting congestive heart failure (Akiyama et al., 2004). In both cases, death occurred during the temporal developmental window of the murine epicardium. Furthermore, the cardiac phenotype seen in *Sox9* null mice is strikingly similar to the phenotype that we found in *sox9b* null zebrafish larvae.

Although the functional role for *Sox9* may be conserved in the zebrafish, we found an interesting divergence in expression pattern. In mice, most myocardial cells do not express *Sox9*. Murine *Sox9* is expressed in epicardial cells undergoing epithelial to mesenchymal transition as they invade the myocardium (Smith et al., 2011). Sox9 is expressed in the developing chick heart around and in the valve cushion mesenchyme, but not broadly across the myocardium. In the zebrafish heart, we found *sox9b* expressed in myocardial cells, but not in epicardial cells.

S*ox9b* and the epicardium

Although loss of *sox9b* was ultimately devastating, *sox9b* expression was dispensable for initial heart chamber formation. A similar pattern was observed in fish exposed to TCDD. In both cases, the appearance of cardiac malformation coincided with the normal timing of PE and epicardium formation. Thus, we speculate that most of the cardiac malformations observed in response to TCDD exposure or loss of *sox9b* can be attributed to loss of the PE and epicardium (Plavicki et al., 2013).

In recent experiments, we demonstrated that ectopic expression of a constitutively active AHR from the *cmlc2* promoter causes cardiac malformations characterized by loss of the epicardium (WH and REP, unpublished). Therefore, events downstream of AHR in myocardial cells disrupt the formation and migration of epicardial cells. Furthermore, while *sox9b* expression was critical for the formation of the epicardium, we found *sox9b* expressed in ventricular cardiomyocytes but not in cells of the PE or epicardium. The genes regulated by the S*ox9* transcription factor are primarily proteins that make up the extracellular matrix (Lincoln et al.,

2007; Rahkonen et al., 2003). Since the epicardium is derived from an extracardiac source of progenitor cells that migrate to and differentiate at the heart (Lie-Venema et al., 2007; Serluca, 2008), we speculate that *sox9b* in cardiomyocytes provides extracellular signals that guide PE development and epicardium migration. In our model, this signal is disrupted by TCDD.

Conclusion

TCDD and related compounds have been known for some time to disrupt development by activating a specific receptor, AHR. However, the identities of genes regulated by AHR that mediate TCDD-induced heart malformation remain largely unknown. Here we show that, as in the developing jaw, *sox9b* is a downstream target of AHR in the heart. We may find that misregulation of *sox9b* becomes a common thread in AHR-mediated developmental toxicity.

While it seems obvious that the outer layer of the heart is needed for normal function, we do not understand how it forms. We show here that expression of *sox9b* is required for assembly of progenitor cells on the pericardium wall, and subsequent formation of the epicardium. We note that *sox9b* is found in cardiomyocytes awaiting the outer layer, not in the epicardial cells that fail to form, and plays an important role in regulating the production of proteins needed for extracellular matrices such as collagen. We speculate that *sox9b* is involved in extracellular signaling to nascent epicardial cells.

ACKNOWLEDGEMENTS

We thank Dorothy Nesbit for expert assistance. We thank K. Poss, V. Korzh, J. Postlethwait, and D. Graham for zebrafish lines and advice.

SOURCES OF FUNDING

Supported by the National Institutes of Health (NIH) grant R01 ES012716 from the National Institute of Environmental Health Sciences (NIEHS) and the University of Wisconsin Sea Grant Institute, National Sea Grant College Program, National Oceanic and Atmospheric Administration, U.S. Department of Commerce grant number NA 16RG2257, Sea Grant Project R/BT-25.

REFERENCES

Akiyama, H., Chaboissier, M.C., Behringer, R.R., Rowitch, D.H., Schedl, A., Epstein, J.A., and de Crombrugghe, B. (2004). Essential role of Sox9 in the pathway that controls formation of cardiac valves and septa. Proceedings of the National Academy of Sciences of the United States of America *101*, 6502-6507.

Andreasen, E.A., Spitsbergen, J.M., Tanguay, R.L., Stegeman, J.J., Heideman, W., and Peterson, R.E. (2002). Tissue-specific expression of AHR2, ARNT2, and CYP1A in zebrafish embryos and larvae: effects of developmental stage and 2,3,7,8-tetrachlorodibenzo-p-dioxin exposure. Toxicol Sci *68*, 403-419.

Antkiewicz, D.S., Burns, C.G., Carney, S.A., Peterson, R.E., and Heideman, W. (2005). Heart malformation is an early response to TCDD in embryonic zebrafish. Toxicol Sci *84*, 368-377.

Antkiewicz, D.S., Peterson, R.E., and Heideman, W. (2006). Blocking expression of AHR2 and ARNT1 in zebrafish larvae protects against cardiac toxicity of 2,3,7,8-tetrachlorodibenzo-p-dioxin. Toxicol Sci *94*, 175-182.

Bartman, T., Walsh, E.C., Wen, K.K., McKane, M., Ren, J., Alexander, J., Rubenstein, P.A., and Stainier, D.Y. (2004). Early myocardial function affects endocardial cushion development in zebrafish. PLoS Biol *2*, E129.

Belair, C.D., Peterson, R.E., and Heideman, W. (2001). Disruption of erythropoiesis by dioxin in the zebrafish. Dev Dyn *222*, 581-594.

Burns, C.G., and MacRae, C.A. (2006). Purification of hearts from zebrafish embryos. Biotechniques *40*, 274, 276, 278 passim.

Carney, S.A., Chen, J., Burns, C.G., Xiong, K.M., Peterson, R.E., and Heideman, W. (2006a). Aryl hydrocarbon receptor activation produces heart-specific transcriptional and toxic responses in developing zebrafish. Molecular pharmacology *70*, 549-561.

Carney, S.A., Prasch, A.L., Heideman, W., and Peterson, R.E. (2006b). Understanding dioxin developmental toxicity using the zebrafish model. Birth defects research *76*, 7-18.

Chang, C.Y., and Puga, A. (1998). Constitutive activation of the aromatic hydrocarbon receptor. Mol Cell Biol *18*, 525-535.

Chiang, E.F., Pai, C.I., Wyatt, M., Yan, Y.L., Postlethwait, J., and Chung, B. (2001). Two sox9 genes on duplicated zebrafish chromosomes: expression of similar transcription activators in distinct sites. Developmental biology *231*, 149-163.

Cook, P.M., Robbins, J.A., Endicott, D.D., Lodge, K.B., Guiney, P.D., Walker, M.K., Zabel, E.W., and Peterson, R.E. (2003). Effects of aryl hydrocarbon receptor-mediated early life stage toxicity on lake trout populations in Lake Ontario during the 20th century. Environ Sci Technol *37*, 3864-3877.

Cross, L.M., Cook, M.A., Lin, S., Chen, J.N., and Rubinstein, A.L. (2003). Rapid analysis of angiogenesis drugs in a live fluorescent zebrafish assay. Arteriosclerosis, thrombosis, and vascular biology *23*, 911-912.

Heideman, W., Antkiewicz, D.S., Carney, S.A., and Peterson, R.E. (2005). Zebrafish and cardiac toxicology. Cardiovasc Toxicol *5*, 203-214.

Henry, T.R., Spitsbergen, J.M., Hornung, M.W., Abnet, C.C., and Peterson, R.E. (1997). Early life stage toxicity of 2,3,7,8-tetrachlorodibenzo-p-dioxin in zebrafish (Danio rerio). Toxicology and applied pharmacology *142*, 56-68.

Hofsteen, P., Mehta, V., Kim, M.S., Peterson, R.E., and Heideman, W. (2013). TCDD inhibits heart regeneration in adult zebrafish. Toxicol Sci *132*, 211-221.

Houston, C.S., Opitz, J.M., Spranger, J.W., Macpherson, R.I., Reed, M.H., Gilbert, E.F., Herrmann, J., and Schinzel, A. (1983). The campomelic syndrome: review, report of 17 cases, and follow-up on the currently 17-year-old boy first reported by Maroteaux et al in 1971. Am J Med Genet *15*, 3-28.

Ishimura, R., Kawakami, T., Ohsako, S., Nohara, K., and Tohyama, C. (2006). Suppressive effect of 2,3,7,8-tetrachlorodibenzo-p-dioxin on vascular remodeling that takes place in the normal labyrinth zone of rat placenta during late gestation. Toxicol Sci *91*, 265-274.

Ivnitski-Steele, I.D., Friggens, M., Chavez, M., and Walker, M.K. (2005). 2,3,7,8-tetrachlorodibenzo-p-dioxin (TCDD) inhibition of coronary vasculogenesis is mediated, in part, by reduced responsiveness to endogenous angiogenic stimuli, including vascular endothelial growth factor A (VEGF-A). Birth defects research *73*, 440-446.

Keegan, B.R., Feldman, J.L., Lee, D.H., Koos, D.S., Ho, R.K., Stainier, D.Y., and Yelon, D. (2002). The elongation factors Pandora/Spt6 and Foggy/Spt5 promote transcription in the zebrafish embryo. Development (Cambridge, England) *129*, 1623-1632.

Kikuchi, K., Gupta, V., Wang, J., Holdway, J.E., Wills, A.A., Fang, Y., and Poss, K.D. (2011). tcf21+ epicardial cells adopt non-myocardial fates during zebrafish heart development and regeneration. Development (Cambridge, England) *138*, 2895-2902.

King Heiden, T.C., Spitsbergen, J., Heideman, W., and Peterson, R.E. (2009). Persistent adverse effects on health and reproduction caused by exposure of zebrafish to 2,3,7,8-tetrachlorodibenzo-p-dioxin during early development and gonad differentiation. Toxicol Sci *109*, 75-87.

Kubota, A., Stegeman, J.J., Woodin, B.R., Iwanaga, T., Harano, R., Peterson, R.E., Hiraga, T., and Teraoka, H. (2011). Role of zebrafish cytochrome P450 CYP1C genes in the reduced mesencephalic vein blood flow caused by activation of AHR2. Toxicology and applied pharmacology *253*, 244-252.

Lanham, K.A., Peterson, R.E., and Heideman, W. (2012). Sensitivity to Dioxin Decreases as Zebrafish Mature. Toxicol Sci.

Lepilina, A., Coon, A.N., Kikuchi, K., Holdway, J.E., Roberts, R.W., Burns, C.G., and Poss, K.D. (2006). A dynamic epicardial injury response supports progenitor cell activity during zebrafish heart regeneration. Cell *127*, 607-619.

Lie-Venema, H., Eralp, I., Markwald, R.R., van den Akker, N.M., Wijffels, M.C., Kolditz, D.P., van der Laarse, A., Schalij, M.J., Poelmann, R.E., Bogers, A.J.*, et al.* (2008). Periostin expression by epicardium-derived cells is involved in the development of the atrioventricular valves and fibrous heart skeleton. Differentiation *76*, 809-819.

Lie-Venema, H., van den Akker, N.M., Bax, N.A., Winter, E.M., Maas, S., Kekarainen, T., Hoeben, R.C., deRuiter, M.C., Poelmann, R.E., and Gittenberger-de Groot, A.C. (2007). Origin, fate, and function of epicardium-derived cells (EPDCs) in normal and abnormal cardiac development. ScientificWorldJournal *7*, 1777-1798.

Lincoln, J., Alfieri, C.M., and Yutzey, K.E. (2004). Development of heart valve leaflets and supporting apparatus in chicken and mouse embryos. Dev Dyn *230*, 239-250.

Lincoln, J., Kist, R., Scherer, G., and Yutzey, K.E. (2007). Sox9 is required for precursor cell expansion and extracellular matrix organization during mouse heart valve development. Developmental biology *305*, 120-132.

Liu, J., and Stainier, D.Y. (2010). Tbx5 and Bmp signaling are essential for proepicardium specification in zebrafish. Circulation research *106*, 1818-1828.

Mehta, V., Peterson, R.E., and Heideman, W. (2008). 2,3,7,8-Tetrachlorodibenzo-p-dioxin Exposure Prevents Cardiac Valve Formation in Developing Zebrafish. Toxicol Sci *104*, 303-311.

Montero, J.A., Giron, B., Arrechedera, H., Cheng, Y.C., Scotting, P., Chimal-Monroy, J., Garcia-Porrero, J.A., and Hurle, J.M. (2002). Expression of Sox8, Sox9 and Sox10 in the developing valves and autonomic nerves of the embryonic heart. Mechanisms of development *118*, 199-202.

Olivey, H.E., and Svensson, E.C. (2010). Epicardial-myocardial signaling directing coronary vasculogenesis. Circulation research *106*, 818-832.

Plavicki, J., Hofsteen, P., Peterson, R.E., and Heideman, W. (2013). Dioxin inhibits zebrafish epicardium and proepicardium development. Toxicol Sci *131*, 558-567.

Poon, K.L., Liebling, M., Kondrychyn, I., Garcia-Lecea, M., and Korzh, V. (2010). Zebrafish cardiac enhancer trap lines: new tools for in vivo studies of cardiovascular development and disease. Dev Dyn *239*, 914-926.

Prasch, A.L., Teraoka, H., Carney, S.A., Dong, W., Hiraga, T., Stegeman, J.J., Heideman, W., and Peterson, R.E. (2003). Aryl hydrocarbon receptor 2 mediates 2,3,7,8-tetrachlorodibenzo-p-dioxin developmental toxicity in zebrafish. Toxicol Sci *76*, 138-150.

Rahkonen, O., Savontaus, M., Abdelwahid, E., Vuorio, E., and Jokinen, E. (2003). Expression patterns of cartilage collagens and Sox9 during mouse heart development. Histochem Cell Biol *120*, 103-110.

Schmidt, J.V., and Bradfield, C.A. (1996). Ah receptor signaling pathways. Ann Rev Cell Dev Biol *12*, 55-89.

Serluca, F.C. (2008). Development of the proepicardial organ in the zebrafish. Developmental biology *315*, 18-27.

Smith, C.L., Baek, S.T., Sung, C.Y., and Tallquist, M.D. (2011). Epicardial-derived cell epithelial-to-mesenchymal transition and fate specification require PDGF receptor signaling. Circulation research *108*, e15-26.

Svensson, E.C. (2010). Deciphering the signals specifying the proepicardium. Circulation research *106*, 1789-1790.

Teraoka, H., Ogawa, A., Kubota, A., Stegeman, J.J., Peterson, R.E., and Hiraga, T. (2010). Malformation of certain brain blood vessels caused by TCDD activation of Ahr2/Arnt1 signaling in developing zebrafish. Aquatic toxicology (Amsterdam, Netherlands) *99*, 241-247.

Xiong, K.M., Peterson, R.E., and Heideman, W. (2008). AHR-Mediated Downregulation of Sox9b Causes Jaw Malformation in Zebrafish Embryos. Molecular pharmacology *74*, 1544-1553.

Yan, Y.L., Willoughby, J., Liu, D., Crump, J.G., Wilson, C., Miller, C.T., Singer, A., Kimmel, C., Westerfield, M., and Postlethwait, J.H. (2005). A pair of Sox: distinct and overlapping functions of zebrafish sox9 co-orthologs in craniofacial and pectoral fin development. Development (Cambridge, England) *132*, 1069-1083.

Chapter V

Proepicardial Cell Migration and Epicardium Formation Require Heart Contraction

Jessica Plavicki, Peter Hofsteen, Kevin Lanham

Richard E. Peterson, and Warren Heideman

ABSTRACT

The epicardium, the outermost layer of the vertebrate heart, forms from a transient cluster of progenitor cells termed the proepicardium (PE). The PE cluster is located outside of the heart, adjacent to the atrioventricular junction. Cells within the PE cluster migrate on to the looped-heart, ultimately enveloping the myocardium to form the epicardium. Once formed, a subset of epicardial cells undergoes epithelial to mesenchymal transitions to form the vascular smooth muscle cells of the coronary arteries and to produce of cardiac fibroblasts. Impaired epicardial formation and function has been associated with defects in valve development, cardiomyocyte proliferation and alignment, cardiac conduction system maturation and adult heart regeneration. Zebrafish are an excellent model for studying cardiac development and regeneration; however, little is known about how the zebrafish epicardium forms. Here, we describe in detail PE migration and epicardium formation in zebrafish. We report that PE cells migrate to the myocardium via a PE bridge followed by release of PE aggregates that continuously supply epicardial progenitors. Lastly, myocardial contraction is required for migration of PE cells to the myocardium and subsequent development of the epicardium.

INTRODUCTION

Zebrafish (*Danio rerio*) are an established teleost model organism for studying heart development due to their high fecundity, translucent external development and the ability, as a result of passive oxygen diffusion, to survive without heart function during the first week of life (Kopp et al., 2005; Stainier et al., 1996; Wells and Pinder, 1996). Consequently, zebrafish are particularly advantageous for identifying genes critical for heart development. In higher vertebrates, mutations in genes required for heart development generally produce severe cardiac phenotypes and result in embryonic lethality. These characteristics make the zebrafish an ideal model to investigate the underlying cause(s) of heart failure as result of gene permutations and heart function.

The heart is derived from three distinct cell types: neural crest, cardiogenic mesoderm and the proepicardium (PE) (reviewed in Buckingham et al., 2005; Martin-Puig et al., 2008; Olson, 2006; Srivastava and Olson, 2000; Vincent and Buckingham, 2010). The PE is a transient extracardiac mesothelial source of progenitors that migrates to the naked heart following heart looping (Bakkers, 2011; Serluca, 2008). Once the epicardium has formed, a subset of epicardial cells undergoes epithelial-to-mesenchymal transitioning (EMT) to assist in the development and maturation of many cardiac tissues, such as the production of cardiac fibroblasts and vascular smooth muscle cells (Lie-Venema et al., 2007; Perez-Pomares et al., 2002). Epicardial impairment is also associated with defects in endocardial valve development, heart looping, cardiomyocyte proliferation and alignment, the cardiac conduction system and cardiac regeneration (reviewed in

Gittenberger-de Groot et al., 2012; Lie-Venema et al., 2007; Riley, 2012; Smart et al., 2012; Smart and Riley, 2012).

PE to epicardium transition varies between vertebrate species. The mammalian PE is thought to populate the myocardium by release of PE cell aggregates that are free floating and produce epicardial islands on the myocardium (Komiyama et al., 1987; Perez-Pomares et al., 1997; Schulte et al., 2007; Sengbusch et al., 2002; Van den Eijnde et al., 1995). In contrast, the avian PE protrudes towards the heart by formation of an extracellular matrix bridge of which PE cells transverse (Ho and Shimada, 1978; Manner, 1993; Nahirney et al., 2003). Amphibian models such as xenopus and axolotl develop a PE bridge prior to epicardium development (Fransen and Lemanski, 1990; Jahr et al., 2008) while it appears sturgeon form an epicardium by a combination of these mechanisms (Icardo et al., 2009).

It has recently been reported that zebrafish have an epicardium and, analogous to other vertebrates, forms from an extracardiac PE located on the pericardial wall adjacent the atrioventricular (AV) junction (Hu et al., 2000; Serluca, 2008). In addition, PE and epicardial expression of the transcription factors *tbx18*, *tcf21* and *wt1* is conserved across vertebrate species. However, how and when the epicardium forms in zebrafish remains poorly understood.

Here, we describe in detail multiple mechanisms of PE migration and the normal course of epicardial development in zebrafish. As in the mouse model, we find the zebrafish PE is a heterogeneous population of epicardium progenitors of

which we speculate are clonally dominant in the epicardium. We report PE migration and epicardium formation is dependent on myocardial contractility.

MATERIAL and METHODS

Zebrafish Strains. Adult zebrafish lines were maintained and zebrafish embryos were reared and housed according to procedures described by (Westerfield, 1995). The AB wild type line was used unless otherwise indicated. Transgenic lines used: *pard3:EGFP* [*ET(krt4:EGFP)*^{sqet27}] (Poon et al., 2010), *tcf21:DsRed* [*Tg(tcf21:DsRed2)*^{pd37}] (Kikuchi et al., 2011), and *cmlc2*:EGFP [*Tg(cmlc2:EGFP)*^{f1}] (Burns et al., 2005). All procedures involving animals were approved by the Animal Care and Use Committee of the University of Wisconsin-Madison, and adhered to the National Institutes of Health's "Guide for the Care and Use of Laboratory Animals."

Immunohistochemistry and Confocal Microscopy. Antibody staining was performed as previously described (Plavicki et al., 2013). The primary antibodies used at the following dilutions: mouse anti- *activated leukocyte cell adhesion molecule* (ALCAM/zn5; ZIRC) 1:50, rabbit anti-DsRed (AnaSpec, Fremont, CA) at 1:200 in PBT. Secondary anti mouse antibodies (Alexa 488, Alexa 568; Invitrogen) were used at 1:200 dilution. Embryos were mounted in Vectashield or Vectashield with Dapi (Vector Laboratories). Confocal images were collected on an Olympus Fluoview FV1000 microscope. Brightest point projections were made using Olympus Fluoview software and images were processed using Adobe Photoshop. Optical sections in z-series were collected at 0.52 μm intervals.

PE Imaging. Live embryos were imaged as previously described (Plavicki et al., 2013). Briefly, fish were imaged at 72 hpf in 3% methylcellulose using a Nikon TE300 inverted microscope attached to a Princeton Instruments Micromax CCD camera. Videos were collected using MotionsScope software and analyzed using Metamorph software.

Morpholinos and 2,3-Butanedione 2-monoxime (BDM). All morpholino oligonucleotides (MOs; Gene Tools, LLC) were used as previously reported (Prasch et al., 2003; Antkiewicz et al., 2006). The TNNT2 MO (5' CAT GTT TGC TCT GAT CTG ACA CGC A 3') was designed to block the translational start site of zebrafish cardiac troponin 2 (tnnt2; *silent heart*, *sih*). The standard Gene Tools Control MO (5'-CCT CTT ACC TCA GTT ACA ATT TAT A-3') was used to control for non-specific responses. One-cell embryos were injected with 2 ng of MO. BDM (Sigma Aldrich) was used at a final concentration of 10 mMol/L embryo water. This concentration reversibly reduces contractility by approximately 90% in zebrafish.

Tissue culture. Hearts from *cmlc2:EGFP*::*tcf21:DsRed* larvae were isolated at 72 hpf as described (Burns and MacRae, 2006) and placed in a matrigel (BD biosciences) coated culture plates. Hearts were incubated at 28°C with 5% CO_2 in cell culture media containing Leibovitz's L-15 (Invitrogen) with 10% fetal bovine serum (Sigma). Images were obtained using an Olympus SZX16 camera mounted on an Olympus DP72 epifluorescence stereomicroscope and imaged with cellSens software.

RESULTS

Zebrafish epicardium development

To better characterize the process of normal zebrafish epicardium development, we collected *pard3:EGFP* embryos at 72, 78, 84, 96, 120 and 168 hpf and counterstained with ALCAM to visualize the myocardium. Consistent with previous findings, we detected a PE cluster located near the AV junction at 72 hpf (Plavicki et al., 2013; Serluca, 2008)(Figure 1 A and A'). Thereafter, at 78, 84, and 96 hpf (Figure 1B through 1D'), we observed epicardial cells on the ventricle, but not the atrium. It was not until 120 hpf that epicardial cells were detected on the atrium. At this stage, epicardial coverage of the atrium was sparse**.** By 168 hpf, epicardial cells were clearly present on both heart chambers, however the epicardial coverage was not complete (Figure 1F and F').

Our results demonstrate an initial development of the PE on the pericardium, migration to the AV junction, a slow spreading of a sparse web of cells across the ventricle, and eventual coverage of the both the ventricle and atrium.

PE migration

We repeatedly observed the PE attached to the heart while still attached to the pericardium at 72 hpf, indicating PE to epicardium migration occurred via formation of a bridge (supplemental video 1). The formation of a PE bridge is more evident from histology and confocal images of the *tcf21* PE/epicardial reporter line (Figure 2A-D; arrows). Furthermore we consistently observe spherical shaped PE

cells undergoing morphogenetic changes as they migrate to the myocardium to become oblong polarized epicardial cells at 78 hpf (Figure 2D).

At 84 hpf, after epicardial cells were detected on the ventricle, we found that *tcf21+* cells were still present on the pericardial wall (Figure 3A). These data indicate PE cells continue to migrate on to the heart as the epicardium forms. While examining live embryos, we observed *tcf21+* cells or cell aggregates moving within the pericardial space. We found examples of cell aggregates clusters at 80 hpf (Figure 3A and A') and at 120 hpf (Figure 3 B and B') as well as *tcf21+* cell aggregates on the pericardial wall (Figure 3C and C'). Thus, suggesting that the migration of epicardial precursors on to the heart is not a discrete event but rather a continuous process. We conclude that epicardial progenitors initially protrude towards the heart during early epicardium development and migrate to the myocardium via a bridge. This is followed by the release of PE cell aggregates later in epicardial development.

The epicardium forms *in vitro* by few resident epicardial cells

Although the epicardium continuously receives PE cells during the first week *in vivo*, this continuous supply of PE cells is dispensable. Following isolation and culture of hearts at 76 hpf, a time when very few epicardial cells are present on the heart, the epicardium formed normally (Figure 4). When hearts were removed prior to PE migration, 40-48 hpf, the epicardium did not form (data not shown). These data indicate individual epicardial cells have proliferative potential.

Zebrafish PE and epicardium is a heterogeneous cell population

The murine PE and epicardium are heterogeneous cell populations that have divergent roles during heart development (Katz et al., 2012). In zebrafish, it is unknown if the PE or epicardium are heterogeneous. We collected z-series of the PE in *tcf21*:DsRed fish at 76 hpf and found that only a subset of PE cells expressed *tcf21* (Figure 5). Thus, indicating that zebrafish PE is a heterogeneous population of cells.

Next, we crossed *pard3* and *tcf21* reporter lines to determine epicardial heterogeneity. As shown in Figure 1, the cell polarity gene, *pard3* was expressed in all epicardial cells at 1-week post fertilization (wpf; Figure 5 A, B, B'). In contrast there were distinct regions of the epicardium that lacked *tcf21* expression (Figure 5 C, C', C", arrow). This was more pronounced later in development. By 6 wpf, we found continuous amorphic regions of the epicardium, which lacked *tcf21* expression (Figure 5 D, D', D"). Thus, indicating that the epicardium is made up of a heterogeneous population of cells.

Myocardial contraction is necessary for epicardial development

Heart function is necessary in late stages of cardiac development events such as the formation of valve cushions and subsequent valve development (Bartman et al., 2004). Interestingly, loss of the epicardium results in an unlooped, elongated heart that resembles the heart phenotype observed in *sih* mutants and morphants. To test if heart function plays a significant role in epicardium formation, we prevented heart contraction by injecting epicardial reporter lines with *sih* MOs and scored for epicardium formation at 96 hpf.

Confocal images taken at 96 hpf showed *tcf21*+ epicardial cells on the ventricle of the control heart, but not on the ventricle of heart from *sih* MO-injected larva (Figure 6A-B'). To confirm our finding, we also examined hearts from *pard3*:EGFP larvae that had been injected with *sih* MOs. Again, *pard3*+ cells were detected on the ventricle of control hearts, but no epicardial cells were found on hearts from *sih* morphants (Figure 6C-D').

As an alternative approach, we impaired myocardial contraction using the reversible myosin ATPase inhibitor, 2,3-butanedione 2-monoxime (BDM) (Bartman et al., 2004). Epicardial reporter lines exposed to BDM between 24 to 120 hpf (data not shown) or 48 to 120 hpf did not form an epicardium when compared to controls (Figure 7A-B'). Furthermore, exposure to BDM after epicardial cells were present on the myocardium (72-120 hpf and 96-120 hpf) resulted in fewer epicardial cells along the outermost surface of the heart when compared to controls (Figure 7C-D'). These results confirm heart contractility is necessary for epicardium formation and maturation in the zebrafish.

PE development occurs in the absence of myocardial contraction

To determine if loss of the epicardium was secondary to the loss of the PE, we examined PE development in *sih* MOs and BDM treated larvae and found the PE developed independent of heart contraction. Brightfield images show PE formation at 72 hpf in control, BDM-treated and *sih* MO-injected fish (Figure 8A and B). Furthermore, when BDM was removed at 72 hpf and heart contraction was restored, the PE was able to migrate to the myocardium and subsequently form an epicardium (Figure 8D-D'). Although it had been shown that *sih* morphants retained *tcf21*

expression at the presumptive site of the PE (Serluca, 2008), these data confirm the PE forms independently of heart contractility.

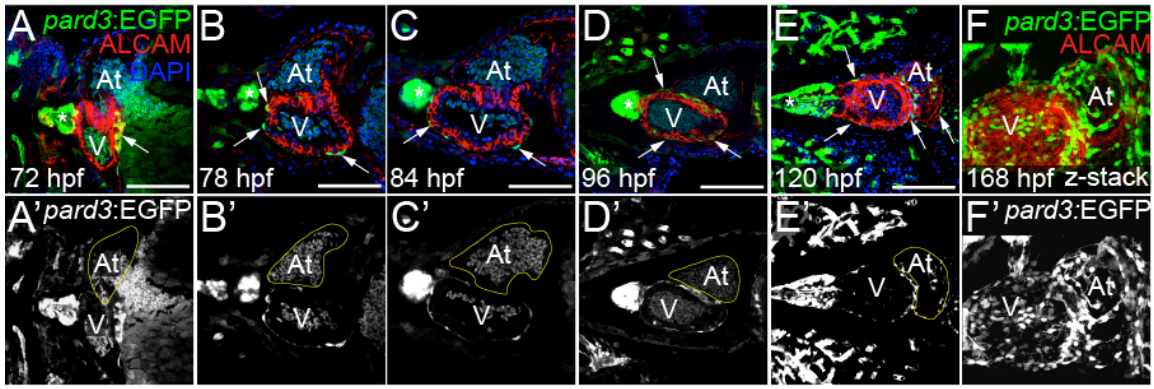

Figure 1: Normal zebrafish epicardium development. Zebrafish carrying a *pard3*:EGFP reporter were analyzed by confocal microscopy coupled with immunohistochemistry during epicardium development (A, A' – F, F'). Representative ventral images are shown with anterior to the left. All fish were counterstained with ALCAM in red and DAPI in blue. Ventricle = V, Atrium = At.

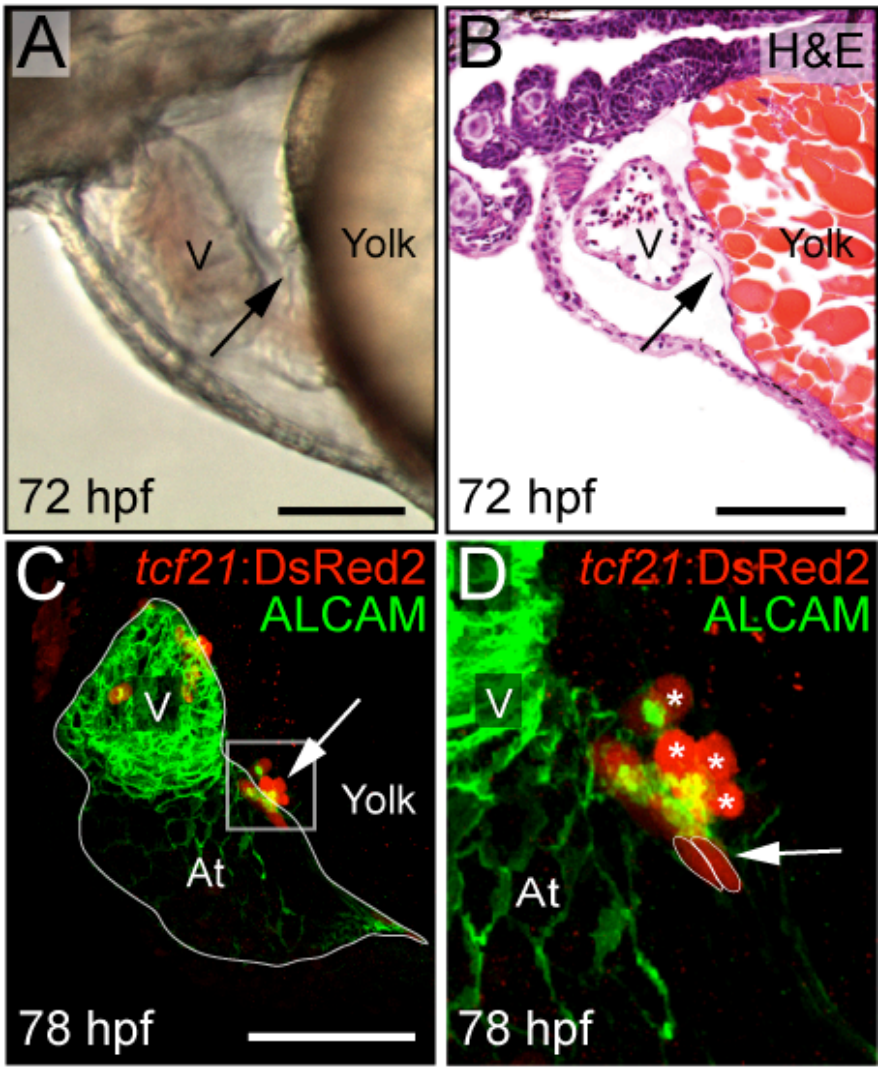

Figure 2: Initial zebrafish proepicardium (PE) to epicardium migration. Wild type (72 hpf; A, B) and *tcf21*:DsRed (78 hpf; C, D) fish were collected and imaged. Representative lateral Brightfield (A), sectioned and stained H&E (B) and confocal (C, D) images are shown with anterior to the left. Black arrows denote PE bridge. Asterisks denote spherical PE cells and white arrow in panel D denote oblong polarized epicardial cells. Immunohistochemistry samples were counterstained with ALCAM (C, D). The ventricle and atrium are indicated by V and At respectively.

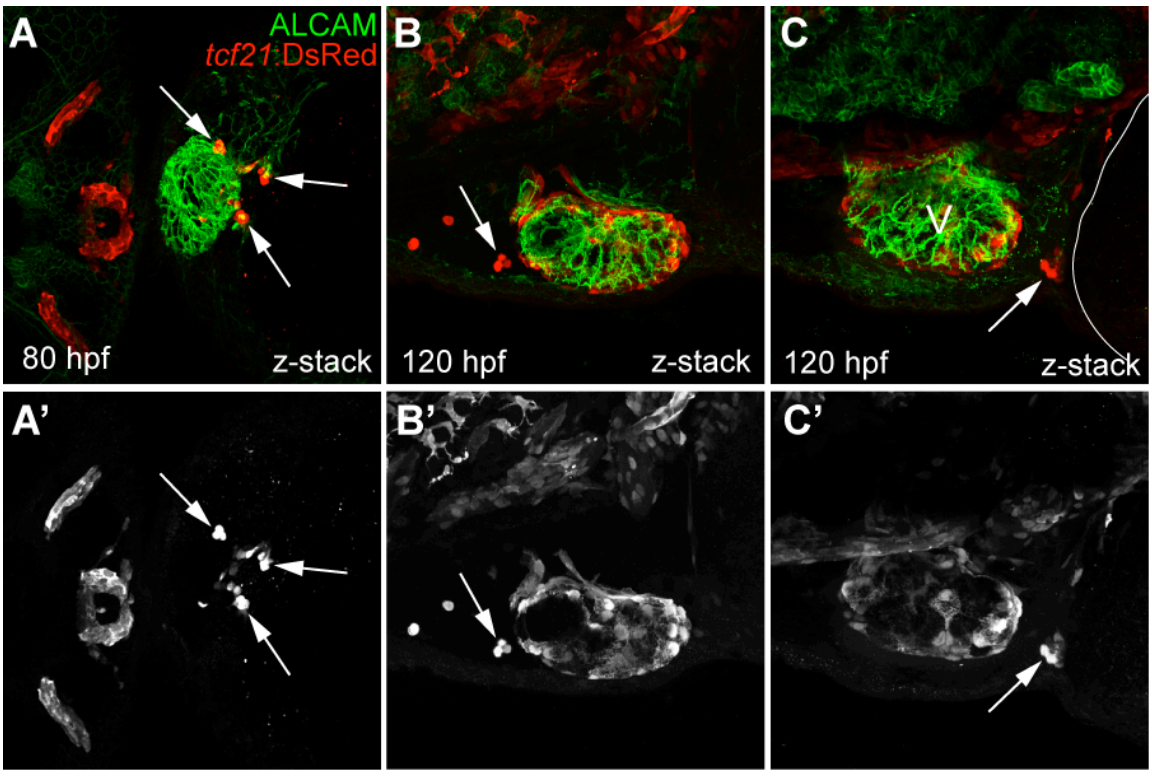

Figure 3: Pericardial PE cell aggregates contribute to late stage epicardium formation in zebrafish. Fish carrying the *tcf21:DsRed* reporter were examined by confocal microscopy and immunohistochemistry at 80 (A, A') and 120 (B, B' and C, C') hpf. All samples were counterstained with ALCAM. Representative ventral lateral images are shown with anterior to the left. Arrows denote PE cell clusters or PE cell aggregates. Ventricle and atrium are denoted as V and At respectively.

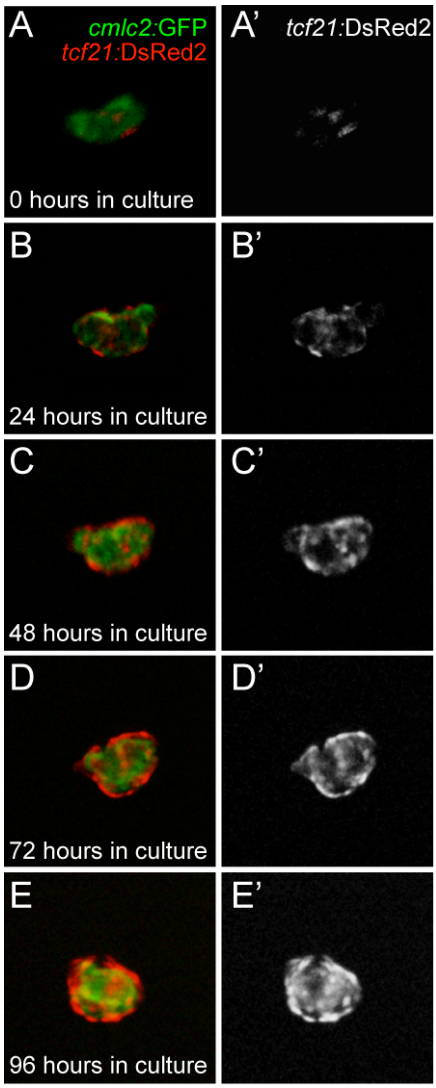

Figure 4: The epicardium forms in the absence of continuous supply of PE cells. Fish carrying *cmlc2:*GFP and *tcf21*:DsRed were euthanized at approximately 76 hpf and hearts were isolated for tissue culture. Cardiomyocytes are shown in green while epicardium is shown in red. Hearts were imaged at 0 (A, A'), 24 (B, B'), 48 (C, C'), 72 (D, D') and 96 (E, E') hours in culture.

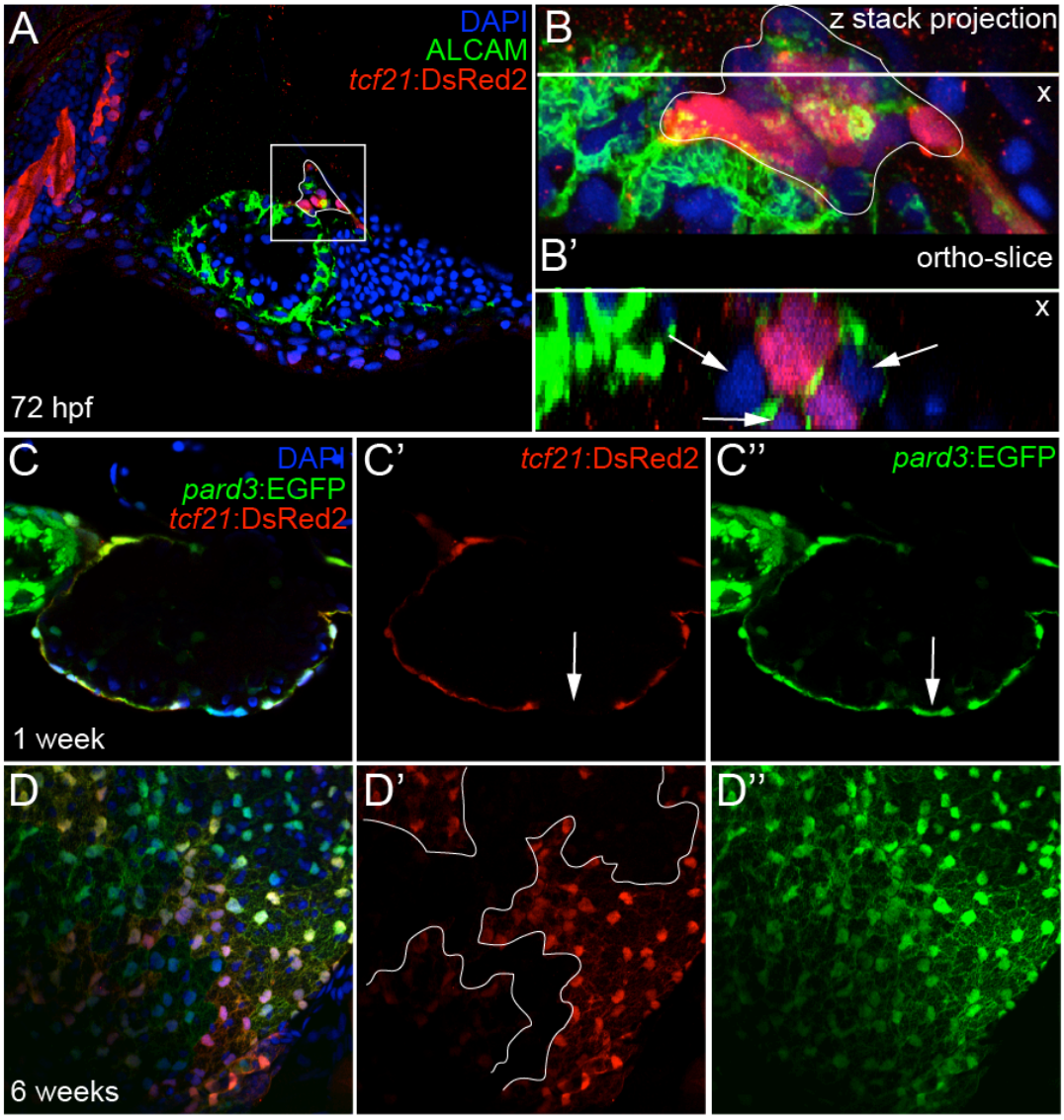

Figure 5: Heterogeneity of the zebrafish PE and epicardium. Zebrafish (*tcf21:DsRed*) were collected at 72 hpf and counterstained with ALCAM and DAPI (A, B, B') and imaged by confocal microscopy. Arrows in panal B' denote non-*tcf21* expressing PE cells. Fish carrying *tcf21:DsRed* and *pard3*:EGFP were collected at 1 week (C, C', C") and 6 weeks (D, D', D"), counterstained with DAPI and imaged by confocal microscopy. Arrows indicate region of the epicardium that is devoid of *tcf21* (B', B").

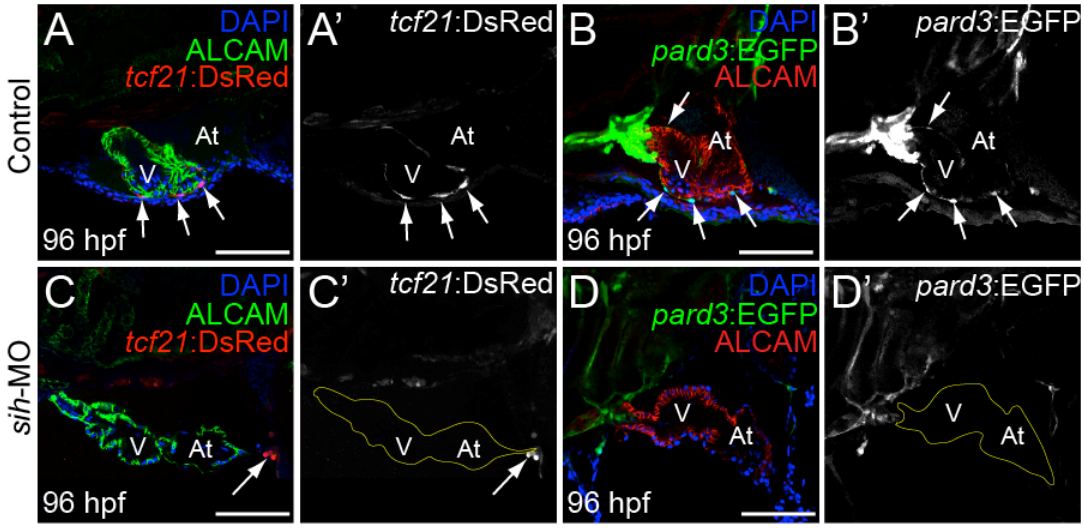

Figure 6: Loss of heart function prevents epicardium formation. Zebrafish carrying either *tcf21*:DsRed (A, A' and C, C') or *pard3*:EGFP (B, B' and D, D') were injected with *sih*MO (C, C' and D, D') or control (A, A' and B, B') at the one cell stage and examined at 96 hpf. Arrows in the control samples denote epicardial cells while arrows in the *sih*MO panels (C, C') denote putative PE cells. All samples were counterstained with ALCAM (green; A and C, red; B and D) and DAPI in blue. Representative ventral lateral images are shown with anterior to the left. Ventricle and atrium are denoted as V and At respectively.

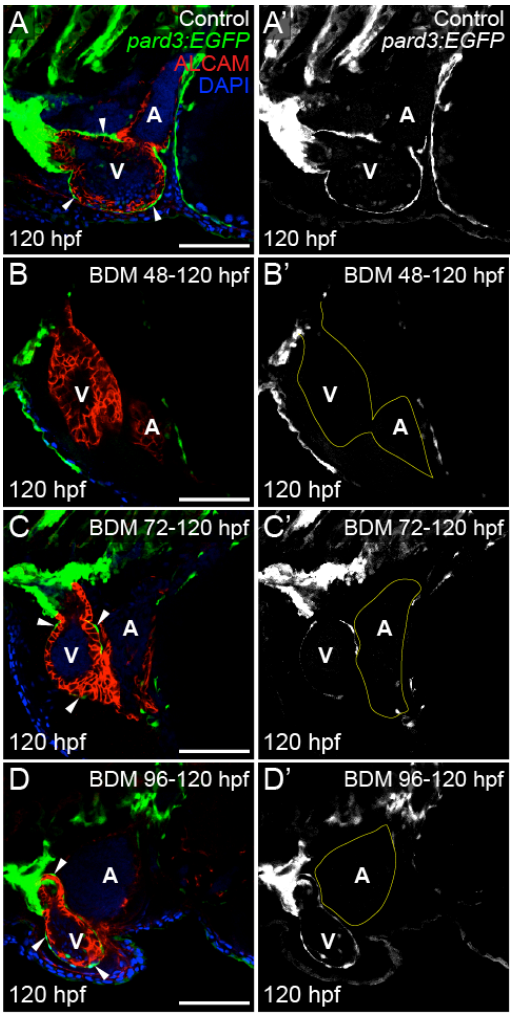

Figure 7: Loss of contractility halts epicardium progression. Zebrafish carrying *pard:*EGFP were exposed to BDM during epicardium development and collected at 120 hpf for confocal microscopy and immunohistochemistry. Representative ventral lateral images are shown with anterior to the left. White arrowheads denote epicardial cells on the heart ventricle. Samples were counterstained with ALCAM and DAPI to visualize the myocardium and nuclei respectively. Ventricle and atrium are denoted as V and A respectively.

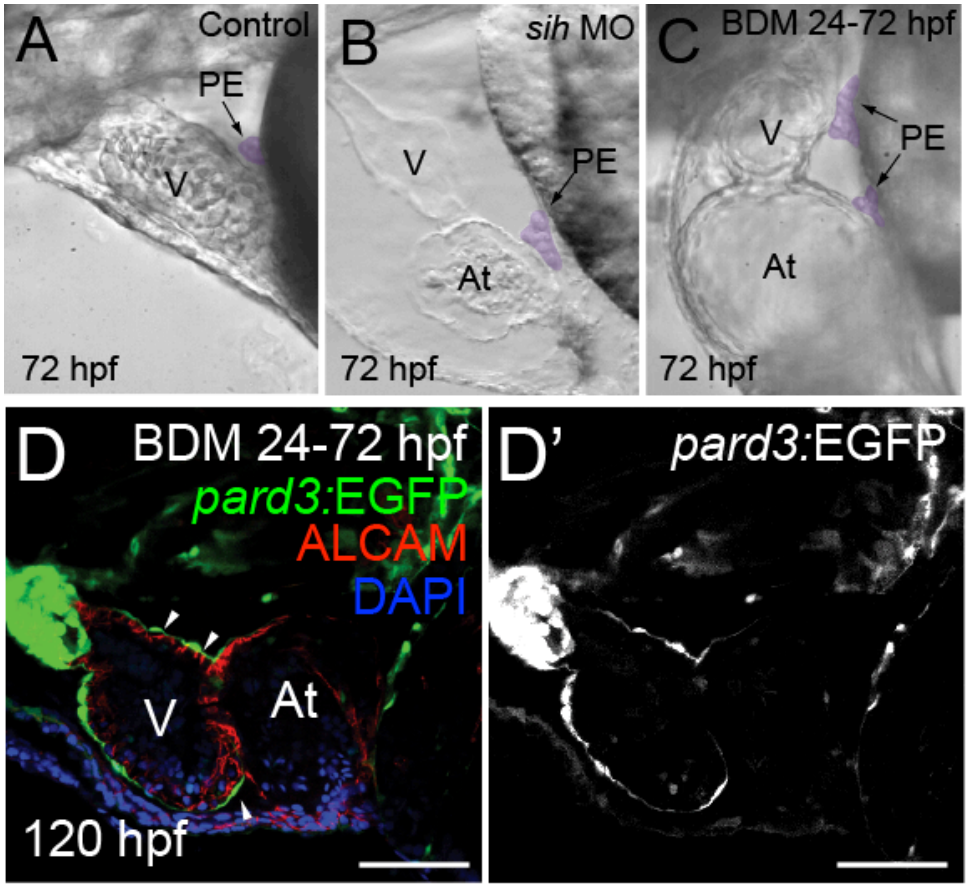

Figure 8: Heart contractility is dispensable for PE formation and heart contractility is required for epicardium formation. Wild type (A) zebrafish were injected with *sih*MO (B) or exposed to BDM (C) to stop heart contractility. Representative lateral brightfield images are shown (A-C) and the PE is pseudocolored in purple as indicated by black arrows. Fish carrying the *pard3:EGFP* were exposed to BDM from 24-72hpf then removed to restore heart contractility and were imaged at 120 hpf. Representative ventral lateral confocal images are shown with anterior to the left. White arrowheads denote epicardial cells. Confocal images were counterstained with ALCAM and DAPI. Ventricle and atrium are denoted as V and At respectively.

DISCUSSION

Here, we detail zebrafish epicardium development. As in other vertebrates, the PE migrates and envelops the myocardium following heart looping. In zebrafish, the epicardium forms over the ventricle followed by atrium envelopment. The epicardium is a late stage developmental event that occurs after the heart has begun beating. Heart contraction is known to affect other late stage steps in cardiac development such as valve development (Bartman et al., 2004). Consequently, we investigated whether heart function was necessary for epicardium formation. The PE formed in the absence of heart function, but failed to migrate to the myocardium and the epicardium did not form. In many cases, we observed the PE in physical contact with the myocardium but migration to the myocardium did not occur. These results suggest loss of contractility disrupts the mechanics of epicardium formation. We used BDM, a reversible inhibitor of heart contraction, to manipulate heart contraction at during different periods of epicardium development. If heart contraction was restored at 72 hpf, when the PE migration normally begins, the epicardium formed.

In the chick embryo, the PE migrates towards to the myocardium by an extracellular matrix bridge (Nahirney et al., 2003) whereas the murine epicardium is formed by release of PE cell aggregates into the pericardial cavity (Schulte et al., 2007). In our experiments, we demonstrate the zebrafish PE protrudes towards the heart in a bridge-like manner to provide the nascent epicardial cells followed by release of PE aggregates during later stages of epicardium development.

Much like the mouse, the zebrafish PE and epicardium are a heterogeneous cell population. In mice, subsets of PE and epicardial cells contribute to divergent

tissue types in the heart such as the coronary vascular endothelial cells (Katz et al., 2012). Furthermore, there has been discussion of two distinct PEs in the chick; the venous pole PE (vPE) and the arterial pole PE (aPE). It is thought the vPE and aPE contribute to divergent tissues types of the heart such as fibroblast and the valves or coronary vessels (Gittenberger-de Groot et al., 2012). It is unknown whether the zebrafish epicardium plays a significant role in downstream tissue development as it does in mice and chick. Very little is known about zebrafish cardiac fibroblasts or coronary vasculature. On the contrary, many of the same abnormalities occur in the zebrafish, when compared to chick and mouse, following epicardial impairment: aberrant endocardial valve defects, heart unlooping and defects in the cardiac conduction system (Bartman et al., 2004; Mehta et al., 2008; Plavicki et al., 2013).

As previously reported, the zebrafish PE forms independently of myocardial contractility (Serluca, 2008). Our experiments indicate the PE forms and is in physical contact with the developing heart, but fails to migrate to form the epicardium. In controls, we observe spherical PE cells that acquire an epithelial oblong shape as they migrate and form the epicardium (Figure 2). With heart contractility impaired, PE cells remain spherical and never attain an epithelial-like shape. Furthermore, *sih* morphants show *tcf21*, but not *pard3,* expression at the atrial pole. This indicates the residual PE cells have potential defects in cell polarity. The planar cell polarity pathway plays a substantial role in PE cell migration. In mice, loss of *Par3* results in failure of PE cell migration (Hirose et al., 2006). In zebrafish, this pathway has also been shown to be important in epicardium development. Serluca showed

knockdown of the cell polarity genes heart and soul (*has/aPKC/PRKCl*) and *nagie oko (nok)* result in aberrant defects in PE morphogenesis (Serluca, 2008). Together, loss of *pard3* and failure of PE cells to undergo cellular morphogenesis to an epithelial-like shape in the *sih* morphant suggests PE cell polarity is dependent on myocardial contractility. Furthermore, when we impaired heart contractility during PE formation (0-72 hpf) but not epicardium formation (72-120), PE cells became polarized, expressed *pard3* and the epicardium formed normally.

This report illustrates the importance of heart function during zebrafish epicardium development. Loss of myocardial contractility resulted in failure of PE cells to become epithelial-like migratory cells. During the course of this study, we have shown evolutionarily conserved elements of epicardium development that are shared between fish, birds and mammals. We speculate the normal process of PE cell polarity and migration to form the epicardium is dependent on heart contractility.

REFERENCES

Bakkers, J. (2011). Zebrafish as a model to study cardiac development and human cardiac disease. Cardiovasc Res *91*, 279-288.

Bartman, T., Walsh, E.C., Wen, K.K., McKane, M., Ren, J., Alexander, J., Rubenstein, P.A., and

Stainier, D.Y. (2004). Early myocardial function affects endocardial cushion development in zebrafish. PLoS Biol *2*, E129.

Buckingham, M., Meilhac, S., and Zaffran, S. (2005). Building the mammalian heart from two sources of myocardial cells. Nat Rev Genet *6*, 826-835.

Burns, C.G., and MacRae, C.A. (2006). Purification of hearts from zebrafish embryos. Biotechniques *40*, 274, 276, 278 passim.

Burns, C.G., Milan, D.J., Grande, E.J., Rottbauer, W., MacRae, C.A., and Fishman, M.C. (2005).

High-throughput assay for small molecules that modulate zebrafish embryonic heart rate. Nat Chem Biol *1*, 263-264.

Fransen, M.E., and Lemanski, L.F. (1990). Epicardial development in the axolotl, Ambystoma mexicanum. The Anatomical record *226*, 228-236.

Gittenberger-de Groot, A.C., Winter, E.M., Bartelings, M.M., Jose Goumans, M., Deruiter, M.C., and Poelmann, R.E. (2012). The arterial and cardiac epicardium in development, disease and repair. Differentiation *84*, 41-53.

Hirose, T., Karasawa, M., Sugitani, Y., Fujisawa, M., Akimoto, K., Ohno, S., and Noda, T. (2006). PAR3 is essential for cyst-mediated epicardial development by establishing apical cortical domains. Development *133*, 1389-1398.

Ho, E., and Shimada, Y. (1978). Formation of the epicardium studied with the scanning electron microscope. Dev Biol *66*, 579-585.

Hu, N., Sedmera, D., Yost, H.J., and Clark, E.B. (2000). Structure and function of the developing zebrafish heart. The Anatomical record *260*, 148-157.

Icardo, J.M., Guerrero, A., Duran, A.C., Colvee, E., Domezain, A., and Sans-Coma, V. (2009). The development of the epicardium in the sturgeon Acipenser naccarii. Anat Rec (Hoboken) *292*, 1593-1601.

Jahr, M., Schlueter, J., Brand, T., and Manner, J. (2008). Development of the proepicardium in Xenopus laevis. Dev Dyn *237*, 3088-3096.
Katz, T.C., Singh, M.K., Degenhardt, K., Rivera-Feliciano, J., Johnson, R.L., Epstein, J.A., and Tabin, C.J. (2012). Distinct compartments of the proepicardial organ give rise to coronary vascular endothelial cells. Dev Cell *22*, 639-650.

Kikuchi, K., Gupta, V., Wang, J., Holdway, J.E., Wills, A.A., Fang, Y., and Poss, K.D. (2011). tcf21+ epicardial cells adopt non-myocardial fates during zebrafish heart development and regeneration. Development *138*, 2895-2902.

Komiyama, M., Ito, K., and Shimada, Y. (1987). Origin and development of the epicardium in the mouse embryo. Anat Embryol (Berl) *176*, 183-189.

Kopp, R., Schwerte, T., and Pelster, B. (2005). Cardiac performance in the zebrafish breakdance mutant. J Exp Biol *208*, 2123-2134.

Lie-Venema, H., van den Akker, N.M., Bax, N.A., Winter, E.M., Maas, S., Kekarainen, T., Hoeben, R.C., deRuiter, M.C., Poelmann, R.E., and Gittenberger-de

Groot, A.C. (2007). Origin, fate, and function of epicardium-derived cells (EPDCs) in normal and abnormal cardiac development. ScientificWorldJournal *7*, 1777-1798.

Manner, J. (1993). Experimental study on the formation of the epicardium in chick embryos. Anat Embryol (Berl) *187*, 281-289.

Martin-Puig, S., Wang, Z., and Chien, K.R. (2008). Lives of a heart cell: tracing the origins of cardiac progenitors. Cell Stem Cell *2*, 320-331.

Mehta, V., Peterson, R.E., and Heideman, W. (2008). 2,3,7,8-Tetrachlorodibenzo-p-dioxin exposure prevents cardiac valve formation in developing zebrafish. Toxicol Sci *104*, 303-311.

Nahirney, P.C., Mikawa, T., and Fischman, D.A. (2003). Evidence for an extracellular matrix bridge guiding proepicardial cell migration to the myocardium of chick embryos. Dev Dyn *227*, 511-523.

Olson, E.N. (2006). Gene regulatory networks in the evolution and development of the heart. Science *313*, 1922-1927.

Perez-Pomares, J.M., Carmona, R., Gonzalez-Iriarte, M., Atencia, G., Wessels, A., and Munoz-Chapuli, R. (2002). Origin of coronary endothelial cells from epicardial mesothelium in avian embryos. Int J Dev Biol *46*, 1005-1013.

Perez-Pomares, J.M., Macias, D., Garcia-Garrido, L., and Munoz-Chapuli, R. (1997). Contribution of the primitive epicardium to the subepicardial mesenchyme in hamster and chick embryos. Dev Dyn *210*, 96-105.

Plavicki, J., Hofsteen, P., Peterson, R.E., and Heideman, W. (2013). Dioxin inhibits zebrafish epicardium and proepicardium development. Toxicol Sci *131*, 558-567.
Poon, K.L., Liebling, M., Kondrychyn, I., Garcia-Lecea, M., and Korzh, V. (2010). Zebrafish cardiac enhancer trap lines: new tools for in vivo studies of cardiovascular development and disease. Dev Dyn *239*, 914-926.

Riley, P.R. (2012). An epicardial floor plan for building and rebuilding the mammalian heart. Curr Top Dev Biol *100*, 233-251.

Schulte, I., Schlueter, J., Abu-Issa, R., Brand, T., and Manner, J. (2007). Morphological and molecular left-right asymmetries in the development of the proepicardium: a comparative analysis on mouse and chick embryos. Dev Dyn *236*, 684-695.

Sengbusch, J.K., He, W., Pinco, K.A., and Yang, J.T. (2002). Dual functions of [alpha]4[beta]1 integrin in epicardial development: initial migration and long-term attachment. J Cell Biol *157*, 873-882.

Serluca, F.C. (2008). Development of the proepicardial organ in the zebrafish. Dev Biol *315*, 18-27.

Smart, N., Dube, K.N., and Riley, P.R. (2012). Epicardial progenitor cells in cardiac regeneration and neovascularisation. Vascul Pharmacol.

Smart, N., and Riley, P.R. (2012). The epicardium as a candidate for heart regeneration. Future Cardiol *8*, 53-69.

Srivastava, D., and Olson, E.N. (2000). A genetic blueprint for cardiac development. Nature *407*, 221-226.

Stainier, D.Y., Fouquet, B., Chen, J.N., Warren, K.S., Weinstein, B.M., Meiler, S.E., Mohideen, M.A., Neuhauss, S.C., Solnica-Krezel, L., Schier, A.F.*, et al.* (1996). Mutations affecting the formation and function of the cardiovascular system in the zebrafish embryo. Development *123*, 285-292.

Van den Eijnde, S.M., Wenink, A.C., and Vermeij-Keers, C. (1995). Origin of subepicardial cells in rat embryos. The Anatomical record *242*, 96-102.

Vincent, S.D., and Buckingham, M.E. (2010). How to make a heart: the origin and regulation of cardiac progenitor cells. Curr Top Dev Biol *90*, 1-41.

Wells, P., and Pinder, A. (1996). The respiratory development of Atlantic salmon. II. Partitioning of oxygen uptake among gills, yolk sac and body surfaces. J Exp Biol *199*, 2737-2744.

Westerfield, M. (1995). The Zebrafish Book. A Guide for the Laboratory Use of Zebrafish (Danio rerio). *3rd Edition*.

SUMMARY

Exposure to the environmental contaminant and prototypical aryl hydrocarbon receptor (AHR) agonist, 2,3,7,8-tetrachlorodibenzo-*p*-dioxin (TCDD) results in deleterious effects on the cardiovascular system in vertebrates (Allen et al., 1977; Cook et al., 2003; Ivnitski et al., 2001; Thackaberry et al., 2005a; Thackaberry et al., 2005b; Walker, 1991). Epidemiological studies have associated TCDD exposure to increased incidence of congenital hypoplastic left heart syndrome and increased risk of ischemic heart disease (Bertazzi et al., 1998; Cronk et al., 2004; Flesch-Janys et al., 1995; Kuehl and Loffredo, 2006; Pesatori et al., 1998). Thus, understanding how TCDD affects the heart is of great concern.

Zebrafish (*Danio rerio*) have been employed to investigate the effects of TCDD on the heart (Antkiewicz et al., 2005; Carney et al., 2006; Heideman et al., 2005). TCDD-exposed zebrafish display marked pericardial edema coupled with heart malformation: an unlooped, elongated and tube shaped heart (Antkiewicz et al., 2005). TCDD-treated hearts also show decreased cardiomyocyte number, failure to form endocardial valve cushions and leaflets, circulation failure and ventricular standstill that culminates in death (Belair et al., 2001; Carney et al., 2006; Mehta et al., 2008). Onset of TCDD-induced heart malformation occurs following heart looping during epicardium development (Lanham et al., 2012; Plavicki et al., 2013; Serluca, 2008). Once the epicardium forms and matures, the zebrafish heart becomes resistant to TCDD exposure. This remains true until the adult zebrafish heart is stimulated to regenerate (Hofsteen et al., 2013a; Lanham et al., 2012).

Unlike humans, zebrafish can completely regenerate new myocardium from spared pre-existing cardiomyocytes (Jopling et al., 2010; Kikuchi et al., 2010; Poss et al., 2002). Resident cardiomyocyte differentiation and proliferation to the regenerating tissue occurs by trophic retinoic acid (RA) signaling from the endocardium and epicardium (Kikuchi et al., 2011). Furthermore, the regenerating heart is thought to revert to an "embryonic-like" state by activating developmental genes, such *tbx18* and the RA synthesizing enzyme *raldh2* along the epicardium (Lepilina et al., 2006). Given TCDD affects early heart development and has shown to inhibit regeneration of the rodent liver and zebrafish fin (Bauman et al., 1995; Mathew et al., 2006; Mitchell et al., 2006; Zodrow and Tanguay, 2003), we sought to determine if TCDD reversed the regenerative capacity of the adult zebrafish heart.

To determine whether TCDD exposure affects adult zebrafish heart regeneration (Chapter II), fish were exposed to TCDD prior to surgical resection of ~20% of the heart ventricle apex. Following regeneration, or lack there of, fish were euthanized at 7, 14 and 21 days post amputation (dpa) and their hearts were imaged. From these experiments it was evident pretreated TCDD amputated hearts could not regenerate new myocardium. This was apparent due to a persistent blood clot that lacked an enveloping epicardial-derived white epithelium. Furthermore, TCDD-treated partially amputated hearts had marked reduction of cardiomyocyte proliferation and epicardial expression of *raldh2* was upregulated and mislocalized. Interestingly, when fish were exposed to TCDD one day after partial heart ventricle amputation, following blood clot formation and initial epicardium-like coverage, regeneration occurred normally. Since TCDD activates the ligand-activated

transcription factor AHR/ARNT, DNA microarray experiments were conducted prior to partial amputation (0 hours post amputation; hpa), at 6 hpa (initial transcriptional response) and at 7 dpa (late stage transcriptional response). From these experiments, we were unable to determine the underlying molecular mechanism of TCDD-induced block in heart regeneration. However, at 6 hpa, several genes that are critical for cardiomyocyte dedifferentiation and proliferation were differentially expressed. While at 7 dpa, genes involved in remodeling of new cardiac tissue were well represented. Together, these results indicate the regenerative capacity of the zebrafish heart is reversed in the presence of TCDD.

The epicardium is the squamous epithelium of the vertebrate heart that is derived from a transient extracardiac cluster of progenitors termed proepicardium (PE) (Manner, 1992; Manner et al., 2001; Viragh and Challice, 1981). In zebrafish, the PE forms adjacent the atrioventricular (AV) junction along the pericardial wall and can be observed as early as 40 hours post fertilization (hpf) (Serluca, 2008).

In Chapter III, we determined when fish are TCDD-exposed prior to PE formation the epicardial progenitors that comprise the PE and subsequently the epicardium did not form. Furthermore, expression of the PE and epicardial marker, *tcf21*, was not expressed at the presumptive PE site following TCDD exposure. When fish were treated with TCDD following PE formation and during epicardium development (between 48-120 hpf) resident epicardial cells were not ablated and heart malformation became less severe. Thus, the onset of TCDD-induced heart malformation can be attributed to the failure to form the PE and subsequently

epicardium. This work identified a critical cell type of the heart that is targeted by TCDD exposure.

TCDD-activation of the AHR/ARNT signaling pathway results in failure to form the PE and epicardium. As discussed above, loss of this cell type can account for most, if not all, onset of TCDD-induced heart malformation. Since this finding was AHR2 dependent, we were curious what gene(s) caused this toxicity. Microarray experiments indicated the chondrogenic transcription factor *sox9b* was significantly downregulated in the heart following TCDD exposure (Carney et al., 2006). Furthermore, a previous report showed AHR-mediated downregulation of *sox9b* led to severe craniofacial malformation (Xiong et al., 2008). Thus, we sought to determine if *sox9b* was also involved in AHR-mediated heart malformation in zebrafish.

In Chapter IV, we show that *sox9b* is expressed in the zebrafish heart during epicardium formation and TCDD cardiotoxicity. This was shown by *in situ* hybridization against *sox9b* mRNA and by analysis of a *sox9b* reporter line *Tg*(-2450/0:*sox9b:EGFP*). It was apparent from these experiments that *sox9b* was mainly expressed in the apical regions of the heart ventricle and in myocardial cells. To determine if TCDD exposure affected *sox9b* expression, TCDD- or DMSO (control)-treated *sox9b* reporter fish were analyzed at 72 hpf by confocal microscopy. Qualitative measurements suggested an approximate two-fold downregulation of *Sox9b* as a result of TCDD exposure. To directly quantify *sox9b* downregulation, qRT-PCR was conducted. Together, these experiments indicated cardiac

expression *sox9b* was downregulated at the protein and mRNA level at the time of TCDD cardiotoxicity.

We next sought to determine if manipulation of *sox9b* would mimic the TCDD-mediated heart phenotype. First, we examined the *sox9b*^{b971} null at 96 hpf and noted a similar phenotype when compared to TCDD-treated fish. The *sox9b*^{b971} null had marked pericardial edema and an unlooped elongated heart. Importantly, the heart shape did not mimic that of a TCDD treated heart and circulation was not as severely affected. To determine if *sox9b* played a role in PE and epicardium development, the *sox9b*^{b971} null was examined at 72 hpf for presence of PE and at 120 hpf for the epicardium. At both times, the PE and epicardium had not formed in these fish. Using an alternative approach to knock down *sox9b,* antisense morpholino oligonucleotides (MO) were injected at the one cell stage in epicardial reporter lines. These experiments confirmed that PE and epicardium formation is dependent on *sox9b*. Subsequently, we overexpressed *sox9b* by mRNA injection prior to TCDD exposure in an attempt to rescue epicardium formation. We were able to rescue TCDD-mediated PE loss but not pericardial edema, the elongated unlooped heart, epicardium formation or cardiac contractility. Together, these sets of experiments suggest TCDD-mediated downregulation of *sox9b* results in loss of PE formation. However, downregulation of *sox9b* by TCDD does not account for all TCDD cardiotoxicity.

Overexpression of *sox9b* mRNA prior to TCDD exposure restored PE formation. However, the epicardium did not form and heart contractility was not restored. In Chapter V, we investigated the role of heart contractility during

epicardium formation. We first sought to fill a gap in the literature. Thus, we detailed zebrafish PE and epicardium development prior to elucidating the role of heart contractility on epicardium formation.

We discovered the PE migrates initially to the heart by a bridge-like structure followed by release of PE cell aggregates. This continuous supply of epicardial progenitors envelops the ventricle (~72-120 hpf) followed by the atrium (~120-168 hpf). We also found the zebrafish PE and epicardium to be a heterogeneous cell population that appear clonally dominant. These findings suggest PE and epicardium development is evolutionarily conserved between fish, birds and mammals.

To test the hypothesis that epicardium formation requires heart contraction we injected antisense MOs against *sih* in epicardial reporter lines (Chapter V, Bartman et al., 2004). *Sih* morphant fish were analyzed for PE presence at 72 hpf and epicardium formation at 120 hpf. The PE, but not the epicardium, formed in these experiments. As an alternative means to impair heart contractility we exposed fish to a reversible myosin ATPase inhibitor, 2,3-butanedione 2-monoxime (BDM) (Bartman et al., 2004). When fish were exposed to BDM during PE and epicardium development (0 - 120 hpf), again the PE formed normally but the epicardium failed to form. When BDM was removed following PE formation (exposure from 0 – 72 hpf) and heart contractility was restored, PE cells expressed the cell polarity gene *pard3* and the epicardium formed normally. These data indicate heart contractility is necessary for PE cell migration and epicardium formation in the zebrafish.

Together, we show TCDD affects two distinct growth-like phases of the zebrafish heart: early heart development and adult heart regeneration. In both growth-like events, the epicardium plays a significant role. If TCDD is present prior to surgical resection of the heart ventricle apex the regenerative capacity of the heart is reversed. We note this is coupled with failure to form the epicardially-derived white epithelium over the newly formed blood clot and a drastic decrease in cell proliferation at the wound site. In the embryo-larvae, TCDD exposure blocks the formation of epicardial progenitors (PE) and subsequent formation of the epicardium. We show normal epicardium formation is dependent on *sox9b* expression and that PE inhibition in the TCDD model is due downregulation *sox9b*. During these studies we have uncovered an evolutionarily conserved role between fish, birds and mammals during PE and epicardium development. Lastly, we show PE cell migration to form the epicardium requires cardiac contractility.

FUTURE DIRECTIONS

This work provides evidence that the epicardial progenitors are a target of TCDD exposure that is potentially the underlying cause of TCDD-induced heart malformation. However, we do not know if this AHR-mediated heart phenotype is a result of only loss of the epicardium. To prove this, one could knockout Ahr2 (dominant negative: dn) in PE cells and expose dnAhr2-PE fish to TCDD in an attempt to rescue the TCDD-induced heart malformation. Theoretically, if Ahr2 is knocked out of PE cells, then the PE will form and presumably migrate to the heart and provide structural support to rescue TCDD heart malformation. Alternatively, we

may find the PE will form but will not migrate to the heart analogous to *sih* morphants and *sox9b*-mRNA injected TCDD hearts. An alternative approach would be to ablate the PE specifically by inducing Ahr2 (constitutively active: ca) in PE cells (caAHR2-PE) to determine if this phenocopies TCDD-mediated heart malformation. In both constructs, dnAhr2 and caAhr2, the BAC clone DKEYP-79F12 of the *tcf21* gene could be fused to previously constructed dnAhr2 (Lanham et al., 2011) and caAHR2$^{zf/m}$ (Lanham et al., unpublished) and injected at the one cell stage into epicardial reporter lines. As an additional method and appropriate control, one could knockout *Tcf21* directly by MO injection in the *tcf21:DsRed* line to determine if this phenocopies TCDD cardiotoxicity. The advantage of this approach is to avoid activation of the Ahr2 signaling pathway. These experiments would confirm that TCDD-induced heart malformation is a direct result of failure to form the PE.

In contrast to higher vertebrates such as aves and mammals, the function and downstream fate of epicardial cells in zebrafish is unknown. To determine this, one could label PE cells with DiI at 50 hpf and analyze fish between 4 and 14 days post fertilization. Regions of particular interest would be the myocardium and valves. Thus, it would be prudent to DiI-label PE cells in fish carrying either *flk1*:GFP or *cmlc2:*GFP to determine if epicardial-derived cells colocalize with GFP. This would strengthen our understanding of the native role of the epicardium and provide insight as to why fish lacking epicardium also fail to form endocardial valves cushions and show decreased cardiomyocyte number.

TCDD-mediated downregulation of *sox9b* prevented PE formation. We show *sox9b* is downregulated 2-fold in the heart during PE and epicardium formation.

However, it is not known whether TCDD-mediated downregulation of cardiac *sox9b* is the reason for the effects on the PE. To answer this there are several experiments that need to be conducted. One experiment would be to activate Ahr in cardiomyocytes by injecting the previously constructed *cmlc2*:caAHR$^{zf/m}$-2AtRFP (Lanham, unpublished) in the *-2450:sox9b:*EGFP reporter line to determine if cardiac *sox9b* is downregulated. An additional experiment would be to knockout *sox9b* in the heart by short hairpin RNA (shRNA) or construction of a dominant negative cardiac *sox9b.* Alternatively, in an attempt to rescue TCDD cardiotoxicity, one could overexpress *Sox9b* in cardiomyocytes by synthesizing *cmlc2*:Sox9b and injecting this construct prior to TCDD treatment. Together, these experiments would indicate TCDD-mediated downregulation of cardiac *sox9b* is the underlying cause of TCDD-induced heart malformation.

Thus far, we have focused on how TCDD-induced activation of the AHR signaling pathway affects gene transcription and heart development. The *sox9b* gene is consistently downregulated by TCDD exposure in multiple tissue types (Carney et al., 2006; Hofsteen et al., 2013b; Mathew et al., 2008; Xiong et al., 2008). However, we have not investigated the role of endogenous *Ahr* and its control of *sox9b*. To test if *Ahr* plays a role in regulating *sox9b* endogenously, one could inject the *ahr2* MO into the *sox9b* reporter line to determine qualitative expression changes. Furthermore, one could also do *in situ* hybridization against *sox9b* in the *ahr2* homozygous null mutant. To quantify changes in *sox9b* directly, *ahr2* morphants could be collected and qRT-PCR for *sox9b* could be conducted with different tissue types.

Together, these experiments would solidify our understanding of the role of epicardium in mediating TCDD cardiotoxicity, elucidate the role of the myocardium in PE formation and recruitment, provide evidence that epicardial-derived cells exist in zebrafish, show what tissue types epicardial cells support developmentally and reveal the endogenous interaction between *Ahr-Sox9b* during embryonic-larvae development.

REFERENCES

Allen, J.R., Barsotti, D.A., Van Miller, J.P., Abrahamson, L.J., and Lalich, J.J. (1977). Morphological changes in monkeys consuming a diet containing low levels of 2,3,7,8-tetrachlorodibenzo-p-dioxin. Food Cosmet Toxicol *15*, 401-410.

Antkiewicz, D.S., Burns, C.G., Carney, S.A., Peterson, R.E., and Heideman, W. (2005). Heart malformation is an early response to TCDD in embryonic zebrafish. Toxicol Sci *84*, 368-377.

Bartman, T., Walsh, E.C., Wen, K.K., McKane, M., Ren, J., Alexander, J., Rubenstein, P.A., and Stainier, D.Y. (2004). Early myocardial function affects endocardial cushion development in zebrafish. PLoS Biol *2*, E129.

Bauman, J.W., Goldsworthy, T.L., Dunn, C.S., and Fox, T.R. (1995). Inhibitory effects of 2,3,7,8-tetrachlorodibenzo-p-dioxin on rat hepatocyte proliferation induced by 2/3 partial hepatectomy. Cell Prolif *28*, 437-451.

Belair, C.D., Peterson, R.E., and Heideman, W. (2001). Disruption of erythropoiesis by dioxin in the zebrafish. Dev Dyn *222*, 581-594.

Bertazzi, P.A., Bernucci, I., Brambilla, G., Consonni, D., and Pesatori, A.C. (1998). The Seveso studies on early and long-term effects of dioxin exposure: a review. Environ Health Perspect *106 Suppl 2*, 625-633.

Carney, S.A., Chen, J., Burns, C.G., Xiong, K.M., Peterson, R.E., and Heideman, W. (2006). Aryl hydrocarbon receptor activation produces heart-specific transcriptional and toxic responses in developing zebrafish. Mol Pharmacol *70*, 549-561.

Cook, P.M., Robbins, J.A., Endicott, D.D., Lodge, K.B., Guiney, P.D., Walker, M.K., Zabel, E.W., and Peterson, R.E. (2003). Effects of aryl hydrocarbon receptor-mediated early life stage toxicity on lake trout populations in Lake Ontario during the 20th century. Environ Sci Technol *37*, 3864-3877.

Cronk, C.E., Pelech, A.N., Malloy, M.E., and McCarver, D.G. (2004). Excess birth prevalence of Hypoplastic Left Heart syndrome in eastern Wisconsin for birth cohorts 1997-1999. Birth Defects Res A Clin Mol Teratol *70*, 114-120.

Flesch-Janys, D., Berger, J., Gurn, P., Manz, A., Nagel, S., Waltsgott, H., and Dwyer, J.H. (1995). Exposure to polychlorinated dioxins and furans (PCDD/F) and mortality in a cohort of workers from a herbicide-producing plant in Hamburg, Federal Republic of Germany. Am J Epidemiol *142*, 1165-1175.

Heideman, W., Antkiewicz, D.S., Carney, S.A., and Peterson, R.E. (2005). Zebrafish and cardiac toxicology. Cardiovasc Toxicol *5*, 203-214.

Hofsteen, P., Mehta, V., Kim, M.S., Peterson, R.E., and Heideman, W. (2013a). TCDD inhibits heart regeneration in adult zebrafish. Toxicol Sci *132*, 211-221.

Hofsteen, P., Plavicki, J., Johnson, S.D., Peterson, R.E., and Heideman, W. (2013b). Sox9b is Required for Epicardium Formation and Plays a Role in TCDD-induced Heart Malformation in Zebrafish. Mol Pharmacol.

Ivnitski, I., Elmaoued, R., and Walker, M.K. (2001). 2,3,7,8-tetrachlorodibenzo-p-dioxin (TCDD) inhibition of coronary development is preceded by a decrease in myocyte proliferation and an increase in cardiac apoptosis. Teratology *64*, 201-212.

Jopling, C., Sleep, E., Raya, M., Marti, M., Raya, A., and Belmonte, J.C. (2010). Zebrafish heart regeneration occurs by cardiomyocyte dedifferentiation and proliferation. Nature *464*, 606-609.

Katz, T.C., Singh, M.K., Degenhardt, K., Rivera-Feliciano, J., Johnson, R.L., Epstein, J.A., and Tabin, C.J. (2012). Distinct compartments of the proepicardial organ give rise to coronary vascular endothelial cells. Dev Cell *22*, 639-650.

Kikuchi, K., Holdway, J.E., Major, R.J., Blum, N., Dahn, R.D., Begemann, G., and Poss, K.D. (2011). Retinoic acid production by endocardium and epicardium is an injury response essential for zebrafish heart regeneration. Dev Cell *20*, 397-404.

Kikuchi, K., Holdway, J.E., Werdich, A.A., Anderson, R.M., Fang, Y., Egnaczyk, G.F., Evans, T., Macrae, C.A., Stainier, D.Y., and Poss, K.D. (2010). Primary contribution to zebrafish heart regeneration by gata4(+) cardiomyocytes. Nature *464*, 601-605.

Kuehl, K.S., and Loffredo, C.A. (2006). A cluster of hypoplastic left heart malformation in Baltimore, Maryland. Pediatr Cardiol *27*, 25-31.

Lanham, K.A., Peterson, R.E., and Heideman, W. (2012). Sensitivity to dioxin decreases as zebrafish mature. Toxicol Sci *127*, 360-370.

Lanham, K.A., Prasch, A.L., Weina, K.M., Peterson, R.E., and Heideman, W. (2011). A dominant negative zebrafish Ahr2 partially protects developing zebrafish from dioxin toxicity. PLoS One *6*, e28020.

Lepilina, A., Coon, A.N., Kikuchi, K., Holdway, J.E., Roberts, R.W., Burns, C.G., and Poss, K.D. (2006). A dynamic epicardial injury response supports progenitor cell activity during zebrafish heart regeneration. Cell *127*, 607-619.

Manner, J. (1992). The development of pericardial villi in the chick embryo. Anat Embryol (Berl) *186*, 379-385.

Manner, J., Perez-Pomares, J.M., Macias, D., and Munoz-Chapuli, R. (2001). The origin, formation and developmental significance of the epicardium: a review. Cells Tissues Organs *169*, 89-103.

Mathew, L.K., Andreasen, E.A., and Tanguay, R.L. (2006). Aryl hydrocarbon receptor activation inhibits regenerative growth. Mol Pharmacol *69*, 257-265.

Mathew, L.K., Sengupta, S.S., Ladu, J., Andreasen, E.A., and Tanguay, R.L. (2008). Crosstalk between AHR and Wnt signaling through R-Spondin1 impairs tissue regeneration in zebrafish. FASEB J *22*, 3087-3096.

Mehta, V., Peterson, R.E., and Heideman, W. (2008). 2,3,7,8-Tetrachlorodibenzo-p-dioxin exposure prevents cardiac valve formation in developing zebrafish. Toxicol Sci *104*, 303-311.

Mitchell, K.A., Lockhart, C.A., Huang, G., and Elferink, C.J. (2006). Sustained aryl hydrocarbon receptor activity attenuates liver regeneration. Mol Pharmacol *70*, 163-170.

Pesatori, A.C., Zocchetti, C., Guercilena, S., Consonni, D., Turrini, D., and Bertazzi, P.A. (1998). Dioxin exposure and non-malignant health effects: a mortality study. Occup Environ Med *55*, 126-131.

Plavicki, J., Hofsteen, P., Peterson, R.E., and Heideman, W. (2013). Dioxin inhibits zebrafish epicardium and proepicardium development. Toxicol Sci *131*, 558-567.

Poss, K.D., Wilson, L.G., and Keating, M.T. (2002). Heart regeneration in zebrafish. Science *298*, 2188-2190.

Serluca, F.C. (2008). Development of the proepicardial organ in the zebrafish. Dev Biol *315*, 18-27.

Thackaberry, E.A., Jiang, Z., Johnson, C.D., Ramos, K.S., and Walker, M.K. (2005a). Toxicogenomic profile of 2,3,7,8-tetrachlorodibenzo-p-dioxin in the murine fetal heart: modulation of cell cycle and extracellular matrix genes. Toxicol Sci *88*, 231-241.

Thackaberry, E.A., Nunez, B.A., Ivnitski-Steele, I.D., Friggins, M., and Walker, M.K. (2005b). Effect of 2,3,7,8-tetrachlorodibenzo-p-dioxin on murine heart development: alteration in fetal and postnatal cardiac growth, and postnatal cardiac chronotropy. Toxicol Sci *88*, 242-249.

Viragh, S., and Challice, C.E. (1981). The origin of the epicardium and the embryonic myocardial circulation in the mouse. The Anatomical record *201*, 157-168.

Walker, M.K., Spitsbergen, J.M., Olson, J.R., and Peterson, R.E. (1991). 2,3,7,8-Tetrachlorodibenzo-p-dioxin toxicity during early life stage development of lake trout (Salvelinus namaycush). Can J Fish Aquat Sci *48*, 875-883.

Xiong, K.M., Peterson, R.E., and Heideman, W. (2008). Aryl hydrocarbon receptor-mediated down-regulation of sox9b causes jaw malformation in zebrafish embryos. Mol Pharmacol *74*, 1544-1553.

Zodrow, J.M., and Tanguay, R.L. (2003). 2,3,7,8-tetrachlorodibenzo-p-dioxin inhibits zebrafish caudal fin regeneration. Toxicol Sci *76*, 151-161.